Basic micrometeorology

Nelson Luís Dias

March 10, 2023

Contents

List of Figures

4

List of Tables

Listings

Preface

Este texto começa com a introdução do conceito de *escala*, que é fundamental em tudo o que se segue. Vamos procurar entender a globalidade do problema descrevendo as várias camadas da atmosfera (troposfera, estratosfera, …) e fazendo depois um "zoom" na Camada-Limite Atmosférica (CLA), que é a parte mais baixa da troposfera. Em seguida, reveremos as equações de Mecânica dos Fluidos aplicáveis à CLA , falaremos de turbulência e da sua abordagem clássica (decomposição de Reynolds e equações de transporte de covariâncias). Algumas soluções particulares simples destas equações proporcionam uma boa idéia da interação das camadas mais altas da atmosfera com a CLA. Estudaremos mais intensamente a parte mais baixa da CLA, chamada Camada Superficial (CS). Na CS, debaixo de algumas hipóteses simplificadoras, podemos utilizar a Teoria de Similaridade de Monin-Obukhov (SMO), que nos permite descrever uma série de grandezas relacionadas com a turbulência de forma extremamente simples. As equações básicas que descrevem a física da turbulência e as previsões da Teoria de Similaridade de Monin-Obukhov são utilizadas para prever o comportamento das grandezas médias $\overline{u}$, $\overline{\theta}$ e $\overline{q}$ na CS. Além do comportamento genérico previsto pela teoria SMO, dois casos-limite cujo significado físico é importante são abordados: a estratificação independente de z numa atmosfera muito *estável*, e a convecção livre local em uma atmosfera muito *instável*. Com as previsões da teoria sobre o comportamento das grandezas médias, é possível então utilizar medições delas para calcular os fluxos τ, H e E. Além de alguns métodos que utilizam exclusivamente a medição de grandezas médias, apresenta-se ao fim do relatório o método da variância, que é um híbrido que utiliza tanto grandezas médias como medições de turbulência.

1

Introduction

1.1 – The regions of the atmosphere

The atmosphere is a relatively thin layer of gas above the Earth's surface. Upwards of $100\,$km above the surface, the density of the atmosphere is very low. Meanwhile, since the Earth's great circle $\mathscr{C}$ is approximately $40\,000\,$km, if we set the thickness of the atmosphere to $\mathscr{L} = 100\,$km, the ratio $\mathscr{L}/\mathscr{C} = 0{,}0025$ shows how thin the atmosphere really is.

Figure 1.1 shows the main regions of the atmosphere in the first $100\,$km, for a standard atmosphere at $10°\,$N in june (Houghton, 1986): in this case, the troposphere extends to $17\,$km; the stratosphere is a strongly stratified region ($\frac{\mathrm{d}T}{\mathrm{d}z} > 0$) between $17\,$km and $50\,$km; the mesosphere displays a marked temperature fall between $50\,$km and $95\,$km; finally, from that point upwards the temperature rises again in the termosphere.

There is a wealth of physical phenomena, still under study today, in the Earth's Atmosphere. The one region of most importance to life on the Planet, and the only one directly experienced by living creatures, is the troposphere. The Earth's highest mountain does not surpass $9\,$km in altitude. The most directly relevant region of the Troposphere is the Atmospheric Boundary Layer (ABL), which rarely extends beyond $2\,$km in height. This represents 2% of figure 1.1.

In the same way that we have used the profile of thermodynamic temperature to characterize the various regions of the atmosphere in figure 1.1, the ABL is characterized by the potential temperature profile; for the time being, suffice it to say that the potential temperature is a density indicator: the greater the potential temperature, the lesser the air density. Figure 1.2 shows a typical potential temperature profile during the day, in fair weather. The potential temperature gradients are large (in absolute value) up to a height of approximately $100\,$m, and configure the surface layer SL; from that point upwards, the potential temperature remains practically constant up to around $1100\,$m (this is the convective, or mixed, layer ML); between 1100 and $1300\,$m, the potential temperature rises gently in the entrainment zone EZ, and above $1300\,$m lies the free atmosphere FA, where a strong density stratification prevails, damping almost all turbulence, and where we can neglect to good approximation the effect of turbulent stresses. This will lead, in Section ??, to the geostrophic wind equations. This brief outline shows the richness of vertical scales involved.
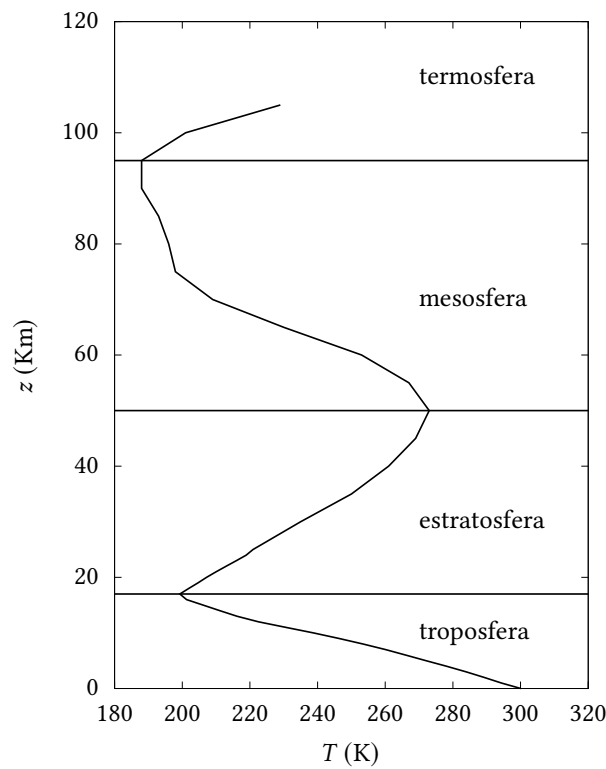
Figure 1.1: Temperature profile in a model atmosphere, at 10°N, in June (Houghton, 1986)
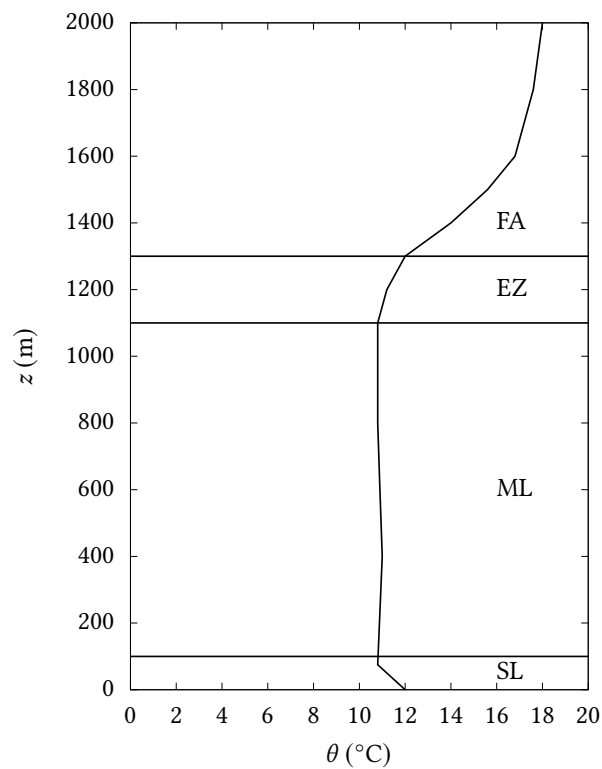
Figure 1.2: A typical daytime potential temperature profile in the ABL (adapted from (Stull, 1988))

Table 1.1: Classification of horizontal scales in meteorology

Name	Characteristic length
macro β	10.000 km
meso α	2.000 km
meso β	200 km
meso γ	20 km
micro α	2 km
micro β	200 m
micro γ	20 m

As one might expect from our discussion on the ratio $\mathscr{L}/\mathscr{C}$, the *horizontal* scales over which atmospheric physical phenomena are observed in meteorology are considerably larger. To make the meaning of the classification in table 1.1, note the following list of phenomena and their corresponding horizontal scales given by Holton (1992):

Table 1.2: Escalas de movimentos atmosféricos (Holton, 1992)

Type of motion	Horizontal scale (m)
Molecular mean free path	10^{-7}
Minute turbulent eddies	10^{-2}–10^{-1}
Small eddies	10^{-1}–10^{0}
Dust devils	10^{0}–10^{1}
Gusts	10^{1}–10^{2}
Tornadoes	10^{2}
Cumulonimbus clouds	10^{3}
Fronts, squall lines	10^{4}
Hurricanes	10^{5}
Synoptic cyclones	10^{6}
Planetary waves	10^{7}

No nosso caso, estaremos trabalhando dentro das fronteiras da micrometeorologia: nossas escalas horizontais são da ordem de 2 km ou menores (micro-α), e nossas escalas verticais da ordem da espessura da camada superficial, cerca de 100 m, ou menores. Este é o domínio por excelência da turbulência: movimentos turbulentos na atmosfera possuem escalas desde algumas centenas de metros (na horizontal) até poucos milímetros, que é a escala onde a turbulência é dissipada por efeitos viscosos. A modelação matemática da CLA é o assunto da próxima seção.

1.2 – The importance of the surface fluxes

A great deal of the physical evolution of the atmosphere is influenced by the exchange of mass, momentum and energy with the surface of the Earth. The surface of these quantities are the *surface fluxes*, and their knowledge is essential for applications in meteorology, hydrology and environmental sciences in general. In particular, the values of the *greenhouse gas* surface fluxes are needed to predict their impact on global warming and climate change.

A emissão de gases de efeito estufa (GEE) da superfície da Terra para a atmosfera é hoje, reconhecidamente, um dos grandes problemas ambientais que enfrentamos. O problema é global, tornando necessária a negociação internacional de limites para as emissões, bem como o desenvolvimento internacional de metodologias que sejam consensualmente aceitas para estimar estas emissões.

Uma das abordagens para a estimativa dos fluxos destes gases é a realização de medições micrometeorológicas. Ao evitar a complexidade dos processos que ocorrem na superfície ou abaixo dela (seja da água ou do solo/vegetação), e ao integrar as emissões e capturas de GEE tanto na vertical quanto sobre o comprimento de pista do vento, medições micrometeorológicas de GEE podem dar respostas importantes sobre o valor dos fluxos superficiais, seu padrão horário e sazonal, e sua relação com outras grandezas importantes tais como temperaturas do ar, água e solo, a qualidade da água, o tipo de vegetação, etc...

Medições micrometeorológicas de gases de efeito estufa em geral consistem em medições de grandezas atmosféricas relativamente próximo da superfície. Convencionalmente, as medições são divididas em "blocos", que podem ser tão curtos quanto 10 minutos, ou tão longos quanto 1 hora. Dentro de cada bloco, é usual supor a estacionariedade das séries temporais medidas. As medições podem ser realizadas por sensores relativamente lentos, quando então "médias" são obtidas, ou com sensores suficientemente rápidos para capturar uma parte signficativa das frequências associadas à turbulência atmosférica. Neste último caso, estatísticas da turbulência dentro do bloco, tais como desvios-padrão, covariâncias, funções de correlação cruzada e espectros podem ser medidos.

Medições de grandezas médias estão associadas ao método fluxo-gradiente (MFG) para a estimativa de fluxos. Medições de turbulência estão associadas ao método de medição de covariâncias turbulentas (MCT).

O MFG é mais antigo, e envolve mais hipóteses, do que as "medições diretas" realizadas pelo MCT. Na verdade, como veremos, estas medições não são tão diretas assim, e o MCT também envolve um grande número de hipóteses, embora talvez não tão restritivas quanto as do MFG. Devido a dificuldades tecnológicas e custo, o MFG ainda é amplamente utilizado para a estimativa de fluxos de gases tais como o CH_4 e o N_2O, para os quais medições (principalmente de longo prazo) de flutuações turbulentas ainda são problemáticas.

O método de medição de covariâncias turbulentas (MCT), originalmente desenvolvido para a medição dos fluxos de quantidade de movimento, calor sensível e massa de vapor d'água, possui uma série de características que o tornam uma opção interessante para a medição de fluxos de GEE: medições contínuas de fluxos

horários ou de 30 minutos são possíveis; as medições possuem uma representatividade espacial da ordem de centenas de metros corrente acima da torre de medição; e as tecnologias de medição envolvidas estão hoje (2011) razoavelmente bem desenvolvidas e possuem custos acessíveis.

2

A primer on the thermodynamics of the Atmospheric Boundary Layer

2.1 – The ideal gas law and specific heats for a pure substance

The ideal gas law applies well for typical conditions of the troposphere. For a *pure substance*, it is

$$pV = nR^{\#}T, \tag{2.1}$$

where p is pressure, V is the volume occupied by the gas, n is the number of moles, $R^{\#} = 8{,}314\,462\,618\,15\,\mathrm{J\,mol^{-1}\,K^{-1}}$ (in the SI) is the universal gas constant, and T is thermodynamic temperature. Still for a pure substance, (2.1) can also be written as

$$p = n\frac{R^{\#}}{V}T = \frac{m}{M}\frac{R^{\#}}{V}T = \frac{m}{V}\frac{R^{\#}}{M}T \;\Rightarrow$$
$$p = \rho R T. \tag{2.2}$$

Above, M is the molar mass; m is the mass of the gas, which is related to the number of moles by

$$m = nM; \tag{2.3}$$

the gas constant is

$$R = \frac{R^{\#}}{M}, \tag{2.4}$$

which depends on the specific gas through M in 2.4; and

$$\rho = \frac{m}{V} \tag{2.5}$$

is the density; its reciprocal

$$v = \frac{1}{\rho} \tag{2.6}$$

is the *specific volume v*. Note that (2.2) is more useful than (2.1) in practice: V does not appear in it, and it only involves intensive quantities (pressure, density and temperature), so it applies at every point in the atmosphere.

The perfect gas law in the form (2.1) or (2.2) is an example of a state equation in thermodynamics. For a *pure substance*, then, the state equation takes one of the forms

$$p = p(v, T) \qquad \text{or} \qquad v = v(p, T) \qquad \text{or} \qquad T = T(p, v).$$

For atmospheric gases, the lower case letters indicate specific quantities (per unit mass or unit volume), and are more convenient since we will not usually treat individual "systems" or "lumps" of air.

Two important thermodynamical functions are the specific internal energy u and the specific enthalpy h defined by

$$h = u + pv. \tag{2.7}$$

For a pure substance, they are functions of two variables, chosen between p, v and T. We usually write

$$u = u(v, T), \tag{2.8}$$

$$h = h(p, T), \tag{2.9}$$

since these pairs lead to useful definitions of measurable quantities such as specific heats. Equations (2.8) and (2.9) lead to perfect differentials

$$du = \left(\frac{\partial u}{\partial v}\right)_T dv + \left(\frac{\partial u}{\partial T}\right)_v dT, \tag{2.10}$$

$$dh = \left(\frac{\partial h}{\partial p}\right)_T dp + \left(\frac{\partial h}{\partial T}\right)_p dT. \tag{2.11}$$

The specific heats at constant volume and constant temperature are defined by

$$c_v = \left(\frac{\partial u}{\partial T}\right)_v, \tag{2.12}$$

$$c_p = \left(\frac{\partial h}{\partial T}\right)_p. \tag{2.13}$$

The subscripts v and p on the right-hand side of the equations above are used in thermodynamics as reminders that u is being taken as a function of v, T, and that h is being taken as a function of p, T.

For a perfect gas, from (2.2) and (2.6), the equation of state takes the form

$$pv = RT, \tag{2.14}$$

where R is a gas constant specific for the pure substance and it is possible to show that in this case u and h are functions of T only (Adkins, 1983). Then, (2.12)–(2.13) become ordinary derivatives. Also,

$$\left(\frac{\partial h}{\partial T}\right)_p = \left(\frac{\partial}{\partial T}[u + pv]\right)_p$$

$$= \left(\frac{\partial u}{\partial T}\right)_p + p\left(\frac{\partial v}{\partial T}\right)_p$$

$$= \frac{du}{dT} + p\frac{R}{p} \implies$$

$$c_p = c_v + R. \tag{2.15}$$

Physically, $c_p > c_v$ due to the extra energy necessary for the expansion of the air against the constant pressure p.

2.2 – The atmosphere as a mixture of ideal gases

The atmosphere however is not a pure substance, but a mixture of gases. The question then is how (2.1) can be reasonably extended to account for mixtures. In fact, from now on, often when we use one of (2.1)–(2.6), we will be referring to the total atmospheric pressure p (of a mixture of gases), the total density ρ, etc..

Therefore, we start by requiring that (2.1) *apply for the mixture*; then, the total number of moles, n, is the sum of the number of moles of each individual constituent. Let i be the index for each gas in a mixture; we have

$$n = \sum_i n_i, \tag{2.16}$$

where n_i is the number of moles of gas i.

We want the perfect gas law to apply for each constituent as well, and if we substitute (2.16) into (2.1), the question is what to do with the left-hand side of (2.1). There are two possibilities: the model of partial pressures, and the model of partial volumes. In the first case, we specify for each gas

$$p_i V = n_i R^\# T. \tag{2.17}$$

In this model all gases occupy a common volume V, each one exerting its own partial pressure p_i, such that the total pressure is

$$p = \sum_i p_i. \tag{2.18}$$

In the second case,

$$p V_i = n_i R^\# T, \tag{2.19}$$

and now all gases are subject to the same pressure p, each one occuping, nominally, a partial volume V_i, with

$$V = \sum_i V_i. \tag{2.20}$$

In both cases, summing the individual equations of state recovers the perfect gas law for the mixture. For example, starting from (2.17),

$$\sum_i \left(p_i V \right) = \sum_i \left(n_i R^\# T \right),$$
$$\left(\sum_i p_i \right) V = \left(\sum_i n_i \right) R^\# T,$$
$$p V = n R^\# T$$

(recovering (2.1)), and similarly for (2.19).

From (2.1), (2.17) and (2.19), it follows that

$$x_i = \frac{p_i}{p} = \frac{V_i}{V} = \frac{n_i}{n} \tag{2.21}$$

defines a concentration (traditionally expressed in %, parts per million (ppm), parts per billion (ppb), etc.) either in partial pressure fraction, partial volume fraction, or *mole fraction*. The gas law for each constituent can also be written

$$p_i = n_i \frac{R^{\#}}{V} T = \frac{m_i}{M_i} \frac{R^{\#}}{V} T = \frac{m_i}{V} \frac{R^{\#}}{M_i} T \implies$$

$$p_i = \rho_i R_i T, \tag{2.22}$$

where (as before for a pure substance)

$$m_i = n_i M_i \tag{2.23}$$

and

$$\rho_i = m_i / V, \tag{2.24}$$

$$v_i = \frac{1}{\rho_i}, \tag{2.25}$$

are the density or the specific mass (with mass m_i occupying the volume V) and the specific volume respectively of the gas i, and M_i is the molar mass of gas i. In (2.22),

$$R_i = \frac{R^{\#}}{M_i} \tag{2.26}$$

is the gas constant for gas i.

Once more, (2.2) holds for the mixture. To see how, note that the total mass of the mixture is

$$m = \sum_i m_i; \tag{2.27}$$

and similarly for the total density:

$$\rho = \frac{m}{V} = \frac{\sum_i m_i}{V} = \sum_i \frac{m_i}{V} = \sum_i \rho_i. \tag{2.28}$$

We will also need to define the *mass concentration*, or *mass fraction* of each constituent,

$$c_i \equiv \frac{m_i}{m} = \frac{\rho_i}{\rho}. \tag{2.29}$$

With (2.27)–(2.28) in hand, we sum (2.22) to obtain

$$\sum_i p_i = \sum_i \rho_i R_i T,$$

$$p = \left(\sum_i \rho_i R_i \right) T \equiv \rho R T.$$

This *defines* the gas constant R of the mixture; now

$$R = \frac{\sum_i \rho_i R_i}{\rho}$$

$$= \frac{\sum_i \frac{m_i}{V} R_i}{\frac{m}{V}}$$

$$= \sum_i \frac{m_i}{m} R_i = \sum_i c_i R_i. \tag{2.30}$$

Thus, given the mass concentrations, we can calculate the equivalent gas constant.

The *mean molar mass* of the mixture is

$$M = \sum_i x_i M_i = \frac{\sum_i n_i M_i}{n} = \frac{m}{n}, \tag{2.31}$$

which recovers (2.3). This finally allows us to close the circuit to recover (2.4) for the mixture. From (2.30),

$$
\begin{aligned}
R &= \frac{1}{m} \left(\sum_i m_i R_i \right) \\
&= \frac{1}{m} \left(\sum_i n_i M_i R_i \right) \\
&= \frac{1}{m} \left(\sum_i n_i R^{\#} \right) = \frac{1}{m} \left(\sum_i n_i \right) R^{\#} \\
&= \frac{n}{m} R^{\#} = \frac{R^{\#}}{M},
\end{aligned}
\tag{2.32}
$$

by virtue of (2.31), which recovers (2.4).

Exercises

2.1 Show that the sum of (2.19) over all gases in a mixture recovers (2.1).

2.2 Show that

$$\sum_i c_i = 1.$$

2.3 – Concentrations

A relationship between x_i and c_i can now be readily obtained:

$$x_i = \frac{n_i}{n} = \frac{\frac{m_i}{M_i}}{\frac{m}{M}} = \frac{m_i}{m} \frac{M}{M_i},$$

or

$$x_i M_i = c_i M. \tag{2.33}$$

Other concentration measures are also in use in meteorology, and need to be defined. The *mixing ratio* can be expressed either as a *mole ratio*,

$$\eta_i = \frac{n_i}{n - n_i}, \tag{2.34}$$

or as a *mass ratio*

$$r_i = \frac{m_i}{m - m_i}. \tag{2.35}$$

It is easy to convert mass fractions c_i to mixing (mass) ratios r_i and vice-versa:

$$r_i = \frac{\rho_i}{\rho - \rho_i} = \frac{\frac{\rho_i}{\rho}}{1 - \frac{\rho_i}{\rho}};$$

$$r_i = \frac{c_i}{1 - c_i} \quad \Rightarrow \tag{2.36}$$

$$c_i = \frac{r_i}{1 + r_i}. \tag{2.37}$$

Table 2.1: Constitution of a "dry" atmosphere (not including water vapor). The values are approximate, and adjusted to ensure that the molar fractions sum up to 1.

Gas	M_i $(\mathrm{g\,mol^{-1}})$	x_i $(\mathrm{mol\,mol^{-1}})$
N_2	28.0134	0.78078700
O_2	31.9988	0.20943200
Ar	39.948	0.00934000
CO_2	44.0095	0.00041390
Ne	20.1797	0.00001818
He	4.002602	0.00000524
CH_4	16.0425	0.00000170
Kr	83.798	0.00000110
H_2	2.01588	0.00000055
N_2O	44.0128	0.00000033
sum		1.00000000

The mixing ratio, therefore, is the ratio of the amount (either in moles or in mass) of substance i to the amount of all *other* substances. It follows that for any substance *other than* water vapor, the denominator includes the amount of water vapor present in the air at the time of measurement. For this reason, *when i is not water vapor*, (2.34)–(2.35) are often called *wet mixing ratios*.

We list on table 2.1 the molar fractions of several atmospheric gases in $\mathrm{g\,m^{-3}}$ in a *dry* atmosphere (a fictitious atmosphere without water vapor). The M_i values were obtained from NIST (2020). The x_i values are given in Dias (2021), and they are *approximations*, based on several existing references (Iribarne and Godson, 1981; COESA, 1976; Wallace and Hobbs, 2006; Wikipedia, 2020); the values of x_i, particularly for CO_2, are updated to the most recent (as of 2023) available data. Morever, the values have been manually adjusted to ensure that

$$\sum_i x_i = 1. \tag{2.38}$$

We are now in a position to calculate the gas constant for *dry air*, R_d, by means of (2.31)– (2.32), using the values in table 2.1, obtaining

$$R_d = 287.0429\,\mathrm{J\,kg^{-1}\,K^{-1}}. \tag{2.39}$$

This value is slightly less than the one adopted for the standard 1976 atmosphere ($R_d = 287.0569$), which is compatible with Iribarne and Godson (1981)'s table I-4. Note however that there has been a steady increase in atmospheric CO_2 since the publication of the 1976 U. S. Standard Atmosphere, so besides not being too different from the COESA (1976) figure, the value adopted here is probably closer to the current (2023) state of the atmosphere.

Exercises

2.3 Obtain the equivalent of (2.36)–(2.37) for the molar fractions x_i and molar ratios η_i.

2.4 Show that

$$\sum_i r_{di} = 1.$$

2.5 A tabela abaixo mostra as frações molares de uma mistura de 3 gases e suas respectivas massas moleculares. Obtenha a constante de gás equivalente R_e da mistura para a equação de estado (para a mistura) $p = \rho R_e T$, onde p é a pressão da mistura, ρ é a densidade da mistura, e T é a temperatura da mistura. Use $R^{\#} = 8.3145\,\mathrm{J\,mol^{-1}\,K^{-1}}$ para a constante universal dos gases. Dê sua resposta no Sistema Internacional de Unidades.

Gas	M_i $(\mathrm{g\,mol^{-1}})$	x_i $(\mathrm{mol\,mol^{-1}})$
N_2	28.0134	0.73
O_2	31.9988	0.22
Ar	39.9480	0.05
soma		1.00

2.4 – Moist air

Note that the equations of section 2.1 are not strictly valid for atmospheric air, which is not a *pure* substance; rather, it is a mixture of many gases. Each new constituent makes the thermodynamical equations more complex; in particular, functions of state such as u and $\hat{h}$ then become also functions of the concentrations of each new constituent.

We will not follow the rigorous path of treating the atmosphere as a mixture of several gases and writing down the full thermodynamical equations for that mixture; instead, we will consider "dry air", discussed in sections 2.2–2.3 and will introduce various humidity indices for the concentration of water vapor (the most important varying component).

Consider now a certain volume V, composed of initally dry air with mass m_d, total number of moles n_d, pressure p_d, and density ρ_d, to which is added water vapor with mass m_v and n_v moles. The equations developed in section 2.2 apply for moist air. Following (2.17), each gas component exerts its own partial pressure as a funcion of temperature T and number of moles n_i. If water vapor is added isothermically, the total pressure after its addition will increase by *the partial pressure of water vapor*, which, from (2.17), is

$$e = \frac{1}{V} n_v R^{\#} T. \tag{2.40}$$

Strictly speaking, we should have used p_v instead of e above, but it is standard in meteorology to call the partial pressure of water vapor e, and we will follow that practice.

The water vapor content of the air, however, is highly variable in the atmosphere; also, in scalar turbulent flux measurements it is often better to employ concentrations measured in (an equivalent) dry atmosphere (see, for example, Butenhoff and Khalil, 2002). Therefore, we revisit several concentration defintions with respect to the *dry* components only. For the mole fraction we now have the *dry* pressure, volume and molar ratios

$$x_{di} = \frac{p_i}{p_d} = \frac{V_i}{V_d} = \frac{n_i}{n_d} \qquad (i \neq v) \tag{2.41}$$

and the *dry* mass fraction or mass concentration,

$$c_{di} = \frac{\rho_i}{\rho_d} \qquad (i \neq v). \tag{2.42}$$

Above, note that after addition of water vapor, the volume of the *dry* constituents will be $V_d < V$. We also have the *dry* mixing ratios

$$\eta_{di} = \frac{n_i}{n_d - n_i}, \qquad (i \neq v) \tag{2.43}$$

and

$$r_{di} = \frac{m_i}{m_d - m_i} \qquad (i \neq v). \tag{2.44}$$

Provided the relative concentrations of the dry components remain unaltered, the previous calculations of dry air properies, M_d and R_d (the mean molecular mass and the gas constant of dry air, respectively) also hold in a moist atmosphere. Running the risk of being tedious, let us verify this. The total pressure now is

$$p = p_d + e. \tag{2.45}$$

where p_d is calculated as

$$p_d = \sum_{i \neq v} p_i = \sum_{i \neq v} \rho_i R_i T \equiv \rho_d R_d T. \tag{2.46}$$

As before, (2.46) defines R_d. Therefore, the value of the dry gas constant in a moist atmosphere is

$$R_d = \frac{\sum_{i \neq v} \rho_i R_i}{\rho_d} = \sum_{i \neq v} \frac{\rho_i}{\rho_d} R_i = \sum_{i \neq v} c_{di} R_i, \tag{2.47}$$

where the weights of the specific gas constants R_i are now the dry mass concentrations c_{di}. Proceeding,

$$
\begin{aligned}
R_d &= \frac{1}{m_d} \sum_{i \neq v} m_i R_i \\
&= \frac{1}{m_d} \sum_{i \neq v} n_i M_i R_i \\
&= \frac{1}{m_d} \sum_{i \neq v} n_i R^{\#} = \frac{1}{m_d} \left(\sum_{i \neq v} n_i \right) R^{\#} \\
&= \frac{n_d}{m_d} R^{\#} \tag{2.48}
\end{aligned}
$$

But the mean molar mass of dry air in the moist atmosphere is, by definition,

$$M_d = \sum_{i \neq v} x_{di} M_i = \frac{\sum_{i \neq v} n_i M_i}{n_d} = \frac{m_d}{n_d} \tag{2.49}$$

so that, as before,

$$R_d = \frac{R^{\#}}{M_d}. \tag{2.50}$$

Also note that if the relative concentrations of the dry components do not change, then the x_{di}'s in (2.49) are the same as the x_i's in table 2.1, which proves the assertion that in this case the values of M_d and R_d do not change.

With these results in hand, we can simplify calculations substantially by dividing air occupying V with total mass m into a dry component and water vapor, *viz.*

$$
\begin{aligned}
m &= m_d + m_v, \\
\frac{m}{V} &= \frac{m_d}{V} + \frac{m_v}{V}, \\
\rho &= \rho_d + \rho_v,
\end{aligned}
\tag{2.51}
$$

where ρ_v is the water vapor density. In itself, ρ_v is an index of water vapor concentration; in meteorology, it is called *the absolute humidity*. Using (2.26) with $M_v = 18.0153\,\mathrm{g\,mol^{-1}}$, we find that

$$
R_v = 461.5230\,\mathrm{J\,kg^{-1}\,K^{-1}}
\tag{2.52}
$$

is the gas constant for water vapor. From (2.22), the partial pressure of water vapor is

$$
e = \rho_v R_v T.
\tag{2.53}
$$

The *specific humidity* q is the same as the mass fraction for water vapor, c_v (see (2.29)) and is defined as

$$
q = \frac{\rho_v}{\rho}.
\tag{2.54}
$$

Again, in meteorology it is standard to use q and not c_v (the latter is also easy to confuse with the specific heat at constant volue, c_v, and will be avoided). Summing (2.46) and (2.53), one obtains

$$
\begin{aligned}
p &= (\rho_d R_d + \rho_v R_v)\,T \\
&= \rho \left(\frac{\rho_d}{\rho} R_d + \frac{\rho_v}{\rho} R_v \right) T \\
&= \rho R_d \left(\frac{\rho_d}{\rho} + \frac{\rho_v}{\rho} \frac{R_v}{R_d} \right) T \\
&= \rho R_d \left((1-q) + \frac{R_v}{R_d} q \right) T.
\end{aligned}
\tag{2.55}
$$

Replacing

$$
\begin{aligned}
\frac{R_v}{R_d} &= 1.608 \approx 1.61 \qquad \Rightarrow \\
p &= \rho R_d \underbrace{(1 + 0.61q) T}_{T_v}.
\end{aligned}
\tag{2.56}
$$

The *virtual temperature* T_v defined above is the temperature of a dry atmosphere with the same density ρ; it is slightly greater than T. A further index atmospheric moisture is the mixing ratio (more specifically, the mass ratio for water vapor). The mixing ratio was introduced in section 2.3; see (2.34)–(2.35). For water vapor, the (mass) mixing ratio is

$$
r_v = \frac{\rho_v}{\rho_d}.
\tag{2.57}
$$

Useful relations for the mixing ratio and specific humidity can be derived as follows:

$$r_v = \frac{\rho_v}{\rho_d} = \frac{\frac{e}{R_v T}}{\frac{(p-e)}{R_d T}}$$

$$= \frac{R_d}{R_v}\frac{e}{p-e} = 0.622\,\frac{e}{p-e}; \tag{2.58}$$

$$q = \frac{\rho_v}{\rho} = \frac{\frac{e}{R_v T}}{\rho_d + \rho_v}$$

$$= \frac{\frac{e}{R_v T}}{\frac{p-e}{R_d T} + \frac{e}{R_v T}}$$

$$= \frac{R_d}{R_v}\frac{e}{p + \left(\frac{R_d}{R_v} - 1\right)e}$$

$$= 0.622\frac{e}{p - 0.378e} \approx 0.622\frac{e}{p}. \tag{2.59}$$

The latent heat of evaporation of water, L, is the amount of energy used to change the phase of a unit of mass from liquid to vapor, in a pure mixture of the two phases. A good approximation for obtaining an expression for L as a function of temperature is the assumption that the heat capacities of the two phases are equal. This leads to (Adkins, 1983, Chap. 10, eq. 10.16)

$$dL = [c_{pv} - c_{pw}]dT \tag{2.60}$$

where c_{pv} and c_{pw} are the specific heats at constant pressure of water vapor and liquid water, respectively. If the specific heats, in turn, are assumed to be constant, we obtain

$$L = a_L + b_L T \tag{2.61}$$

with $b_L = [c_{pv} - c_{pw}]$. In the SI, with T in Kelvins, Dake (1972) gives

$$L = 3.142689 \times 10^6 - 2.365601 \times 10^3 T \tag{2.62}$$

in $J\,kg^{-1}$. Henderson-Sellers (1984) argues that a more accurate expression is

$$L = 1.91846 \times 10^6 \left[T/(T - 33.91)\right]^2. \tag{2.63}$$

A reasonable alternative is to use a constant value, given the very small variation of L with T. At $T = 288.15$ K, (2.62) gives $L = 2.464 \times 10^6\,J\,kg^{-1}$.

For a system composed of water vapor and liquid water in equilibrium, an equation can be derived relating the derivative with respect to temperature of the *saturation vapor pressure* e^* (the vapor pressure of the gas in equilibrium with the liquid water) to the change in specific volume v between the two phases and the latent heat, *viz.*

$$\frac{de^*}{dT} = \frac{L}{T\Delta v}; \tag{2.64}$$

it is the *Clausius-Clapeyron* equation (Adkins, 1983, Chap. 10, eq. (10.11)). Assuming the validity of the perfect-gas law, and that the specific volume of the liquid phase is negligible in comparison with that of the vapor phase, the Clausius-Clapeyron equation takes the form (Adkins, 1983, Chap. 10, eq. (10.12))

$$\frac{de^*}{dT} = \frac{Le^*}{R_v T^2}. \tag{2.65}$$

Note that Eqs. (2.61)– (2.62) can be used to integrate (2.65), yielding

$$e^*(T) = \left(\frac{T}{T_0}\right)^{\frac{b_L}{R_v}} e^*(T_0) \exp\left[\frac{a_L}{R_v}\left(\frac{1}{T_0} - \frac{1}{T}\right)\right], \qquad (2.66)$$

where T_0 is a reference temperature. With $b_L = 0$, (2.66) is the same as the equation proposed by Huang (2018), and bears a strong resemblance to (but is not the same as) Teten's empirical formula (Murray, 1966; Dilley, 1968; Stull, 1995; Alduchov and Eskridge, 1996):

$$e^*(T) = e_0 \exp\left[\frac{b(T - T_1)}{T - T_2}\right], \qquad (2.67)$$

with $e_0 = 610.78$ Pa, $b = 17.2693882\,\mathrm{K}^{-1}$, $T_1 = 273.16$ K and $T_2 = 35.86$ K. For ice, the constants change to $b = 21.8745584$ and $T_2 = 7.66$.

For most meteorological applications, Teten's formula is more than enough. Note however that the constants change for saturation vapor pressure over *ice*; also, note that the presence of salts in the water alters e^* significantly. Finally, Richards' equation (Brutsaert, 1982) is

$$e^*(T) = 101\,325 \exp\left[13.3185 t_r - 1.9760 t_r^2 - 0.6445 t_r^3 - 0.1299 t_r^4\right] \qquad (2.68)$$

$$\frac{de^*}{dT} = \frac{373.15}{T^2} e^*(T)\left[13.3185 - 3.9520 t_r - 1.9335 t_r^2 - 0.5996 t_r^3\right], \qquad (2.69)$$

$$t_r = 1 - \frac{373.15}{T}. \qquad (2.70)$$

The concept of saturation now allows for the definition of several humidity indices based on it. The *relative humidity* y is the ratio of the actual mixing ratio and the mixing ratio in water vapor saturated air at the same temperature and pressure:

$$y = \frac{r}{r^*}. \qquad (2.71)$$

Note that, because it is specified at the same temperature and pressure, the density of dry air in the saturated atmosphere (ρ_{d*}) is actually smaller than the density of dry air in the non-saturated atmosphere (ρ_d). The gas law equations are

$$p - e = \rho_d R_d T, \qquad\qquad e = \rho_v R_v T, \qquad (2.72)$$
$$p - e^* = \rho_{d*} R_d T, \qquad\qquad e^* = \rho_v^* R_v T. \qquad (2.73)$$

Therefore,

$$\begin{aligned}
y = \frac{r}{r^*} &= \frac{\frac{\rho_v}{\rho_d}}{\frac{\rho_v^*}{\rho_{d*}}} = \frac{\rho_{d*}}{\rho_d} \times \frac{\rho_v}{\rho_v^*} \\
&= \frac{\frac{p - e^*}{R_d T}}{\frac{p - e}{R_d T}} \times \frac{\frac{e}{R_v T}}{\frac{e^*}{R_v T}} \\
&= \frac{p - e^*}{p - e} \times \frac{e}{e^*} \\
&= \frac{p(1 - e^*/p)}{p(1 - e/p)} \times \frac{e}{e^*} \\
&\approx (1 - e^*/p)(1 + e/p)\frac{e}{e^*} \\
&\approx \frac{e}{e^*}. \qquad (2.74)
\end{aligned}$$

A

$e_a, \; \rho_v, \; T_a$

$e_a = \rho_v R_v T_a$

$y_a \approx \dfrac{e_a}{e_a^*}$

constant T

increase in water
vapor content

B

$e_a^*, \; \rho_{va}^*, \; T_a$

$e_a^* = \rho_{va}^* R_v T_a$

$y_a = 100\%$

A

$e_a, \; \rho_v, \; T_a$

$e_a = \rho_v R_v T_a$

$y_a \approx \dfrac{e_a}{e_a^*}$

constant e

heat removal;
temperature
reduction

C

$e_a, \; \rho_{vd}^*, \; T_d$

$e_d^* = \rho_{vd}^* R_v T_d$

$y_a = 100\%$

$e_a = e_d^*$
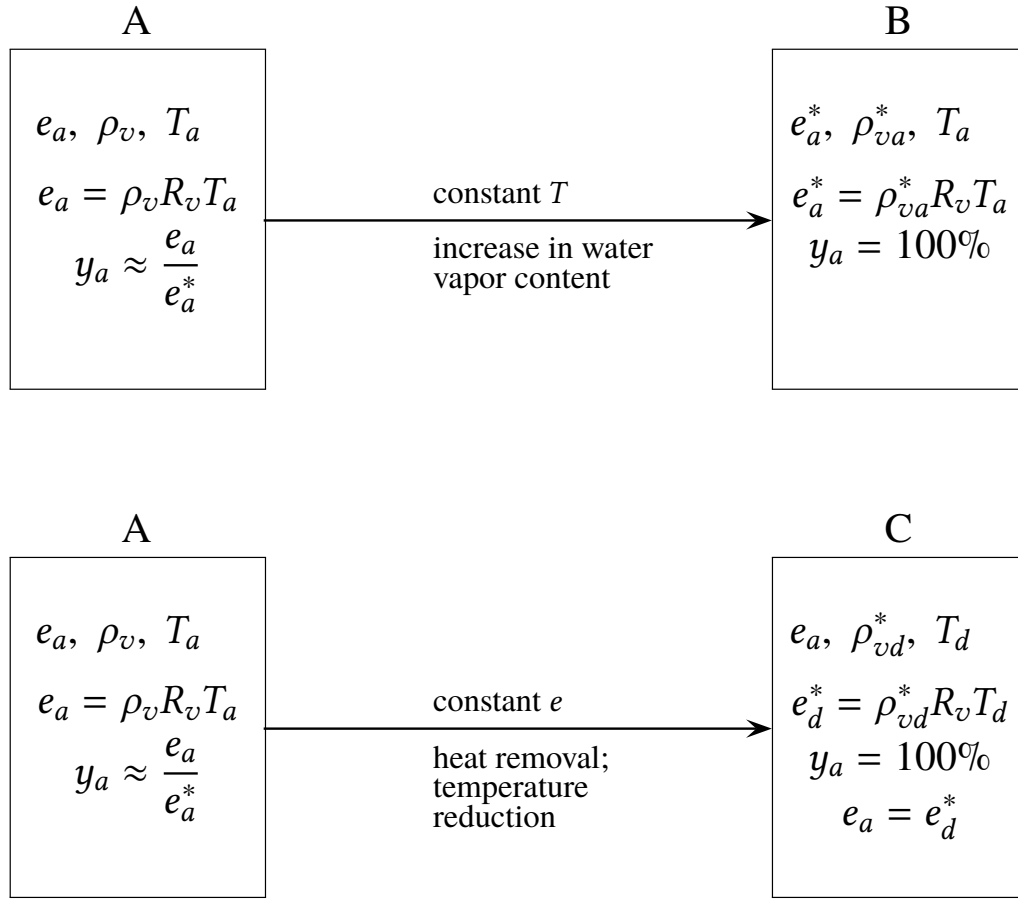
Figure 2.1: The concepts of atmospheric saturation, relative humidity and dew-point. Adapted from Dias (1986).

The last form, (2.74), is the one commonly used in calculations, but see Problem 2.7.

The *dewpoint temperature* T_d is the temperature at which the water vapor pressure in the air becomes the saturated vapor pressure:

$$e^*(T_d) = e_a. \tag{2.75}$$

Usually, temperature varies with height in the atmospheric boundary layer. A subscript like T_x or e_x will often be used to specify temperature, water vapor pressure, etc., at some specified level. Also, we will often use the simplified notation

$$e_x^* = e^*(T_x), \tag{2.76}$$

$$d_x = \frac{\mathrm{d}e^*(T_x)}{\mathrm{d}T}, \tag{2.77}$$

$$\rho_{vx}^* = \rho_v^*(T_x). \tag{2.78}$$

In figure 2.1, we show in frame A the prevailing conditions in the atmosphere. In frame B, saturation is reached, from A, through an increase in water vapor content. In frame C, saturation conditions are also reached, but this time through a continuous drop in temperature down to the dew point temperature T_d.

Exercises

2.6 Show that after the isothermal addition of water vapor, the partial volume of the dry constituents will be $V_d < V$.

2.7 Show that the *exact* expression for e as a function of y also depends on p and is

$$e = \frac{ye^*}{1 + (y - 1)\frac{e^*}{p}}.$$

Of course, e^* itself is a function of temperature.

Let us now build an example moist atmosphere. We follow from section 2.4, where we assumed an initally dry atmosphere with molar fractions given by table 2.1 and total pressure p_d, to which water vapor is added isothermally, raising the total pressure by e to p, while the partial pressures of the dry components remain unaltered. We will assume a total pressure $p = 100\,000$ Pa, an air temperature $T = 20\,°\text{C} = 293.15$ K, and a relative humidty $y = 0.70$. The exact vapor pressure (Problem 2.7) is then $e = 1647.6712$ Pa, and $p_d = p - e = 98\,352.3288$ Pa.

The molar fractions of the *dry components* for the moist atmosphere are now

$$x_i = \frac{p_i}{p} = \frac{p_i}{p_d} \times \frac{p_d}{p} = x_{di}\frac{p_d}{p}, \qquad i \neq v, \tag{2.79}$$

where the x_{di} are the same as the x_i in a dry atmosphere from table 2.1. The molar fraction of water vapor is

$$x_v = \frac{e}{p}. \tag{2.80}$$

The densities are obtained from (2.21) and (2.22). From there, mass concentrations (or mass fractions) c_i, mixing ratios r_i and dry mixing ratios r_{di} are obtained from (2.29), (2.36) and (2.44).

The results are given in table 2.2. The table is ordered by x_i. We can see that H_2O is the third most abundant element, followed by Ar. Note the drastic progressive density reduction of the greenhouse gases H_2O, CO_2, CH_4 and N_2O. All gases after the first four in the table are referred to as *trace gases*. Note how the molar fractions and the mass concentrations add up to 1, but not the mixing ratio and the dry mixing ratio. Also note that, except for N_2 and O_2, the difference betwen c_i, r_i and r_{di} is very small.

What table 2.2 reveals is that the measurement of CO_2 is much more difficult than the measurement of H_2O; similarly, CH_4 measurement is harder than CO_2's, and so on, by the simple fact that it is necessary to measure increasingly smaller concentrations. Although this is possible in controlled laboratory conditions with various types of chemical analyzers, *in situ* measurements, necessary to obtain continuous data series, are substantially more difficult. Thus, the task of measuring fluxes and performing greenhouse gas material balances is also extraordinarily hard, and one of its greatest scientific challenges is still the obtention of accurate error estimates.

Table 2.2: Constitution of an example moist atmosphere.

Gas	M_i (g mol^{-1})	x_i (mol mol^{-1})	ρ_i (kg m^{-3})	c_i (kg kg^{-1})	r_i (kg kg^{-1})	r_{di} (kg kg^{-1})
N_2	28.0134	0.76792220	0.88258991	0.74732474	2.95764908	3.08348888
O_2	31.9988	0.20598125	0.27041906	0.22897480	0.29697448	0.30100013
H_2O	18.0153	0.01647671	0.01217834	0.01031189	0.01041934	—
Ar	39.948	0.00918611	0.01505575	0.01274832	0.01291294	0.01304924
CO_2	44.0095	0.00040708	0.00073503	0.00062238	0.00062276	0.00062926
Ne	20.1797	0.00001788	0.00001480	0.00001253	0.00001254	0.00001267
He	4.002602	0.00000515	0.00000085	0.00000072	0.00000072	0.00000072
CH_4	16.0425	0.00000167	0.00000110	0.00000093	0.00000093	0.00000094
Kr	83.798	0.00000108	0.00000372	0.00000315	0.00000315	0.00000318
H_2	2.01588	0.00000054	0.00000004	0.00000004	0.00000004	0.00000004
N_2O	44.0128	0.00000032	0.00000059	0.00000050	0.00000050	0.00000050
Air	28.785494	1.00000000	1.18099919	1.00000000	—	—

2.5 – Potential temperature

Consider the adiabatic expansion of a parcel of air, from a level (higher up) where the ambient pressure is p down to a level where the ambient pressure is p_0. The first law of thermodynamics is (q is heat per unit mass added to the system; w is work per unit mass performed on the system)

$$\mathrm{d}u = \text{đ}q + \text{đ}w;$$

For an adiabatic ($\text{đ}q = 0$) and reversible process,

$$\mathrm{d}u = -p\mathrm{d}v \tag{2.81}$$

Differentiation of (2.14) and use of (2.12) (keeping in mind that $u = u(T)$ for a perfect gas) produce

$$p\mathrm{d}v + v\mathrm{d}p = R\mathrm{d}T$$
$$c_v\mathrm{d}T = v\mathrm{d}p - R\mathrm{d}T$$
$$(c_v + R)\mathrm{d}T = v\mathrm{d}p = \frac{RT}{p}\mathrm{d}p$$
$$c_p\mathrm{d}T = v\mathrm{d}p = \frac{RT}{p}\mathrm{d}p \tag{2.82}$$
$$\frac{\mathrm{d}T}{T} = \frac{R}{c_p}\frac{\mathrm{d}p}{p}. \tag{2.83}$$

We now integrate between the temperature-pressure pairs (T, p) and (θ, p_0):

$$\theta = T\left(\frac{p_0}{p}\right)^{\frac{R}{c_p}}. \tag{2.84}$$

The potential temperature θ, defined above, is therefore the temperature of a parcel of air brought adiabatically and reversibly from state p, T to a reference pressure p_0.

Equation (2.84) needs to be used with the correct value of R/c_p in the case of moist air. This is because in this case the effective gas constant and the effective specific heat at constant pressure for moist air depend on the specific humidity q. To see this, suppose that the total enthalpy (not the *specific enthalpy*) for a parcel of air with total mass m can be calculated by adding the enthalpies of dry and moist air:

$$m\hbar = m_d \hbar_d + m_v \hbar_v.$$

This produces

$$\hbar = \frac{\rho_d}{\rho}\hbar_d + \frac{\rho_v}{\rho}\hbar_v,$$

$$\hbar = (1-q)\hbar_d + q\hbar_v,$$

$$c_p = \left(\frac{\partial \hbar}{\partial T}\right)_p = (1-q)c_{pd} + qc_{pv} = (1 + 0.84q)c_{pd} \tag{2.85}$$

(using tabulated values for c_{pd} and c_{pv}).

On the basis of (2.56), the effective gas constant for moist air can be written as

$$R = R_d(1 + 0.61q) \tag{2.86}$$

(note that this is an alternative interpretation to (2.56): we are now changing the gas constant R, and keeping the absolute temperature T, so that 2.14 still applies.) Therefore,

$$\frac{R}{c_p} = \frac{R_d}{c_{pd}}\frac{1 + 0.61q}{1 + 0.84q}. \tag{2.87}$$

Using the identity

$$\frac{1 + ax}{1 + bx} \equiv 1 - (b-a)x + \frac{(b-a)bx^2}{1 + bx} \approx 1 - (b-a)x, \tag{2.88}$$

we find (for small $x = q$)

$$\frac{R}{c_p} \approx (1 - 0.23q)\frac{R_d}{c_{pd}} \tag{2.89}$$

for moist air. Therefore,

$$\theta = T\left(\frac{p_0}{p}\right)^{(1-0.23q)\frac{R_d}{c_{pd}}} \tag{2.90}$$

It is also straightforward to obtain the specific heat at constant volume for moist air:

$$c_v = \left(\frac{\partial u}{\partial T}\right)_v = (1-q)c_{vd} + qc_{vv} \tag{2.91}$$

Finally, these definitions extend to virtual temperature, *but not uniquely*, as discussed by Brutsaert (1982, section 3.2b). The *virtual potential temperature* is the virtual temperature that a parcel of moist air would have if changed adiabatically from its actual state to the standard pressure p_0:

$$\theta_{vp} = T_v\left(\frac{p_0}{p}\right)^{(1-0.23q)\frac{R_d}{c_{pd}}}. \tag{2.92}$$

This is slightly different from *potential virtual temperature*, which is the potential temperature of dry air at the same initial pressure and density, and which is given by

$$\theta_{pv} = T_v \left(\frac{p_0}{p} \right)^{\frac{R_d}{c_{pd}}} . \tag{2.93}$$

The two quantities defined by (2.92) and (2.93) are, evidently, numerically very similar. From here on, we will always use the virtual potential temperature (2.92). Also, for simplicity, we will refer to it simply as θ_v.

3

The dynamical equations for the ABL

The transport equations express the principles of conservation of total mass, momentum, energy and mass of a mixed substance (for instance water vapor) at a point in space and instant in time. In principle, any fluid mechanics problem can be solved if we know the constitutive equation (the rate of strain – stress relation) and the boundary conditions.

In practice, the problem is much more complicated. The momentum equations are non-linear, making the solution (either analytical or numerical) much more difficult. Morever, they display chaotic behavior, which causes very small differences in the boundary conditions to amplify very fast (Ruelle, 1994). Finally, their full solution requires the resolution of extremely small scales (the Kolmogorov microscales), rendering the problem impossible to solve on the basis of the fundamental equations alone, and requiring additional hypothesis regarding their closure at some level: this is the well known turbulence closure problem (Wyngaard, 1981).

3.1 – Differential operators

It is convenient to adopt a double notation for the position and velocity vectors, and the basis for $\mathbb{R}^3$, *viz.*

$$\boldsymbol{x} = (x, y, z) \equiv (x_1, x_2, x_3), \tag{3.1}$$

$$\boldsymbol{u} = (u, v, w) \equiv (u_1, u_2, u_3), \tag{3.2}$$

$$(\boldsymbol{i}, \boldsymbol{j}, \boldsymbol{k}) \equiv (\boldsymbol{e}_1, \boldsymbol{e}_2, \boldsymbol{e}_3). \tag{3.3}$$

The equations of fluid mechanics involve four differential operators: the divergence, the curl, the laplacian, and the operator for the material derivative. They are:

$$\boldsymbol{\nabla} \cdot \boldsymbol{u} = \frac{\partial u}{\partial x} + \frac{\partial v}{\partial y} + \frac{\partial w}{\partial z}$$

$$= \sum_{k=1}^{3} \frac{\partial u_k}{\partial x_k}; \tag{3.4}$$

$$\nabla \times \boldsymbol{u} = \left(\frac{\partial w}{\partial y} - \frac{\partial v}{\partial z}\right)\boldsymbol{i} + \left(\frac{\partial u}{\partial z} - \frac{\partial w}{\partial x}\right)\boldsymbol{j} + \left(\frac{\partial v}{\partial x} - \frac{\partial u}{\partial y}\right)\boldsymbol{k}$$

$$= \sum_{k=1}^{3}\sum_{i=1}^{3}\sum_{j=1}^{3} \epsilon_{ijk}\frac{\partial u_j}{\partial x_i}\boldsymbol{e}_k; \tag{3.5}$$

$$\nabla^2 a = \frac{\partial^2 a}{\partial x \partial x} + \frac{\partial^2 a}{\partial y \partial y} + \frac{\partial^2 a}{\partial z \partial z}$$

$$= \sum_{k=1}^{3}\frac{\partial^2 a}{\partial x_k \partial x_k}; \tag{3.6}$$

$$\frac{Da}{Dt} = \frac{\partial a}{\partial t} + u\frac{\partial a}{\partial x} + v\frac{\partial a}{\partial y} + w\frac{\partial a}{\partial z}$$

$$= \frac{\partial a}{\partial t} + \sum_{k=1}^{3} u_k\frac{\partial a}{\partial x_k}, \tag{3.7}$$

where a represents any scalar field and ∇ is the "symbolic" vector $(\frac{\partial}{\partial x}, \frac{\partial}{\partial y}, \frac{\partial}{\partial z})$. The first line in each of the equations above gives the formula for each operator in x, y, and z notation. The second line shows that all operators can be written in a compact form as sums. For the curl, the permutation symbol $\epsilon_{ijk} = +1$ for cyclic permutations (1,2,3), (2,3,1), (3,1,2); $\epsilon_{ijk} = -1$ for anti-cyclic permutations (1,3,2), (2,1,3), (3,1,2); and $\epsilon_{ijk} = 0$ if $i = j$, $j = k$, $k = i$ or $i = j = k$.

In the equations that follow, we will adopt most of the time the compact sum notation. In particular cases, it will be more frutiful to shift back to the notation involving (x, y, z) and (u, v, w).

3.2 – The hydrostatic reference state

Consider again the first law for an adiabatic atmosphere, as in 2.82, repeated here,

$$c_p \mathrm{d}T_r = v_r \mathrm{d}p_r, \tag{3.8}$$

together with the hydrostatic equation

$$\frac{\mathrm{d}p_r}{\mathrm{d}z} = -\rho_r g. \tag{3.9}$$

Above, the subscript r means the reference state for a hydrostatic equation. Together with the state equation (2.14), equations (3.8)–(3.9) form a system from which we can eliminate either T_r, p_r or $v_r = 1/\rho_r$. Three equations result for the reference pressure, temperature or density as a function of z (bear in mind that in a moist atmosphere c_p, c_v and R are given by 2.85, (2.91) and 2.86 respectively):

$$T_r(z) = T_0 - \frac{g}{c_p}z, \tag{3.10}$$

$$p_r(z) = p_0 \left(\frac{T_0 - \frac{g}{c_p}z}{T_0}\right)^{c_p/R}, \tag{3.11}$$

$$\rho_r(z) = \rho_0 \left(\frac{T_0 - \frac{g}{c_p}z}{T_0}\right)^{c_v/R}. \tag{3.12}$$
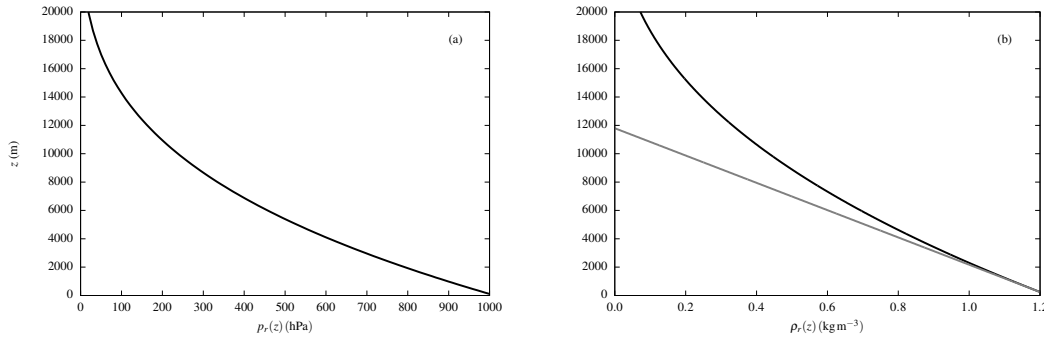
Figure 3.1: Reference pressure p_r and density ρ_r in a hydrostatic and adiabatic equation.

Figure 3.1 shows the pressure and density reference states in the atmosphere as functions of z, for $T_0 = 15\,°\mathrm{C}$ and $p_0 = 101\,325\,\mathrm{Pa}$. The *scale height* is defined as

$$D = \left| \frac{1}{\rho_0} \frac{\mathrm{d}\rho_r(0)}{\mathrm{d}z} \right|^{-1} ; \tag{3.13}$$

it is obtained by extrapolating the straight line with the same slope as the reference density profile at the surface up to $\rho_r = 0$, as seen in figure 3.1-b.

3.3 – Reynolds's decomposition and averaging

The Reynolds decomposition for turbulent flows

The Reynolds decomposition is the formal proceedure by which we decompose any variable a measured in the atmosphere into its average $\overline{a}$ and its turbulent fluctuation a'. The Reynolds decomposition consists of writing

$$a = \overline{a} + a', \tag{3.14}$$

but the subsequent manipulation of $\overline{a}$ and a' in the Navier-Stokes equation and the transport equation for a gas χ depends on the precise definition of the average.

Ensemble averages

We will adopt here a variation of Kundu (1990)'s approach to calculate ensemble averages. In this approach, the realizations k of a random variable a, $a^{(k)}(x, y, z, t)$, are seen as a four-dimensional stochastic process. The realizations are considered in a countable, possibly infinite, sample space. The probability of realization k is p_k (in this context, we see no danger of confusing p_k with "pressure"). The ensemble average of $a(x, y, z, t)$ is defined as

$$\overline{a}(x, y, z, t) \equiv \sum_{k=1}^{\infty} a^{(k)}(x, y, z, t) p_k. \tag{3.15}$$

The fluctuation a' (that is also an stochastic process) is thence defined by (3.14). In turbulence, *we do not adopt the usual notation of writing uppercase letters for random variables*: the nature of the variables must be understood from the context or made explicit by the author.

When the stochastic process is stationary, the left side of (3.15) is reduced to $\overline{a}(x, y, z)$; if moreover the process is horizontally homogeneous, the dependence is reduced yet to $\overline{a}(z)$.

Having (3.15), it is possible now to prove the so-called Reynolds's postulates (that in this context should be properly called Reynolds's Theorems or, even better, Reynolds's Lemmas). They are:

$$\overline{\overline{a}(x, y, z, t)} = \sum_{k=1}^{\infty} \overline{a}(x, y, z, t)p_k$$

$$= \overline{a}(x, y, z, t) \underbrace{\left[\sum_{k=1}^{\infty} p_k\right]}_{=1}$$

$$= \overline{a}(x, y, z, t); \tag{3.16}$$

$$\overline{a'(x, y, z, t)} = \sum_{k=1}^{\infty} \left[a^{(k)}(x, y, z, t) - \overline{a}(x, y, z, t)\right] p_k$$

$$= \sum_{k=1}^{\infty} a^{(k)}(x, y, z, t)p_k - \overline{a}(x, y, z, t) \sum_{k=1}^{\infty} p_k$$

$$= \overline{a}(x, y, z, t) - \overline{a}(x, y, z, t) = 0; \tag{3.17}$$

$$\overline{\overline{a}(x, y, z, t)b'(x, y, z, t)} = \sum_{k=1}^{\infty} \overline{a}(x, y, z, t) \left[b^{(k)}(x, y, z, t) - \overline{b}(x, y, z, t)\right] p_k$$

$$= \overline{a}(x, y, z, t) \sum_{k=1}^{\infty} b^{(k)}(x, y, z, t)p_k$$

$$- [\overline{a}(x, y, z, t)] \left[\overline{b}(x, y, z, t)\right] \sum_{k=1}^{\infty} p_k$$

$$= [\overline{a}(x, y, z, t)] \left[\overline{b}(x, y, z, t)\right]$$

$$- [\overline{a}(x, y, z, t)] \left[\overline{b}(x, y, z, t)\right] = 0; \tag{3.18}$$

$$\overline{\frac{\partial a}{\partial x}} = \sum_{k=1}^{\infty} \frac{\partial a^{(k)}}{\partial x} p_k$$

$$= \frac{\partial}{\partial x} \sum_{k=1}^{\infty} a^{(k)}(x, y, z, t)p_k$$

$$= \frac{\partial \overline{a}}{\partial x}. \tag{3.19}$$

The last equation, (3.19), tells us that the partial derivatives commute with the ensemble average. Identical results hold, obviously, for any other independent variable than x.

3.4 – Mass conservation and the Boussinesq approximation

The derivation of the transport equations for u, v, w, θ, q, θ_v, ... is a long process involving a fair amount of physics and mathematics. It can be found in various texts, such as Batchelor (1967), Bird et al. (1960) and Landau and Lifshitz (1959). An excellent itroduction to the equations in a form often used in the ABL is Stull (1988)'s book.

We will briefly analyze the dynamical equations in light of the *Boussinesq approximation*. First we define a thickness ℓ such that the reference density changes little between $z = 0$ and $z = \ell$. From figure 3.1-b, it can be seen that

$$\frac{\Delta \rho_r}{\rho_0} \leq \frac{\ell}{D} \equiv \epsilon_b \ll 1, \tag{3.20}$$

where $\rho_0 = \rho_r(0)$. In (3.20), we use any appropriately small value of ϵ_b (say $\epsilon_b = 0.01$), to define ℓ rigorously.

Next we define the *Boussinesq decompositions*

$$u_i = 0 + u_{\delta i}, \tag{3.21}$$
$$\rho = \rho_r + \rho_\delta, \tag{3.22}$$
$$p = p_r + p_\delta, \tag{3.23}$$
$$T = T_r + T_\delta. \tag{3.24}$$

Above, u_δ, ρ_δ, p_δ and T_δ are the fluctuations of velocity, density, pressure, and temperature of an actual ("dynamic") atmosphere with respect to the reference hydrostatic state.

Of course, (3.21)–(3.24) can be further expanded by means of a Reynolds' decomposition, yielding

$$\overline{u_i} + u_i' = \overline{u_{\delta i}} + u_{\delta i}', \tag{3.25}$$
$$\overline{\rho} + \rho' = \rho_r + \overline{\rho_\delta} + \rho_\delta', \tag{3.26}$$
$$\overline{p} + p' = p_r + \overline{p_\delta} + p_\delta', \tag{3.27}$$
$$\overline{T} + T' = T_r + \overline{T_\delta} + T_\delta'. \tag{3.28}$$

Then, the following relations hold (trivially) between the Reynolds decomposition and the Boussinesq decomposition:

$$\overline{u_i} = \overline{u_{\delta i}} \qquad\qquad u_i' = u_{\delta i}', \tag{3.29}$$
$$\overline{\rho} = \rho_r + \overline{\rho_\delta} \qquad\qquad \rho' = \rho_\delta', \tag{3.30}$$
$$\overline{p} = p_r + \overline{p_\delta} \qquad\qquad p' = p_\delta', \tag{3.31}$$
$$\overline{T} = T_r + \overline{T_\delta} \qquad\qquad T' = T_\delta', \tag{3.32}$$

whence

$$u_i = 0 + \overline{u_{\delta i}} + u', \tag{3.33}$$
$$\rho = \rho_r + \overline{\rho_\delta} + \rho', \tag{3.34}$$
$$p = p_r + \overline{p_\delta} + p', \tag{3.35}$$
$$T = T_r + \overline{T_\delta} + T'. \tag{3.36}$$

Clearly, the notations $\overline{u_{\delta i}}$ and $u'_{\delta i}$, ρ'_δ, p'_δ and T'_δ in (3.29)–(3.32) are excessive, and will not be used any further.

Only now we introduce the Boussinesq approximation proper: it is the assumption that the dynamic density fluctuations ρ_δ are of the same order of magnitude of the variation of the reference density ρ_r within the layer of thickness ℓ. In view of the definition of D in (3.13) and (3.20), it is

$$\rho_\delta \sim \rho_0 \frac{\ell}{D} \ll \rho_r, \qquad 0 \leq z \leq \ell. \tag{3.37}$$

Now consider the full form for the equation for (total) mass conservation, which reads

$$\frac{\partial \rho}{\partial t} + \sum_{k=1}^{3} \frac{\partial(\rho u_k)}{\partial x_k} = 0. \tag{3.38}$$

Its ensemble average is

$$\frac{\partial \overline{\rho}}{\partial t} + \sum_{k=1}^{3} \frac{\partial \overline{\rho u_k}}{\partial x_k} = 0. \tag{3.39}$$

Expanding all terms with the help of (3.33)–(3.36) and Reynolds' postulates (3.16)–(3.19),

$$\underbrace{\frac{\partial \overline{\rho_\delta}}{\partial t}}_{\text{I}} + \underbrace{\sum_{k=1}^{3} \overline{u_k} \frac{\partial \rho_r}{\partial x_k}}_{\text{II}} + \underbrace{\sum_{k=1}^{3} \overline{u_k} \frac{\partial \overline{\rho_\delta}}{\partial x_k}}_{\text{III}} + \underbrace{\sum_{k=1}^{3} \rho_r \frac{\partial \overline{u_k}}{\partial x_k}}_{\text{IV}} + \underbrace{\sum_{k=1}^{3} \overline{\rho_\delta} \frac{\partial \overline{u_k}}{\partial x_k}}_{\text{V}} + \underbrace{\sum_{k=1}^{3} \frac{\partial \overline{\rho' u'_k}}{\partial x_k}}_{\text{VI}} = 0. \tag{3.40}$$

The order of magnitude of each individual term in the sums above can be established relatively easily. For that, we need to define in some useful way a density scale $\tilde{\rho}$ and a velocity scale $\tilde{u}$. Due to (3.34) and (3.37), we will define

$$\tilde{\rho} \sim \overline{\rho_\delta} \sim \rho', \tag{3.41}$$

and

$$\tilde{u} \sim \overline{u_k}; \qquad \tilde{\rho}\tilde{u} \sim \overline{\rho' u'_k}. \tag{3.42}$$

With that, one finds

$$\text{I} \sim \frac{\tilde{\rho}\tilde{u}}{\ell};$$

$$\text{II} \sim \frac{\rho_0 \tilde{u}}{D} \sim \frac{\tilde{\rho}\tilde{u}}{\ell};$$

$$\text{III} \sim \frac{\tilde{\rho}\tilde{u}}{\ell};$$

$$\text{IV} \sim \frac{\rho_0 \tilde{u}}{\ell};$$

$$\text{V} \sim \frac{\tilde{\rho}\tilde{u}}{\ell};$$

$$\text{VI} \sim \frac{\tilde{\rho}\tilde{u}}{\ell}.$$

The upshot is that all individual terms in I–III, and V–VI, are much smaller than the individual terms in IV. The *sum* of all three terms in IV must be of the same order of the other terms, whence

$$\sum_{k=1}^{3} \frac{\partial \overline{u_k}}{\partial x_k} \sim \frac{\tilde{\rho}}{\rho_0} \frac{\tilde{u}}{\ell} \ll \frac{\tilde{u}}{\ell} \implies \sum_{k=1}^{3} \frac{\partial \overline{u_k}}{\partial x_k} \approx 0. \tag{3.43}$$

Equation (3.43) is often first found in fluid mechanics in the context of mass conservation in an incompressible flow. Here, it is only *approximately valid* (we are in the context of the Boussinesq *approximation*); it is valid (at this point) for the mean velocity field $\overline{u}$ only; and *it does not mean that there are no density fluctuations*.

The same approach can be taken for the full momentum equation, which is (for a Newtonian fluid)

$$\left[\frac{\partial(\rho u_i)}{\partial t} + \sum_{k=1}^{3} \frac{\partial(\rho u_i u_k)}{\partial x_k} + \sum_{k=1}^{3} \sum_{j=1}^{3} 2\epsilon_{ijk}\Omega_j u_k \right] = \rho g_i - \frac{\partial p}{\partial x_i} + $$
$$\frac{\partial}{\partial x_i} \left(\lambda \sum_{k=1}^{3} \frac{\partial u_k}{\partial x_k} \right) + \nu\rho \sum_{k=1}^{3} \frac{\partial s_{ik}}{\partial x_k}, \qquad i = 1,\dots,3, \tag{3.44}$$

where Ω is the angular velocity of the Earth; $\sum_{k=1}^{3} \sum_{j=1}^{3} 2\epsilon_{ijk}\Omega_j u_k$ is the Corilis acceleration along x_i; $g = (0, 0, -g)$ is the accelration of gravity, and ν is the kinematic viscosity. Expanding and estimating orders of magnitude for (3.44) however, is now a lengthy and somewhat tedious procedure. Perhaps the most revealing part is the effect that the Boussinesq decomposition has on the gravity and pressure terms:

$$\rho g_i - \frac{\partial p}{\partial x_i} = (\rho_r + \rho_\delta)g_i - \frac{\partial(p_r + p_\delta)}{\partial x_i}$$
$$= \rho_\delta g_i - \frac{\partial p_\delta}{\partial x_i}, \tag{3.45}$$

in view of the hydrostatic equation (3.9). Equation (3.45) shows very clearly that an important part of the acceleration in the fluid is caused by the differences in bouyancy caused *Boussinesq fluctuations* in density, ρ_δ.

If one now proceeds with the Boussinesq and Reynolds decomposition for the momentum equation, followed by averaging and simplification with (3.38) (which we omit, but encourage the reader to undertake!), the final result is

$$\rho_r \left[\frac{\partial \overline{u_i}}{\partial t} + \overline{u_k} \frac{\partial \overline{u_i}}{\partial x_k} + \frac{\partial \overline{u_i' u_k'}}{\partial x_k} \right] - \left[\overline{\rho_\delta} g_i - \frac{\partial \overline{p_\delta}}{\partial x_i} \right] \sim \frac{\tilde{\rho}\tilde{u}^2}{\ell}. \tag{3.46}$$

Each of the individual terms above can be shown to be $\sim \rho_0 \tilde{u}^2/\ell$. The Coriolis terms, which do not appear above, are of the order of $\rho_0 \tilde{u}^2/(\text{Ro}\ell)$ (where Ro $= \tilde{u}/(f\ell)$ is the Rossby number, and $f = 2\Omega\sin(\phi)$ is the Coriolis parameter, and ϕ is the latitude). At the scale of the flow, ℓ, the Rossby number is very large and consequently Coriolis effects are negligible. For the left-hand side of (3.46),

therefore, one has

$$g\tilde{\rho} \sim \rho_0 \frac{\tilde{u}^2}{\ell}, \tag{3.47}$$

$$\frac{\tilde{p}}{\ell} \sim \rho_0 \frac{\tilde{u}^2}{\ell} \quad \Rightarrow \tag{3.48}$$

$$\tilde{p} \sim \tilde{\rho} g \ell. \tag{3.49}$$

Pressure fluctuations are extremely difficult to measure in the atmosphere. Wyngaard (2010) gives the estimate $p' \sim \rho_0 \tilde{u}^2$; this is the same as (3.48). Hauf et al. (1996) observed values of p' of the order of 2.5 Pa, which again is the same order as given by Wyngaard. The main consequence of (3.49) is that the effects of the pressure fluctuations p_δ and p' can often be neglected in the atmosphere.

The order of magnitude of the Boussinesq pressure fluctuations now leads to the following approximation in the state equation:

$$p = \rho R_d T_v,$$
$$[p_r + p_\delta] = [\rho_r + \rho_\delta] R_d [T_{vr} + T_{v\delta}],$$
$$p_r + p_\delta \approx \rho_r R_d T_{vr} + \rho_r R_d T_{v\delta} + \rho_\delta R_d T_{vr},$$

where the product $\rho_\delta R_d T_{v\delta}$ has been neglected. By definition, the equation of state, $p_r = \rho_r R_d T_{vr}$ holds for the hydrostatic reference state; therefore,

$$p_\delta \approx \rho_r R_d T_{v\delta} + \rho_\delta R_d T_{vr},$$
$$\underbrace{\frac{p_\delta}{p_r}}_{\sim \frac{\tilde{p}}{p_0}} \approx \underbrace{\frac{T_{v\delta}}{T_{vr}}}_{\sim \frac{\tilde{T}}{T_0}} + \underbrace{\frac{\rho_\delta}{\rho_r}}_{\sim \frac{\tilde{\rho}}{\rho_0}}$$

But

$$\frac{\tilde{\rho}}{\rho_0} \sim \epsilon_b = 0.01 \qquad \text{by definition,}$$
$$\frac{\tilde{p}}{p_0} \sim \frac{2.5}{101\,325} = 2.47 \times 10^{-5} \ll 0.01.$$

Therefore, the Boussinesq pressure fluctuations can be safely dismissed. This leads to a much simpler linear equation of state that does not include pressure, namely

$$\frac{\rho_\delta}{\rho_r} = -\frac{T_{v\delta}}{T_r}. \tag{3.50}$$

Finally, there are the scalar transport equations. Interestingly, they are subsumed by the momentum equation (3.44), if a special notation is assumed. We start letting the indices i of u_i assume values greater than 3, one for each scalar, namely

$$u_4 = \theta, \qquad u_5 = q, \qquad u_6 = \theta_v, \qquad u_7 = c, \tag{3.51}$$

etc.. We must also keep the sums over k up to 3 only, naturally, and specify that

$$\frac{\partial}{\partial x_i} = 0, \qquad i > 3; \tag{3.52}$$

$$g_i = 0, \qquad i > 3. \tag{3.53}$$

Finally, the kinematic viscosity v must be replaced by the corresponding molecular diffusivity for heat of mass, *viz.*

$$v_\theta, \qquad v_q, \qquad v_{\theta_v}, \qquad v_c.$$

The case for the transport equation for the virtual temperature is rather obscure: it is not clear if there is such a thing as a molecular diffusivity v_{θ_v} for θ_v, but we will assume there is, purely for notational convenience.

Then, for $i > 3$, (3.44) simplifies (with the help of the continuity equation!) to

$$\frac{\partial u_i}{\partial t} + \sum_{k=1}^{3} u_k \frac{\partial u_i}{\partial x_k} = v_{u_i} \sum_{k=1}^{3} \frac{\partial^2 u_i}{\partial x_k \partial x_k}. \tag{3.54}$$

This is correct. For example, for temperature the transport equation reads

$$\frac{\partial \theta}{\partial t} + \sum_{k=1}^{3} u_k \frac{\partial \theta}{\partial x_k} = v_\theta \sum_{k=1}^{3} \frac{\partial^2 \theta}{\partial x_k \partial x_k}. \tag{3.55}$$

Exercise

3.1 Using Reynolds' decomposition (3.14) and Reynolds' postulates (3.16)–(3.19), show that

$$\frac{\overline{\rho_\delta}}{\rho_r} = -\frac{\overline{T_{v\delta}}}{T_r},$$

$$\frac{\rho'}{\rho_r} = -\frac{T_v'}{T_r}.$$

3.5 – The Reynolds-averaged Navier-Stokes equations

Under the validity of the Boussinesq approximation (3.37), the mass and momentum conservation equations (3.43) and (3.46) are correct to order ϵ_b. We are unaware of works that deal with the extension of the Boussinesq approximation to the higher-order, second-moment equations that are essential to understand the mechanics of turbulent flow, and which were introduced by O. Reynolds in 1895 (Reynolds, 1895). We will however *assume* that the equations for the turbulent fluctuations of velocity and other quantities are analogous to (3.43) and (3.46) for the means.

Under these further assumptions, application of Reynolds' decomposition (3.14) to the mass and momentum equations (3.38) and (3.44), and subtraction of the equations for means,(3.43) and (3.46), eventually results in

$$\sum_{k=1}^{3} \frac{\partial u_k'}{\partial x_k} = 0 \tag{3.56}$$

$$\frac{\partial u_i'}{\partial t} + \sum_{k=1}^{3} \overline{u_k} \frac{\partial u_i'}{\partial x_k} = \sum_{k=1}^{3} \left[-u_k' \frac{\partial \overline{u_i}}{\partial x_k} - \frac{\partial u_i' u_k'}{\partial x_k} + \frac{\partial \overline{u_i' u_k'}}{\partial x_k} \right] - \sum_{j=1}^{3} \sum_{k=1}^{3} 2\epsilon_{ijk} \Omega_j u_k'$$

$$- \frac{1}{\overline{\rho}} \frac{\partial p'}{\partial x_i} - \frac{g_i}{\overline{\theta_v}} \theta_v' + 2v \sum_{k=1}^{3} \frac{\partial s_{ik}'}{\partial x_k}, \tag{3.57}$$

where $\boldsymbol{g} = (0, 0, -g)$ with $g = 9.81\,\mathrm{m\,s^{-2}}$. Note that the average of (3.56) and (3.57) above is zero. Multiplication of (3.57) by u'_j, exchange of the indices i and j and summation of the two resulting equations, followed by averaging, leads the the second-order equations

$$
\underbrace{\frac{\partial \overline{u'_i u'_j}}{\partial t}}_{\text{I}} + \underbrace{\sum_{k=1}^{3} \overline{u_k} \frac{\partial \overline{u'_i u'_j}}{\partial x_k}}_{\text{II}} = \underbrace{\sum_{k=1}^{3} -\overline{u'_i u'_k} \frac{\partial \overline{u_j}}{\partial x_k} - \overline{u'_j u'_k} \frac{\partial \overline{u_i}}{\partial x_k}}_{\text{III}} - \underbrace{\sum_{k=1}^{3} \frac{\partial \overline{u'_i u'_j u'_k}}{\partial x_k}}_{\text{IV}}
$$

$$
\underbrace{-\frac{1}{\theta_{vr}} \left[g_i \overline{u'_j \theta'_v} + g_j \overline{u'_i \theta'_v} \right]}_{\text{V}}
$$

$$
\underbrace{-2 \sum_{k=1}^{3} \sum_{l=1}^{3} \Omega_l \left(\epsilon_{ilk} \overline{u'_j u'_k} + \epsilon_{jlk} \overline{u'_i u'_k} \right)}_{\text{VI}}
$$

$$
\underbrace{-\frac{1}{\rho_r} \left(\frac{\partial \overline{u'_i p'}}{\partial x_j} + \frac{\partial \overline{u'_j p'}}{\partial x_i} \right)}_{\text{VII}} - \underbrace{\frac{\overline{p'}}{\rho_r} \left(\frac{\partial u'_i}{\partial x_j} + \frac{\partial u'_j}{\partial x_i} \right)}_{\text{VIII}}
$$

$$
\underbrace{+ 2\nu \sum_{k=1}^{3} \frac{\partial}{\partial x_k} \left[\overline{u'_j s'_{ik}} + \overline{u'_j s'_{jk}} \right]}_{\text{IX}}
$$

$$
\underbrace{- 2\nu \sum_{k=1}^{3} \left[\overline{s'_{ik} \frac{\partial u'_j}{\partial x_k}} + \overline{s'_{jk} \frac{\partial u'_i}{\partial x_k}} \right]}_{\text{X}} \tag{3.58}
$$

In (3.58),

$$
s'_{ik} = \frac{1}{2} \left(\frac{\partial u'_i}{\partial x_k} + \frac{\partial u'_k}{\partial x_i} \right) \tag{3.59}
$$

is the fluctuation rate of deformation.

The set (3.58) is essential to understand the physics of turbulence. We borrow from (Stull, 1988) their meanings:

I. Is the local rate of change of the covariance $\overline{u'_i u'_j}$.

II. Is the advection of $\overline{u'_i u'_j}$ by the mean wind $\overline{u_k}$.

III. Is the *gradient production/destruction term*. A loose interpretation is that the average profiles are subject to perturbations that generate large-scale structures that progressively break into smaller structures, and so on. The larger structures are anisotropic, an evidence of this fact being the very existence of the mean gradients $\partial \overline{u_j}/\partial x_k$, but the smaller structures ("eddies") become more and more isotropic, and their statistics more homogeneous and stationary.

IV. This is the *transport term*: it reflects turbulence's *closure problem*: note that in equation (3.46) for the mean $\overline{u_i}$ there are $2^{\underline{nd}}$-order moments $\overline{u_i' u_k'}$; here, in the equation for the second-order moments $\overline{u_i' u_j'}$ the $3^{\underline{rd}}$-*order moments* $\overline{u_i' u_j' u_k'}$ appear, and so on *ad infinitum*. Indeed, Reynold's decomposition always leads to more equations than unknowns to any order. In the atmospheric boundary layer, the divergence of $3^{\underline{rd}}$-order moments is often important and reflects *non-local* redistribution of covariances: it adds considerable difficulty in modeling and understanding its physics.

V. This is the buoyancy term: the buoyancy flux $\overline{\rho' u_j'}$ has a counterpart in the virtual sensible heat flux $\overline{u_j' \theta_v'}$, via the simplified equation of state (3.50) that emerges from the Boussinesq approximation. Depending on the sign of $\overline{u_j' \theta_v'}$, it can either produce or destroy the covariance $\overline{u_i' u_j'}$. Production of turbulence by buoyancy makes the atmosphere more *unstable*, and destrution makes it more *stable*.

VI. This is the Coriolis term: it is negligible in the atmospheric boundary layer (Stull, 1988).

VII. Like III, this is a divergence term: it is called the *pressure redistribution* term, and also like III it redistributes $\overline{u_i' u_j'}$ without creating nor destroying covariances in the overall flow domain Tennekes and Lumley (1972).

VIII. This is the *return to isotropy* term (Rotta, 1951a,b; Hinze, 1975; Lumley and Newman, 1977; CHOI and LUMLEY, 2001). Its sum for the 3 components $\overline{u_1' u_1'}$, $\overline{u_2' u_2'}$ and $\overline{u_3' u_3'}$ is zero, showing that it acts to reduce the anisotropy of turbulence, and to nudge the Reynolds stress tensor $\overline{u_i' u_j'}$ to become isotropic.

IX. This term accounts for the molecular diffusion of $\overline{u_i' u_j'}$: it is very small and can be neglected.

X. This is the viscous dissipation term. It can be shown to be small for the case $i \neq j$ Wyngaard (1981), but is always very important when $i = j$; then, it accounts for the dissipation of turbulence kinetic energy, and is of the same order of the other important terms in (3.58), such as gradient production and buoyancy.

An equation that has a central role in the understanding of the physics (or, at least, the phenomenology) of turbulence is the turbulence kinetic energy (TKE) equation. It is obtained by setting $i = j$ in (3.58), summing from 1 to 3, and dividing by two. The quantities

$$e' = \frac{1}{2} \sum_{i=1}^{3} u_i' u_i', \tag{3.60}$$

$$\overline{e'} = \frac{1}{2} \sum_{i=1}^{3} \overline{u_i' u_i'} \tag{3.61}$$

are the kinetic energy of the fluctuations and their mean, respectively. Note that being the average of a quadratic quantity, $\overline{e'} \neq 0$. The TKE equation is

$$
\underbrace{\frac{\partial \overline{e'}}{\partial t}}_{\text{I}} + \underbrace{\sum_{k=1}^{3} \overline{u_k} \frac{\partial \overline{e'}}{\partial x_k}}_{\text{II}} = - \underbrace{\sum_{i=1}^{3} \sum_{k=1}^{3} \overline{u_i' u_k'} \frac{\partial \overline{u_i}}{\partial x_k}}_{\text{III}} - \underbrace{\sum_{k=1}^{3} \frac{\partial \overline{e' u_k'}}{\partial x_k}}_{\text{IV}}
$$

$$
+ \underbrace{\frac{g}{\theta_r} \overline{w' \theta_v'}}_{\text{V}} - \underbrace{2 \sum_{i=1}^{3} \sum_{k=1}^{3} \sum_{l=1}^{3} \epsilon_{ilk} \Omega_l \overline{u_i' u_k'}}_{\text{VI}} - \underbrace{\frac{1}{\rho_r} \sum_{i=1}^{3} \left[\frac{\partial \overline{u_i' p'}}{\partial x_i} \right]}_{\text{VII}}
$$

$$
+ \underbrace{2\nu \sum_{i=1}^{3} \sum_{k=1}^{3} \frac{\partial \overline{u_i' s_{ik}'}}{\partial x_k}}_{\text{VIII}} - \underbrace{2\nu \sum_{i=1}^{3} \sum_{k=1}^{3} \overline{s_{ik}' s_{ik}'}}_{\text{IX}}. \quad (3.62)
$$

In (3.62),

  I is the time rate of change of $\overline{e'}$;

  II is the advection of $\overline{e'}$ (the advective derivative of $\overline{e'}$);

  III is the gradient production term;

  IV is the transport term;

  V is the buoyancy production of $\overline{e'}$;

  VI is the (negligible) Coriolis term;

  VII is the pressure redistribution term;

VIII is the (negligible) diffusive transport of $\overline{e'}$;

  IX is the dissipation of TKE.

Note that, on account of the mass conservation equation for the fluctuations, (3.56), the return to isotropy term in (3.58) now sums to zero:

$$
\sum_{i=1}^{3} \overline{\frac{p'}{\rho_r} \frac{\partial u_i'}{\partial x_i}} = \overline{\frac{p'}{\rho_r} \left[\sum_{i=1}^{3} \frac{\partial u_i'}{\partial x_i} \right]} = 0. \quad (3.63)
$$

Further simplification can be achieved if we assume the conditions under which the Monin-Obukhov Similarity Theory is valid: horizontal homogeneity, stationarity, mean flow along the x direction only. Then one has

$$
0 = -\overline{u' w'} \frac{\partial \overline{u}}{\partial z} - \frac{\partial \overline{e' w'}}{\partial z} + \frac{g}{\theta_r} \overline{w' \theta_v'} - \frac{1}{\rho_r} \frac{\partial \overline{w' p'}}{\partial z} - 2\nu \sum_{i=1}^{3} \sum_{k=1}^{3} \overline{s_{ik}' s_{ik}'}
$$

$$
0 = -\overline{u' w'} \frac{\partial \overline{u}}{\partial z} - \frac{\partial \overline{e' w'}}{\partial z} + \frac{g}{\theta_r} \overline{w' \theta_v'} - \frac{1}{\rho_r} \frac{\partial \overline{w' p'}}{\partial z} - \epsilon_e \quad (3.64)
$$

Using the notation set out with (3.51)–(3.53), we can also start from (3.58) to write down the equations for the scalars semivariances, represented by

$$\frac{1}{2}\overline{c'c'}$$

where c is the scalar's concentration (it can also be θ, q, etc.). These equations now read

$$\frac{\partial \frac{1}{2}\overline{c'c'}}{\partial t} + \sum_{k=1}^{3} \overline{u_k}\frac{\partial \frac{1}{2}\overline{c'c'}}{\partial x_k} = \sum_{k=1}^{3} -\overline{u_k'c'}\frac{\partial \overline{c}}{\partial x_k} - \sum_{k=1}^{3} \frac{\partial \frac{1}{2}\overline{c'c'u_k'}}{\partial x_k}$$
$$+ \nu_c \sum_{k=1}^{3} \frac{\partial}{\partial x_k}\left(\overline{c'\frac{\partial c'}{\partial x_k}}\right) - \nu_c \sum_{k=1}^{3} \overline{\frac{\partial c'}{\partial x_k}\frac{\partial c'}{\partial x_k}}. \tag{3.65}$$

The term

$$\epsilon_{cc} = \nu_c \sum_{k=1}^{3} \overline{\frac{\partial c'}{\partial x_k}\frac{\partial c'}{\partial x_k}} \tag{3.66}$$

is the rate of molecular dissipation of the semivariance of c. Also, the next-to-last term above can be shown to be very small, and will be ommitted from now on. Then, under conditions of stationarity and horizonal homogeneity, (3.65) simplifies to

$$0 = -\overline{w'c'}\frac{\partial \overline{c}}{\partial z} - \frac{\partial \frac{1}{2}\overline{c'c'w'}}{\partial z} - \nu_c \sum_{k=1}^{3} \overline{\frac{\partial c'}{\partial x_k}\frac{\partial c'}{\partial x_k}}. \tag{3.67}$$

4

Monin-Obukhov Similarity Theory (MOST)

The Monin-Obukhov Similarity Theory (Obukhov, 1971) — MOST for short — appeared in the Soviet Union during the Second World War. It became known in the West in the 1950s and since the 1960s it has become a standard tool for micrometeorological analysis. Before we look at the theory itself, however, we we analyze the basis of the modern measurement of surface fluxes: the eddy covariance method.

4.1 – Physical basis of the eddy covariance method (ECM)

Figure 4.1 shows the essence of the eddy covariance method. We will illustrate it for several pairs of intensive quantity ↔ extensive quantity (Fox and McDonald, 1981) (indentified by the extensive quatities in the following list): the mass of dry air, the mass of water vapor, and the mass of CO_2.

For the control volume $\mathcal{V}$, limited by the closed surface $\mathcal{S}$, the mass balance equation of an atmospheric gas χ is

$$\int_{\mathcal{V}} s_\chi \, dV - \oint_{\mathcal{S}} (\boldsymbol{n} \cdot \boldsymbol{j}_\chi) \, dS = \frac{\partial}{\partial t} \int_{\mathcal{V}} \rho_\chi \, dV + \oint_{\mathcal{S}} \rho_\chi (\boldsymbol{n} \cdot \boldsymbol{u}) \, dS. \qquad (4.1)$$

In (4.1), $\boldsymbol{j}_\chi$ is the diffusive mass flux of the gas χ on the surface of $\mathcal{V}$ and s_χ are the production sources of the gas χ inside $\mathcal{V}$ (for example, the production of CO_2 by the respiration of plants). These terms form the *total flux* of the gas χ into the control volume $\mathcal{V}$:
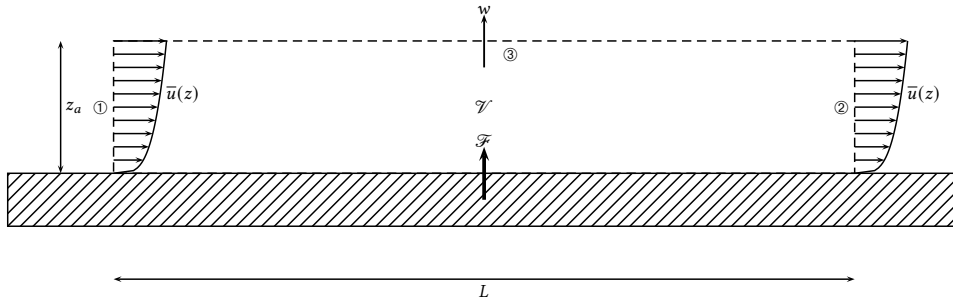
Figure 4.1: Mass balance to a virtual "box" (a control volume) of a height z_a over a homogeneous surface of length L in the wind direction.

$$\mathscr{F}_\chi \equiv \int_{\mathscr{V}} s_\chi \, dV - \oint_{\mathscr{S}} (\boldsymbol{n} \cdot \boldsymbol{j}_\chi) \, dS. \tag{4.2}$$

To proceed, it is necessary to take into consideration the gaseous composition of the atmosphere, and the importance of the contributions to the sources and the diffusive fluxes at the boundaries of $\mathscr{V}$. Consider the atmosphere constituted essentially by 3 components. The "dry" part consists mainly of O_2 e N_2, taken together as a simple gas with constant $R_s = 287{,}05$ $J\,kg^{-1}\,K^{-1}$ (the gas constant for dry air; see (2.26)). The wet component is the water vapor H_2O, whose gas constant is $R_v = 461{,}52\,J\,kg^{-1}\,K^{-1}$. Now, consider a third component formed by a greenhouse gas. To fix the ideas, suppose it is CO_2, whose gas constant is $R_c = 188{,}92\,J\,kg^{-1}\,K^{-1}$. The air density is the sum of each component:

$$\rho = \rho_d + \rho_v + \rho_c, \tag{4.3}$$

where ρ_d is the density of dry air, ρ_v is the density of water vapor, and ρ_c is the density of CO_2. Similarly, the diffusive fluxes and the sources add up:

$$s = s_d + s_v + s_c, \tag{4.4}$$

$$\boldsymbol{j} = \boldsymbol{j}_d + \boldsymbol{j}_v + \boldsymbol{j}_c. \tag{4.5}$$

For dry air, $s_d = 0$, and $\boldsymbol{j}_d = 0$ at the surface-atmosphere interface (Finnigan, 2009). According to Lee and Massman (2011), this hypotheses is a fundamental novelty of the theory proposed by Webb et al. (1980).

Expanding the derivative with respect to time in (4.1),

$$\mathscr{F}_\chi = \int_V \frac{\partial \rho_\chi}{\partial t} \, dV + \oint_S \rho_\chi (\boldsymbol{n} \cdot \boldsymbol{u}) \, dS. \tag{4.6}$$

The term involving the mass advection through the control surface needs to be evaluated for each of the surfaces ①, ② and ③:

$$\int_① \rho_\chi (\boldsymbol{n} \cdot \boldsymbol{u}) \, dS = - \int_{y=0}^{b} \int_{z=0}^{z_a} \rho_\chi u(x=0,y,z,t) \, dz \, dy, \tag{4.7}$$

$$\int_② \rho_\chi (\boldsymbol{n} \cdot \boldsymbol{u}) \, dS = + \int_{y=0}^{b} \int_{z=0}^{z_a} \rho_\chi u(x=L,y,z,t) \, dz \, dy, \tag{4.8}$$

$$\int_③ \rho_\chi (\boldsymbol{n} \cdot \boldsymbol{u}) \, dS = + \int_{x=0}^{L} \int_{y=0}^{b} \rho_\chi w(x,y,z=z_a,t) \, dy \, dx. \tag{4.9}$$

Consider now the average of (4.6). Using the commutation properties of the average with the derivative, expressed by (3.19) for the ensemble average,

$$\overline{\mathscr{F}_\chi} = \int_V \frac{\partial \overline{\rho}}{\partial t} \, dV + \oint_S \overline{\rho(\boldsymbol{n} \cdot \boldsymbol{u})} \, dS. \tag{4.10}$$

Note that $\overline{\mathscr{F}_\chi}$ is a mass transfer rate into $\mathscr{V}$, in $kg_\chi\,s^{-1}$ in the SI.

If the flow is *homogeneous* in x and y, then, for the ensemble average,

$$\overline{[\rho_\chi u]}(x=0,y,z) = \overline{[\rho_\chi u]}(x=L,y,z), \quad \forall y,z \tag{4.11}$$

note that this *is valid only on average*; proceeding,

$$\int_① \overline{\rho_\chi(\boldsymbol{n} \cdot \boldsymbol{u})}\, dS + \int_② \overline{\rho_\chi(\boldsymbol{n} \cdot \boldsymbol{u})}\, dS = 0. \tag{4.12}$$

Also note that in the case of block and running averages, (4.11) and (4.12) are valid only approximately.

Horizontal homogeneity also implies that $\overline{[\rho_\chi w]}(x, y, z = z_a)$ is independent of both x and y, whence

$$\int_{x=0}^{L} \int_{y=0}^{b} \overline{[\rho_\chi w]}(x, y, z = z_a)\, dy\, dx = \overline{[\rho_\chi w]}(z = z_a) bL. \tag{4.13}$$

For the average density $\overline{\rho_\chi}$ the hypothesis of horizontal homogeneity produces

$$\overline{\rho_\chi} = \overline{\rho_\chi}(z, t), \tag{4.14}$$

where (4.6), using (4.12) and (4.13), reduces to

$$\overline{\mathscr{F}_\chi} = bL \int_0^{z_a} \frac{\partial \overline{\rho_\chi}}{\partial t}\, dz + bL\overline{[\rho_\chi w]}(z = z_a),$$

$$\frac{\overline{\mathscr{F}_\chi}}{bL} \equiv F_\chi = \int_0^{z_a} \frac{\partial \overline{\rho_\chi}}{\partial t}\, dz + \overline{[\rho_\chi w]}(z = z_a), \tag{4.15}$$

where F_χ is the specific mass flux (flux per unit of surface area) of the gas. The transient term is kept in (4.15) to allow an analysis of its importance, which now follows.

By the mean value theorem of differential and integral calculus, if $0 \leq z^* \leq z_a$:

$$F_\chi = \frac{\partial}{\partial t} \left\{ z_a \overline{\rho_\chi}(z^*) \right\} + \overline{[\rho_\chi w]}(z = z_a). \tag{4.16}$$

The transient term can be neglected if

$$z_a \frac{\partial}{\partial t} \left\{ \overline{\rho_\chi}(z^*) \right\} \ll \overline{[\rho_\chi w]}(z = z_a); \tag{4.17}$$

in this case, we get the standard equation of the eddy covariance method for the surface flux of gas χ:

$$F_\chi = \overline{[\rho_\chi w]}(z = z_a). \tag{4.18}$$

Note that the choice of z_a is crucial: the bigger the value, the more important becomes the effect of $\partial \overline{\rho_\chi}/\partial t$; as one would expect the value of $\overline{\rho_\chi}$ to evolve over over time as a funcion of the flux F_χ, it is not realistic to assume that the transient term is identically null in a real atmosphere; strictly speaking, it is a combination of a small value of the time derivative with a "low" height of measurement (besides of course the horizontal homogeneity hypothesis) that assures that (4.18) gives us an accurate value of F_χ in the surface.

As we saw above, for dry air $\mathscr{F}_d \equiv 0$, where (4.18) with $\chi = d$, gives

$$\frac{\overline{\mathscr{F}_d}}{bL} = 0 = \overline{[\rho_d w]}(z = z_a). \tag{4.19}$$

This is a fundamental hypothesis in the deduction of the WPL correction (Webb et al., 1980), that however is only briefly mentioned in that paper. In this text, (4.19) is rigorously derived from the horizontal homogeneity hypothesis and from the stationarity and dry air budget for a control volume, in essentially the same way as in Finnigan (2009), and Lee and Massman (2011).

Under the same hypothesis of homogeneity and stationarity, and taking respectively $\chi = v$ e $\chi = c$, the specific fluxes (*i.e.*, per unit of area) of water vapor mass and CO_2 mass are

$$E \equiv \frac{\overline{\mathscr{F}_v}}{bL} = \overline{[\rho_v w]}(z = z_a), \tag{4.20}$$

$$F \equiv \frac{\overline{\mathscr{F}_c}}{bL} = \overline{[\rho_c w]}(z = z_a). \tag{4.21}$$

Besides the mass fluxes described above, also indispensable in micrometeorological measurements are the momentum flux,

$$\tau \equiv \frac{\overline{\mathscr{F}_u}}{bL} = \overline{[\rho u w]}(z = z_a), \tag{4.22}$$

and the sensible heat flux,

$$H \equiv \frac{\overline{\mathscr{F}_\theta}}{bL} = \overline{[\rho c_p w \theta]}(z = z_a), \tag{4.23}$$

where θ is potential temperature.

In the name of simplicity, from now on we will omit the measurement level; in this way, for example, we write $\overline{\rho_v w}$ instead of $\overline{[\rho_v w]}(z = z_a)$.

4.2 – Physical justification

The fundamental hypotheses of the MOS theory are the following:

- The flow is nearly stationary on average:

$$\frac{\partial \overline{(\cdot)}}{\partial t} = 0. \tag{4.24}$$

- The flow is unidirectional:

$$\overline{\boldsymbol{u}} = (\overline{u}, 0, 0), \quad \overline{v} = \overline{w} = 0. \tag{4.25}$$

They assumption $\overline{w} = 0$ is strictly not valid; instead, $\overline{w}$ is very small but nonzero, in a way that actually impacts flux measurements where the density of a gas (ρ_χ), instead of its mass concentration c_χ, or mixing ratio r_χ, is measured. We will revisit this when we discuss the WPL correction.

- The flow is homogeneous in x and y, on average:

$$\frac{\partial \overline{(\cdot)}}{\partial x} = \frac{\partial \overline{(\cdot)}}{\partial y} = 0. \tag{4.26}$$

In these conditions, the *local advection* of any quantity in the x direction is null:

$$\bar{u}\frac{\partial \overline{(\cdot)}}{\partial x} = 0. \tag{4.27}$$

In particular, the vertical fluxes of momentum τ, sensible heat H, mass of water vapor E and greenhouse gas mass F are constant along x. These surface fluxes are the desired quantities, for example: by hydrologists interested in evaporation (or evapotranspiration) and meteorologists interested in using them as boundary conditions for their weather forecast models, atmospheric dispersion models, etc..

As seen in section **??**, from the turbulence theory point of view, the surface fluxes are turbulence statistics, next to the surface, in which one of the variables is the vertical velocity w:

$$\tau = \bar{\rho}u_*^2 = -\overline{\rho w u} \tag{4.28}$$

$$H = \bar{\rho}c_p u_* \theta_* = \overline{\rho c_p w \theta} \tag{4.29}$$

$$E = \bar{\rho}u_* q_* = \overline{\rho_v w} \tag{4.30}$$

$$H_v = \bar{\rho}c_p u_* \theta_{v*} = \overline{\rho c_p w \theta_v} \tag{4.31}$$

$$F = \bar{\rho}u_* c_* = \overline{\rho_c w} \tag{4.32}$$

These equations define new types of *scales*: the velocity scale u_*, the temperature scale θ_* the specific humidity scale q_*, the greenhouse gas scale q_* and the virtual temperature scale θ_{v*}. The latter is associated to the virtual heat flux H_v. According to what we discussed in the previous section, it is necessary to measure the turbulent statistics close to the surface.

The set (4.28–(4.32) is not the most common form to present the turbulent fluxes and scales. Instead, the rightmost terms can be further simplified. We will do this for the momentum flux, and list the remaining simplifications for the reader to verify it. First note that the total mass flux $\overline{\rho w} \approx \overline{\rho_v w}$; moreover, because $\rho_v \sim 0.01\rho_d$ in the surface layer, clearly

$$\overline{\rho w} = \bar{\rho}\,\bar{w} + \overline{\rho' w'} \sim \tilde{\rho}\tilde{u} \tag{4.33}$$

using the notation introduced in section 3.4. Therefore, $\bar{\rho}\,\bar{w} \sim \tilde{\rho}\tilde{u}$ *at most*. This leads immediately to

$$\bar{w} \sim \frac{\tilde{\rho}\tilde{u}}{\rho_0}. \tag{4.34}$$

Note that this is a weaker condition than $\bar{w} = 0$! We now expand $\overline{\rho w u}$ by means of a standard Reynolds decomposition:

$$\overline{\rho w u} = \overline{[\bar{\rho} + \rho'][\bar{w} + w'][\bar{u} + u']}$$

$$= \overline{\bar{\rho}\,\bar{w}\,\bar{u}} + \overline{\bar{\rho}\,\bar{w}\,u'}^{\,0} + \overline{\bar{\rho}\,w'\,\bar{u}}^{\,0} + \bar{\rho}\,\overline{w'\,u'}$$

$$+ \overline{\rho'\,\bar{w}\,\bar{u}}^{\,0} + \overline{\rho'\,\bar{w}\,u'} + \overline{\rho'\,w'\,\bar{u}} + \overline{\rho'w'u'}$$

$$= \underbrace{\bar{u}[\bar{\rho}\,\bar{w} + \overline{\rho'w'}]}_{\text{I}} + \underbrace{\bar{\rho}\overline{w'u'}}_{\text{II}} + \underbrace{\bar{w}\overline{\rho'u'}}_{\text{III}} + \underbrace{\overline{\rho'w'u'}}_{\text{IV}}. \tag{4.35}$$

The order of each term in (4.35) can now be readily estimated:

$$\text{I} \sim \tilde{\rho}\tilde{u}^2,$$

$$\text{II} \sim \rho_0\tilde{u}^2,$$

$$\text{III} = \frac{\tilde{\rho}}{\rho_0}\tilde{\rho}\tilde{u}^2,$$

$$\text{IV} = \tilde{\rho}\tilde{u}^2,$$

whence

$$\overline{\rho w u} \approx \overline{\rho}\,\overline{w'u'}. \tag{4.36}$$

Similar analyses can be performed for the remainder of (4.28)–(4.32), and will be omitted, leading (in higher order) to

$$\tau = \overline{\rho}u_*^2 \approx -\overline{\rho}\,\overline{w'u'} \tag{4.37}$$

$$H = \overline{\rho}c_p u_* \theta_* \approx \overline{\rho}c_p\overline{w'\theta'} \tag{4.38}$$

$$E = \overline{\rho}u_* q_* \approx \overline{\rho}\,\overline{w'q'} \tag{4.39}$$

$$H_v = \overline{\rho}c_p u_* \theta_{v*} \approx \overline{\rho}c_p\overline{w'\theta'_v} \tag{4.40}$$

$$F = \overline{\rho}u_* c_* \approx \overline{\rho}\,\overline{w'c'}. \tag{4.41}$$

A standard justification (but not derivation!) for Monin-Obukhov Similarity Theory can be obtained from the TKE equation with *further simplifications*. Note that in a moist atmosphere we should use the virtual temperature θ_v for the buyoancy term. Also, assuming that all fluxes are constant with height, and that the TKE transport term and pressure terms can both be neglected, (3.64) simplifies to

$$\underbrace{-\overline{u'w'}\frac{\mathrm{d}\overline{u}}{\mathrm{d}z}}_{P} + \underbrace{\frac{g}{\theta_{vr}}\overline{w'\theta'_v}}_{B} - \epsilon_e = 0, \tag{4.42}$$

$$-u_*^2\frac{\mathrm{d}\overline{u}}{\mathrm{d}z} + \frac{g}{\theta_{vr}}u_*\theta_* - \epsilon_e = 0,$$

$$\frac{\kappa(z-d)}{u_*}\frac{\mathrm{d}\overline{u}}{\mathrm{d}z} + \frac{\kappa g(z-d)\theta_{v*}}{\theta_{vr}u_*^2} - \frac{\kappa(z-d)\epsilon_e}{u_*^3} = 0. \tag{4.43}$$

Equation (4.42) states that to first order mechanical production (P) plus buoyant production (B) equals molecular dissipation (ϵ_e) and is often use to analyze the degree to which a dataset conforms to MOST (see Chamecki et al. (2018)).

In applications, one typically replaces θ_{vr} by $\overline{\theta_v}$, a mean virtual temperature measured close to the surface. The Obukhov stability variable is now defined by

$$\zeta = \frac{z-d}{L_O} = -\frac{\kappa g(z-d)\theta_{v*}}{\overline{\theta_v}u_*^2} \tag{4.44}$$

and indicates the relative magnitude of the turbulent kinetic energy production by buoyancy (θ_{v*} appears in the numerator) and by friction (u_* appears in the denominator). In (4.44), d is the "zero plane" displacement. It takes into consideration the height of the vegetation, and establishes a level d above the ground from which the effects of the surface turbulent fluxes on the atmosphere above the vegetation are felt.

The other two terms in (4.43) can now be defined as

$$\phi_\tau \equiv \frac{\kappa(z-d)}{u_*}\frac{\mathrm{d}\overline{u}}{\mathrm{d}z},\tag{4.45}$$

$$\phi_{\epsilon_e} \equiv \frac{\kappa(z-d)\epsilon_e}{u_*^3},\tag{4.46}$$

whence

$$\phi_\tau - \zeta - \phi_{\epsilon_e} = 0.\tag{4.47}$$

The surface layer (SL) is the region inside the atmospheric boundary layer where, roughly, the surface fluxes τ, H, H_v, etc., are approximately constant with z. In other words, in principle, turbulence measurements inside the SL produce the surface fluxes. The SL has many sub-layers: the interfacial sublayer, the roughness sublayer, the dynamic sublayer, the dynamic-convective sublayer and the local free convection sublayer. The latter, depending on the author, may or may not be considered a part of the SL. The nomenclature also varies according to the author. The three first classifications are reasonably universal (Brutsaert, 1982; Garratt, 1994); the term dynamic-convective sublayer is due to Kader and Yaglom (1990); the term free convection sublayer (or layer, depending on it being considered or not a part of the SL) is due to Wyngaard et al. (1971). We refer the reader to these references for details on the many sublayers of the SL.

The SL is unstable when $\zeta < 0$, and the buoyancy term in the turbulence kinetic energy equation contributes to produce turbulence. The SL is stable when $\zeta > 0$, and that term helps to destroy the turbulence. The SL is neutral when $\zeta = 0$.

MOST predicts that all the turbulent fluctuation moments, non-dimensionalized correctly by the proper combination of z, u_*, θ_*, q_*, θ_{v*} and c_*, are functions of the independent variable ζ. In the following, we cover some of these funcions.

It is often necessary to relate θ_{v*}, θ_* and q_*. This can be done as follows:

$$\begin{aligned}
\theta_v &= (1+0.61q)\theta,\\
\overline{\theta_v} + \theta_v' &= (1+0.61[\overline{q}+q'])(\overline{\theta}+\theta'),\\
\overline{\theta_v} + \theta_v' &= (1+0.61\overline{q}+0.61q')(\overline{\theta}+\theta'),\\
\overline{\theta_v} + \theta_v' &= (1+0.61\overline{q})\overline{\theta} + (1+0.61\overline{q})\theta' + 0.61q'\overline{\theta} + 0.61q'\theta',\\
\theta_v' &\approx (1+0.61\overline{q})\theta' + 0.61q'\overline{\theta},\\
\overline{w'\theta_v'} &\approx (1+0.61\overline{q})\overline{w'\theta'} + 0.61\overline{\theta}\,\overline{w'q'},\\
u_*\theta_{v*} &\approx (1+0.61\overline{q})u_*\theta_* + 0.61\overline{\theta}\,u_*q_*,\\
\theta_{v*} &\approx (1+0.61\overline{q})\theta_* + 0.61\overline{\theta}\,q_*.
\end{aligned}\tag{4.48}$$

4.3 – Gradients of mean quantities

The MOST functions for the gradients are

$$\frac{\kappa(z-d)}{u_*}\frac{\mathrm{d}\overline{u}}{\mathrm{d}z} = \phi_\tau(\zeta), \tag{4.49}$$

$$\frac{\kappa(z-d)}{\theta_*}\frac{\mathrm{d}\overline{\theta}}{\mathrm{d}z} = \phi_H(\zeta), \tag{4.50}$$

$$\frac{\kappa(z-d)}{q_*}\frac{\mathrm{d}\overline{q}}{\mathrm{d}z} = \phi_E(\zeta), \tag{4.51}$$

$$\frac{\kappa(z-d)}{c_*}\frac{\mathrm{d}\overline{c}}{\mathrm{d}z} = \phi_F(\zeta). \tag{4.52}$$

The use of the ordinary derivative $\mathrm{d}/\mathrm{d}z$ in the above equations, instead of the partial derivative, simply indicates that we consider that the flow is stationary and horizontally homogeneous, so that the only independent variable (from the statistical point of view of turbulence) is z.

The equations (4.49–4.52), which define the dimensionless gradients of Monin-Obukhov Similarity Theory, are equivalent to postulate turbulent diffusivities. For example, consider a turbulent flow in a boundary layer with density stratification. The turbulent diffusivity of momentum, K_τ, is defined by analogy with the molecular diffusivity as

$$\tau \equiv \overline{\rho}K_\tau\frac{\mathrm{d}\overline{u}}{\mathrm{d}z}. \tag{4.53}$$

From (4.28) and (4.49), the turbulent diffusivity is

$$K_\tau = \kappa(z-d)u_*/\phi_\tau(\zeta). \tag{4.54}$$

Now, consider (4.49) for the profile of horizontal mean velocity $\overline{u}$ and $\zeta = 0$ ($L_O = +\infty$):

$$\frac{\kappa(z-d)}{u_*}\frac{d\overline{u}}{dz} = \phi_\tau(0) = 1 \tag{4.55}$$

where the value $\phi_\tau(0) = 1$ is classically obtained in non-stratified flows (Brutsaert, 1982). Integrating,

$$\frac{dz}{z-d} = \kappa\frac{d\overline{u}}{u_*}$$

$$\int_{x=d+z_{0\tau}}^{z-d}\frac{dx}{x-d} = \kappa\frac{\overline{u}}{u_*}$$

$$\frac{\overline{u}}{u_*} = \frac{1}{\kappa}\ln\frac{z-d}{z_{0\tau}} \tag{4.56}$$

Note that the integral over z has lower limit $d + z_{0\tau}$, and not d, because (4.56) is valid only in the so-called inertial sublayer of the SL, but is no longer valid in the roughness sublayer (where the flow is turbulent but does not obey MOST) and in the thin viscous sublayer very close to the surface where the transport by molecular diffusion is significant. The integration constant $z_{0\tau}$ is called the roughness length for momentum.

We need a drawing here

Equation (4.56) is the logarithmic profile of velocity that appears in turbulent boundary layers without density stratification. Clearly, $\phi_\tau(\zeta)$ "corrects" this profile for non-null stratification ($\zeta \neq 0$).

The general integration procedure for the case $\zeta \neq 0$ is the following:

$$\frac{\kappa(z-d)}{u_*}\frac{d\overline{u}}{dz} = \phi_\tau(\zeta),$$

$$\frac{\kappa\zeta}{u_*}\frac{d\overline{u}}{d\zeta} = \phi_\tau(\zeta),$$

$$\phi_\tau(\zeta)\frac{d\zeta}{\zeta} = \kappa\frac{d\overline{u}}{du_*},$$

$$\int_{\zeta_1}^{\zeta_2}\frac{\phi_\tau(x)\,dx}{x} = \kappa\frac{\overline{u}_2 - \overline{u}_1}{u_*}, \tag{4.57}$$

for $\zeta_1 < \zeta_2$. It is convenient to define

$$\Phi_\tau(\zeta) \equiv \int_{\zeta_{0\tau}}^{\zeta}\frac{\phi_\tau(x)\,dx}{x}, \tag{4.58}$$

where the lower limit of integration is set at

$$\zeta_{0\tau} = \frac{(z_{0\tau}+d)-d}{L_O} = \frac{z_{0\tau}}{L_O}. \tag{4.59}$$

Then

$$u_* = \kappa\frac{\overline{u}_2 - \overline{u}_1}{\Phi_\tau(\zeta_2) - \Phi_\tau(\zeta_1)} \tag{4.60}$$

Similarly, integrating the dimensionless gradients of temperature, specific humidity and greenhouse effect gas concentration,

$$\theta_* = \kappa\frac{\overline{\theta}_1 - \overline{\theta}_2}{\Phi_H(\zeta_2) - \Phi_H(\zeta_1)}, \tag{4.61}$$

$$q_* = \kappa\frac{\overline{q}_1 - \overline{q}_2}{\Phi_E(\zeta_2) - \Phi_E(\zeta_1)}, \tag{4.62}$$

$$c_* = \kappa\frac{\overline{c}_1 - \overline{c}_2}{\Phi_F(\zeta_2) - \Phi_F(\zeta_1)}, \tag{4.63}$$

where, in analogy with (4.58)–(4.59),

$$\Phi_{H,E,F}(\zeta) \equiv \int_{\zeta_{0H,0E,0F}}^{\zeta}\frac{\phi_\tau(x)\,dx}{x}, \tag{4.64}$$

$$\zeta_{0H,0E,0F} = \frac{z_{0H,0E,0F}}{L_O}. \tag{4.65}$$

Similarly to the case of a neutral atmosphere ($\zeta = 0$), the relations (4.49)–(4.52) (the first of which was used in obtaining of (4.60)) are not valid down to $z - d = 0$. That way, when level "1" is the surface, we use $z_1 - d = z_{0\tau}$ in (4.60), $z_1 - d = z_{0H}$ in (4.61), $z_1 - d = z_{0E}$ in (4.62) and $z_1 - d = z_{0F}$ in (4.63). Note that $\Phi_{H,E,F}(\zeta_{0H,0E,0F}) = 0$

It is common to assume $\phi_H = \phi_E = \phi_F$ in the SL. The equality of the turbulent diffusivities of heat and water vapor was supposed explicitly in the first time in the micrometeological context by Bowen in 1926 (Brutsaert, 1982), and constantly used ever since, but this hypothesis was only proved by Hill (1989) by means of dimensional analysis, and Dias (1994) and Dias and Brutsaert (1996) from the Reynolds equations for the case of homogeneous turbulence in the vertical axis. In the following, we will assume that the similarity functions ϕ for heat, water vapor and trace gases are always identical, *i.e.*: $\phi_H = \phi_E = \phi_F$. Strictly speaking, z_{0H}, z_{0E} and z_{0F} are not equal (Brutsaert, 1982); however, we'll assume in this text that they are sufficiently close ($z_{0H} \approx z_{0E} \approx z_{0F}$) for practical purposes.

4.4 – Classical formulas of the MOS theory

The classical profiles for the velocity $\overline{u}$ and scalars ($\overline{\theta}$, $\overline{q}$, $\overline{c}$) most used probably are the Businger-Dyer functions (Brutsaert, 1982). For unstable conditions ($\zeta < 0$):

$$\phi_\tau^2 = \phi_H = \phi_E = \phi_F (1 - 16\zeta)^{-1/2} \tag{4.66}$$

and for stable conditions ($\zeta > 0$):

$$\phi_\tau = \phi_H = \phi_E = \phi_F = 1 + 5\zeta. \tag{4.67}$$

Although there is still some discussion about the constants's values and even the form of these functions, they still represent a reasonable consent; a more recent revision on the ϕ profiles that are similar to the ones in this text can be found in (Högström, 1988). Stimulated by the findings of Kader and Yaglom (1990), Brutsaert (1992) suggested, for example, new formulations for unstable conditions. In stable conditions, Cheng and Brutsaert (2005) also re-evaluated the similarity functions using data from the CASES-99 experiment.

Note that in a neutral atmosphere $\zeta = 0$, where $\Phi_\tau(0) = \Phi_H(0) = \Phi_E(0) = \Phi_F(0) = -\infty$. This makes it difficult, if not impossible, to use equations (4.60)–(4.62), because of the singularity in the denominator. Therefore, it is preferable to work with functions Ψ that define the *deviation* of $\overline{u}$, $\overline{\theta}$ and $\overline{q}$ in relation of the logarithmic profiles due to the stability $\zeta \neq 0$:

$$\Psi(\zeta) \equiv \int_{\zeta_0}^{\zeta} \frac{1 - \phi(x)}{x}\, dx = \ln\left|\frac{\zeta}{\zeta_0}\right| - \Phi(\zeta) = \ln\left|\frac{z - d}{z_0}\right| - \Phi(\zeta). \tag{4.68}$$

Starting with Ψ_τ,

$$\begin{aligned}
\Psi_\tau(\zeta) &= \int_{\zeta_{0\tau}}^{\zeta} \frac{1 - (1 - 16u)^{-1/4}}{u}\, du \\
&= \int_{\zeta_{0\tau}}^{\zeta} \left[\frac{1}{u} - \frac{1}{u(1 - 16u)^{1/4}}\right] du
\end{aligned} \tag{4.69}$$

To calculate the integral, do

$$x = (1 - 16u)^{1/4}; \qquad x^4 = (1 - 16u); \qquad \frac{1 - x^4}{16} = u; \qquad du = -\frac{u^3}{4}\, dx. \tag{4.70}$$

The limits of integration in the variable x change to

$$a = (1 - 16\zeta_{0\tau})^{1/4} \approx 1 \text{ (due to the smallness of } \zeta_{0\tau}), \tag{4.71}$$

$$b = (1 - 16\zeta)^{1/4}. \tag{4.72}$$

Then,

$$\Psi_\tau(\zeta) = \int_a^b \left[\frac{16}{1 - x^4} - \frac{16}{x(1 - x^4)} \right] \left(-\frac{x^3}{4} \right) dx$$

$$= 4 \int_a^b \left[\frac{x}{x(x^4 - 1)} - \frac{1}{x(x^4 - 1)} \right] x^3 \, dx$$

$$= \int_a^b \frac{4(x - 1)x^2}{x^4 - 1} \, dx$$

$$= \int_a^b \left[\frac{2x}{x^2 + 1} - \frac{2}{x^2 + 1} + \frac{2}{x + 1} \right] dx$$

$$= \ln(x^2 + 1) + 2\ln(x + 1) - 2\arctan x \Big|_a^b, \tag{4.73}$$

whence

$$\Psi_\tau(\zeta) = \ln(b^2 + 1) + 2\ln(b + 1) - 2\arctan b - [\ln(2) + 2\ln(2) - 2\arctan(1)]$$

$$= \ln \frac{b^2 + 1}{2} + 2\ln \frac{b + 1}{2} - 2\arctan b + \frac{\pi}{2}. \tag{4.74}$$

Note that $\Psi_\tau(b = 1) \equiv 0$.

For Ψ_H:

$$\Psi_H(\zeta) = \int_{\zeta_{0\tau}}^\zeta \frac{1 - (1 - 16u)^{-1/2}}{u} \, du$$

$$= \int_{\zeta_{0\tau}}^\zeta \left[\frac{1}{u} - \frac{1}{u(1 - 16u)^{1/2}} \right] du \tag{4.75}$$

Using the same change of variables given by (4.70),

$$\Psi_H(\zeta) = \int_a^b \left[\frac{16}{1 - x^4} - \frac{16}{x^2(1 - x^4)} \right] \left(-\frac{x^3}{4} \right) dx$$

$$= 4 \int_a^b \left[\frac{x^2}{x^2(x^4 - 1)} - \frac{1}{x^2(x^4 - 1)} \right] x^3 \, dx$$

$$= \int_a^b \frac{4(x^2 - 1)x}{x^4 - 1} \, dx$$

$$= 2\ln(x^2 + 1) \Big|_a^b$$

$$= 2\ln \frac{b^2 + 1}{2}. \tag{4.76}$$

Note that, again, we have $\Psi_H(b = 1) \equiv 0$. Also note that on account of the assumed equality $\phi_H = \phi_E = \phi_F$, it also follows now that $\Psi_H(\zeta) = \Psi_E(\zeta) = \Psi_F(\zeta)$.

Finally, in stable conditions, using (4.67):

$$\Psi_{\tau,H,E,F} = \int_{\zeta_{0\tau,0H,0E,0F}}^{\zeta} \frac{1-(1+5x)}{x}\, dx$$
$$= -5(\zeta - \zeta_{0\tau,0H,0E,0F}) \approx -5\zeta. \tag{4.77}$$

Thus, equations (4.60)–(4.62) are now written as

$$u_* = \kappa \frac{\overline{u}_2 - \overline{u}_1}{\ln\frac{\zeta_2}{\zeta_1} - [\Psi_\tau(\zeta_2) - \Psi_\tau(\zeta_1)]}, \tag{4.78}$$

$$\theta_* = \kappa \frac{\overline{\theta}_1 - \overline{\theta}_2}{\ln\frac{\zeta_2}{\zeta_1} - [\Psi_H(\zeta_2) - \Psi_H(\zeta_1)]}, \tag{4.79}$$

$$q_* = \kappa \frac{\overline{q}_1 - \overline{q}_2}{\ln\frac{\zeta_2}{\zeta_1} - [\Psi_E(\zeta_2) - \Psi_E(\zeta_1)]}, \tag{4.80}$$

$$c_* = \kappa \frac{\overline{c}_1 - \overline{c}_2}{\ln\frac{\zeta_2}{\zeta_1} - [\Psi_F(\zeta_2) - \Psi_F(\zeta_1)]}. \tag{4.81}$$

Along with (4.44), which defines L_O in terms of u_*, θ_*, q_* and c_*, this provides a non-linear system in the variables u_*, θ_*, q_*, c_* and L_O, that can be iteratively solved from the measurement of the mean profiles $\overline{u}(z)$, $\overline{\theta}(z)$, $\overline{q}(z)$ and $\overline{c}(z)$. In general, this is done postulating $|L_O| = +\infty$ initially, where $\Psi_{\tau,H,E,F} = 0$; with the values of u_*, θ_* and q_* obtained from the initial logarithmic profiles, we re-calculate L_O and then ζ_1, ζ_2, that can be used in a new estimate of the turbulent scales, and so on until the process converges.

4.5 – The flux-gradient method (FGM)

The transfer equations quantify the surface fluxes as a function of the differences in wind velocity, temperature, humidity and greenhouse gas between the surface and one or more measurement levels. We will assume that temperature $\overline{\theta}_a$, specific humidity $\overline{q}_a$, and mass concentration $\overline{c}_a$ are measured at height z_a, while the wind velocity $\overline{u}_b$ is measured at height z_b. The sub-index 0 indicates the surface. In his case, the transfer equations are

$$\tau = \overline{\rho} C_\tau \, \overline{u}_b^2, \tag{4.82}$$

$$H = \overline{\rho} c_p C_H \, \overline{u}_b \left(\overline{\theta}_0 - \overline{\theta}_a\right), \tag{4.83}$$

$$E = \overline{\rho} C_E \, \overline{u}_b \left(\overline{q}_0 - \overline{q}_a\right), \tag{4.84}$$

$$F = \overline{\rho} C_F \, \overline{u}_b \left(\overline{c}_0 - \overline{c}_a\right), \tag{4.85}$$

where C_τ, C_H, C_E and C_F are *dimensionless transfer coefficients* (respectively for momentum, heat, H_2O mass and (an unspecified?) gas mass). The use of the transfer equations for the estimation of surface fluxes is often called the *flux-gradient method*.

To derive (4.82)–(4.84), we start from (4.78)–(4.80). We set $z_2 = z_b$ for the momentum flux τ, and $z_2 = z_a$ for the scalar fluxes. At the surface, we already know that we need to specify $z_1 = d + z_{0\tau,0H,0E,0F}$. Then, keeping in mind that $a \approx 1$ (Equation 4.71), $\Psi_{\tau,H,E,F}(\zeta_{0\tau,0H,0E,0F}) = 0$, and using (4.28)–(4.20) and (4.78)–(4.81):

$$\tau = \overline{\rho} \frac{\kappa^2}{\left[\ln \frac{z_b - d}{z_{0\tau}} - \Psi_\tau \left(\frac{z_b - d}{L_O} \right) \right]^2} \, \overline{u}_b^2, \tag{4.86}$$

$$H = \overline{\rho} c_p \frac{\kappa^2}{\left[\ln \frac{z_b - d}{z_{0\tau}} - \Psi_\tau \left(\frac{z_b - d}{L_O} \right) \right] \left[\ln \frac{z_a - d}{z_{0H}} - \Psi_H \left(\frac{z_a - d}{L_O} \right) \right]} \, \overline{u}_b \left(\overline{\theta}_0 - \overline{\theta}_a \right), \tag{4.87}$$

$$E = \overline{\rho} \frac{\kappa^2}{\left[\ln \frac{z_b - d}{z_{0\tau}} - \Psi_\tau \left(\frac{z_b - d}{L_O} \right) \right] \left[\ln \frac{z_a - d}{z_{0E}} - \Psi_E \left(\frac{z_a - d}{L_O} \right) \right]} \overline{u}_b \left(\overline{q}_0 - \overline{q}_a \right), \tag{4.88}$$

$$F = \overline{\rho} \frac{\kappa^2}{\left[\ln \frac{z_b - d}{z_{0\tau}} - \Psi_\tau \left(\frac{z_b - d}{L_O} \right) \right] \left[\ln \frac{z_a - d}{z_{0F}} - \Psi_E \left(\frac{z_a - d}{L_O} \right) \right]} \overline{u}_b \left(\overline{c}_0 - \overline{c}_a \right). \tag{4.89}$$

The penultimate equation above is, naturally, "Dalton's Law". In the same way that occurs in the energy balance method, it is more commonly written with vapor pressure e instead of the specific humidity q,

$$E = \frac{0{,}622\overline{\rho}}{\overline{p}} \frac{\kappa^2}{\left[\ln \frac{z_b - d}{z_{0\tau}} - \Psi_\tau \left(\frac{z_b - d}{L_O} \right) \right] \left[\ln \frac{z_a - d}{z_{0E}} - \Psi_E \left(\frac{z_a - d}{L_O} \right) \right]} \overline{u}_b \left(\overline{e}_0 - \overline{e}_a \right). \tag{4.90}$$

This equation should be compared with many empirical formulas of evaporation of the nineteenth century and the first half of the twentieth century, of the kind

$$E = (a + b\overline{u})(\overline{e}_0 - \overline{e}_a). \tag{4.91}$$

From the micrometeorological point of view, a does not have physical meaning (*i.e.*: shouldn't be in the equation) if (4.91) is used over time scales that are not compatible with atmospheric turbulence, between 30 minutes and one hour. Historically, however, we find that equations like (4.91) are widely used at the daily and monthly scales. Finally notice that, strictly speaking, b is not constant; for fixed measurement heights z_a and z_b and roughness lengths (note that the surface roughness can vary over an agricultural area, or with wind direction), b still depends on the MO stability length, which varies in a (semi-)hourly scale along the day.

4.6 – Other similarity functions

Some of the most relevant 2$^{\underline{nd}}$order dimensionless MOST functions are

$$\frac{\overline{w'w'}}{u_*^2} = \phi_{ww}(\zeta), \tag{4.92}$$

$$\frac{\overline{\theta'\theta'}}{\theta_*^2} = \phi_{\theta\theta}(\zeta), \tag{4.93}$$

$$\frac{\overline{q'q'}}{q_*^2} = \phi_{qq}(\zeta), \tag{4.94}$$

where (Tillman, 1972; Hicks, 1981; Wesely, 1988):

$$\phi_{ww}^{1/2} = \begin{cases} 1.3(1 - 2\zeta)^{1/3} & \zeta \leq 0 \\ 1.3 & \zeta > 0 \end{cases} \tag{4.95}$$

$$\phi_{\theta\theta}^{1/2} = \phi_{qq}^{1/2} = \begin{cases} (2 - \zeta)^{-1/3} & \zeta \leq 0 \\ 2 & \zeta > 0 \end{cases} \tag{4.96}$$

The constants in the equations above are obtained experimentally, and may vary considerably depending on the author, experiment, etc.. The values presented here are an attempt at a reasonable consensus among several studies.

For the dimensionless dissipation of TKE,

$$\frac{\kappa z \epsilon_e}{u_*^3} = \phi_{\epsilon_e}(\zeta), \tag{4.97}$$

Högström (1990) gives

$$\phi_{\epsilon_e}(\zeta) = \begin{cases} 1.24[(1 - 19\zeta)^{-1/4} - \zeta], & \zeta \leq 0, \\ 1.24 + 4.7\zeta, & \zeta > 0. \end{cases} \tag{4.98}$$

4.7 – Classical applications

4.7.1 – The Energy-Budget Bowen Ratio (EBBR) Method

Consider a surface receiving a net irradiance R_n (SI units $\mathrm{W\,m^{-2}}$). Historically, the same quantitiy has often been called (and, often, still is) "net radiation" This available energy (per unit area and unit time) is used at the surface as follows:

- to warm or cool the air, by means of the sensible heat flux H;

- to evaporate or to condense surface humidity; if the latent heat of evaporation at the surface is L and the water vapor mass flux is E, the corresponding latent heat flux is LE; and

- to warm or cool the soil (or water) underneath, by means of the "ground" heat flux G.

The surface energy budget is then

$$R_l = H + LE + G. \tag{4.99}$$

From equations (4.28)–(4.20) for the surface fluxes and equations (4.61) and (4.62) for the mean profiles, and under the hypotheses $\phi_H = \phi_E$ and $z_{0H} \approx z_{0E}$ mentioned in the previous section, the *Bowen ratio* B_o is

$$B_o = \frac{H}{LE} = \frac{c_p}{L} \frac{\overline{\theta_1} - \overline{\theta_2}}{\overline{q_1} - \overline{q_2}} \tag{4.100}$$

Now, from (2.59),

$$B_o = \underbrace{\frac{c_p p}{0{,}622L}}_{\gamma} \frac{\overline{\theta_1} - \overline{\theta_2}}{\overline{e_1} - \overline{e_2}} \tag{4.101}$$

where γ is known as the psychrometric constant. From 4.99 and 4.101, one can obtain LE as

$$LE = \frac{R_n - G}{1 + \gamma \frac{\overline{\theta_1 - \theta_2}}{\overline{e_1 - e_2}}} \tag{4.102}$$

which is the Energy-Budget Bowen ratio method for the estimation of E.

4.7.2 – The psychrometric equation

A second example is the measurement of atmospheric humidity with an aspirated psychrometer. If we consider the energy budget of the wet bult at temperature $\overline{\theta_w}$ over which air flows at the air temperature $\overline{\theta_a}$, we have

$$R_n - G = 0 \Rightarrow B_o = -1.$$

The water vapor pressure of air in contact with the wet bulb is the saturation vapor pressure at $\overline{\theta_w}$, $e^*(\overline{\theta_h})$, and the water vapor pressure in the air that we wish to measure is $\overline{e_a}$. From (4.101),

$$-1 = \gamma \frac{\overline{\theta_w} - \overline{\theta_a}}{e^*(\overline{\theta_w}) - \overline{e_a}}$$

$$\overline{e_a} - e^*(\overline{\theta_w}) = -\gamma \left(\overline{\theta_a} - \overline{\theta_w} \right)$$

$$\overline{e_a} = e^*(\overline{\theta_w}) - \gamma \left(\overline{\theta_a} - \overline{\theta_w} \right). \tag{4.103}$$

4.8 – Atmosferas muito estáveis e muito instáveis

4.8.1 – Estratificação independente de z

The effect of atmospheric stability is to produce a restorative buoyancy force that tends to return vertically displaced air parcels to their equilibrium positions. Therefore, in a strongly stratified atmosphere, the buyancy term works to destroy turbulence kinetic energy (TKE). The stronger the stratification, the smaller the vertical excursions become, until a point when the distance to the zero-plane displacement, $z - d$, ceases to be a relevant scale to the problem. Another way of looking at this situation is to assume that the turbulence is independent of z, *i.e.*, that the turbulence is also *homogeneous* in the vertical.

The consequence of this situation in 3.64 then is that the derivatives with respect to z of $\overline{w'e'}$ and $\overline{w'p'}$ drop, and all remaining terms must become asymptoticall independent of z. This immediately implies that $\partial \overline{u}/\partial z = $ constant, so that mean velocity profile becomes linear. There must be transition, however, between neutral and very stable conditions, which are then given by the log-linear profile (4.67).

O mesmo raciocínio pode ser aplicado para as equações de balanço de $\overline{\theta'\theta'}$ e $\overline{q'q'}$, com o resultado de que $\partial\overline{\theta}/\partial z$ e $\partial\overline{q}/\partial z$ também são constantes em condições de estratificação independente de z. No que concerne aos momentos de ordem 2 em condições estáveis, a previsão teórica passa a ser

$$\phi_{ww} = \text{cte} \quad \phi_{\theta\theta} = \text{cte} \quad \phi_{qq} = \text{cte} \tag{4.104}$$

Isto está de acordo com as formas de (4.95) e (4.96) na região estável. Entretanto, evidências muito recentes (Pahlow et al., 2001) sugerem que estas funções de similaridade de Monin-Obukhov voltam a crescer para valores de ζ muito grandes.

4.8.2 – Convecção livre local

No topo da CS, a influência da produção de energia cinética turbulenta por gradiente tende a se reduzir, porque $\partial \overline{u}/\partial z \downarrow 0$, já que o perfil de velocidade tende a ser muito mais uniforme na camada convectiva CC sobrejacente; o mesmo acontece com a produção de variância $\overline{\theta'\theta'}$ e com o perfil de temperatura média $\overline{\theta}$. A importância da velocidade de atrito u_* nestas condições desaparece, e se torna necessário encontrar uma outra escala de velocidade representativa destas condições locais. Considere portanto um balanço de energia cinética turbulenta altamente simplificado e irrealista, no qual se retém entretanto uma característica física fundamental do topo da CS: a produção por empuxo e a dissipação molecular devem ser da mesma ordem de grandeza:

$$\frac{g}{\overline{\theta}_v} \overline{w'\theta'_v} \sim \epsilon_e \tag{4.105}$$

Ao multiplicarmos ambos os lados pela escala de comprimento z "natural" do problema, obtemos

$$1 \sim \frac{z\epsilon_e}{\left[\dfrac{zg\,\overline{w'\theta'_v}}{\overline{\theta}_v}\right]} \tag{4.106}$$

e agora, por analogia com $\phi_{\epsilon_e} = \kappa z \epsilon_e / u_*^3$ fica fácil identificar a escala convectiva de velocidade

$$w_f = \left[\frac{zg\,\overline{w'\theta'_v}}{\overline{\theta}_v}\right]^{1/3} \tag{4.107}$$

É preciso compreender que o conceito de convecção livre local não implica que $u_* = 0$, mas sim que a importância relativa do termo de produção de turbulência por gradiente é assintoticamente decrescente. De fato, $u_* \neq 0$ na CS sempre, e é possível formar o grupo adimensional

$$\frac{w_f}{u_*} = \frac{1}{\sqrt[3]{\kappa}} \left[\frac{\kappa z g u_* \theta_{v*}}{\overline{\theta}_v u_*^3}\right]^{1/3} = \frac{1}{\sqrt[3]{\kappa}} \left(\frac{-z}{L_O}\right)^{1/3} \tag{4.108}$$

Da mesma maneira que z, g, $\overline{w'\theta'_v}$ e $\overline{\theta}_v$ formam uma escala de velocidade convectiva w_*, z, g, $\overline{w'\theta'}$ e $\overline{\theta}$ são capazes de formar uma escala de temperatura convectiva, que nós chamaremos de ϑ_*. Para vermos isso, lançamos mão do balanço de variância de temperatura turbulento sem o termo de produção por gradiente,

$$-\frac{\partial \overline{w'\theta'\theta'}}{\partial z} - 2\epsilon_{\theta\theta} = 0 \tag{4.109}$$

Ambos os termos têm que ser estimados. Uma análise clássica de ordem de grandeza dos momentos turbulentos envolvidos (Tennekes and Lumley, 1972) fornece:

$$-\frac{\partial \overline{w'\theta'\theta'}}{\partial z} \quad \sim \quad \frac{\overline{w'\theta'}\,\vartheta_*}{z} \tag{4.110}$$

$$\epsilon_{\theta\theta} \quad \sim \quad \frac{w_* \vartheta_*^2}{z} \tag{4.111}$$

substituindo estas estimativas em (4.109) obtém-se

$$\vartheta_* = \left[\frac{(\overline{w'\theta'})^2 \overline{\theta}}{zg} \right]^{1/3} \tag{4.112}$$

Novamente, é possível relacionar a "nova" escala ϑ_* com a "velha" escala θ_*,

$$\frac{\vartheta_*}{\theta_*} = \kappa^{1/3} \left(\frac{-z}{L_O} \right)^{-1/3} \tag{4.113}$$

Vale a pena analisar o que acontece com diversas funções de similaridade neste limite; por exemplo,

$$\begin{aligned}
\phi_\tau &= \frac{\kappa z}{u_*} \frac{\partial \overline{u}}{\partial z} \\
&= \frac{\kappa z}{u_*} \frac{w_*}{w_*} \frac{\partial \overline{u}}{\partial z} \\
&= \frac{\kappa z}{w_*} \frac{\partial \overline{u}}{\partial z} \frac{1}{\sqrt[3]{\kappa}} (-\zeta)^{1/3} .
\end{aligned} \tag{4.114}$$

Se nós supusermos que w_* é uma grandeza natural para definir a escala do gradiente de velocidade média nesta região (Garratt (1994) faz o mesmo),

$$\frac{\partial \overline{u}}{\partial z} \sim \frac{w_*}{z} \tag{4.115}$$

e, no limite de convecção livre,

$$\phi_\tau(\zeta) = \text{cte}(-\zeta)^{1/3}. \tag{4.116}$$

No caso de ϕ_{H_v},

$$\begin{aligned}
\phi_{H_v} &= -\frac{\kappa z}{\theta_{v*}} \frac{\theta_{v*}}{\theta_{v*}} \frac{\partial \overline{\theta}_v}{\partial z} \\
&= -\frac{\kappa z}{\vartheta_*} \frac{\partial \overline{\theta}_v}{\partial z} (-\zeta)^{-1/3}.
\end{aligned} \tag{4.117}$$

Supondo, de forma análoga ao que fizemos com w_*, que ϑ_* é uma escala válida para o gradiente de temperatura potencial virtual nesta região,

$$\frac{\partial \overline{\theta}_v}{\partial z} \sim \frac{\vartheta_*}{z}, \tag{4.118}$$

donde

$$\phi_{H_v} = \text{cte}(-\zeta)^{-1/3}. \tag{4.119}$$

Da mesma forma, os momentos de 2ª ordem de w e θ_v produzem

$$\phi_{ww} = \frac{\overline{w'w'}}{w_*^2} \left(\frac{w_*}{u_*} \right)^2 = \text{cte} \left(\frac{-z}{L_O} \right)^{2/3} \tag{4.120}$$

$$\phi_{\theta\theta} = \frac{\overline{\theta'\theta'}}{\vartheta_*^2} \left(\frac{\vartheta_*}{\theta_*} \right)^2 = C_{\theta\theta}^2 \left(\frac{-z}{L_O} \right)^{-2/3} \tag{4.121}$$

Novamente, note que a forma de (4.95) e (4.96) é assintoticamente correta e corresponde às equações (4.95) e (4.96) acima.

Note também que w_* já tem a altura z "embutida" em sua definição; assim, enquanto que a Teoria de Similaridade de Monin-Obukhov trabalha com quatro escalas,

$$u_*, \quad \theta_{v*}, \quad g/\overline{\theta}_v \quad \text{e} \quad z,$$

em condições de convecção livre nós "perdemos" u_*, ficando com

$$g/\overline{\theta}_v, \quad z \quad \text{e} \quad \overline{w'\theta'_v}|_0.$$

Em particular, isto significa que

$$\frac{\overline{w'w'}}{w_*^2} = \text{cte} \quad \text{(e independente de } u_*\text{)}. \tag{4.122}$$

Consequentemente, não se pode mais usar $\overline{w'w'}$ para estimar u_* em condições de convecção livre.

4.9 – O método da variância

Existem muitas maneiras de calcular os fluxos τ, H e E a partir de medições micrometeorológicas. Nós já vimos duas delas: o método do balanço de energia – razão de Bowen, e o método de medição de perfis médios. Ambos utilizam apenas grandezas médias. A medição "direta" de fluxos consiste em medir as flutuações turbulentas w', u', θ' e q' com instrumentos de resposta rápida (frequências de medição típicas situam-se entre 10 e 100 Hz). Estas entretanto são medidas caras e difíceis, que ainda não podem ser feitas rotineiramente. Por outro lado, os métodos baseados em medição de perfis médios sofrem do fato de que as diferenças de temperatura $\overline{\theta_1} - \overline{\theta_2}$ na CS podem ser de apenas alguns décimos, ou mesmo centésimos, de Kelvin. "Um híbrido" muito interessante é a estimativa de u_* e θ_* por meios diferentes. Por exemplo, pode-se estimar u_* a partir de medidas de velocidade média do vento $\overline{u}$ em dois níveis, com 2 anemômetros, por meio de (4.78), e medir apenas as flutuações de temperatura θ', obtendo

$$\theta_* = \sqrt{\frac{\overline{\theta'\theta'}}{\phi_{\theta\theta}}} \tag{4.123}$$

e então calcular H por meio de (4.29). Este método, que é uma das variantes do método da variância (Tillman, 1972; Hicks, 1981; Wesely, 1988) obviamente envolve algumas iterações partindo do perfil logarítmico, da mesma forma que no caso de medição de perfis médios. Ele apresenta uma considerável economia em relação a medições turbulentas de fluxo, e é um candidato a um sistema contínuo de monitoramento de fluxos superficiais Kustas et al. (1994).

O método original de Tillman (1972) envolvia também o conhecimento da assimetria da temperatura:

$$\gamma_\theta \equiv \frac{\overline{\theta^3}}{\sigma_\theta^3}. \tag{4.124}$$

Tillman (1972) constatou que γ_θ depende de ζ. Supondo-se a validade da Teoria de Similaridade de Monin-Obukhov, isto pde ser previsto:

$$\begin{aligned}
\gamma_\theta &= \frac{\overline{\theta^3}}{\sigma_\theta^3} \\
&= \frac{\overline{\theta^3}}{\theta_*^3}\frac{\theta_*^3}{\sigma_\theta^3} \\
&= \phi_{\theta\theta\theta}\left[\phi_{\theta\theta}\right]^{-3/2}.
\end{aligned} \tag{4.125}$$

A relação obtida por Tillman é

$$\zeta = -A\exp(B\gamma_\theta), \tag{4.126}$$

com $A = 0{,}0137$, $B = 4{,}39$. Seja agora uma relação de variância para a temperatura na forma (Dias et al., 2009)

$$\frac{\sigma_\theta}{\theta_*} = A(1 + B|\zeta|)^{-1/3}; \tag{4.127}$$

rearranjando a equação:

$$\frac{\sigma_\theta}{H}\wp c_p u_* = A(1 + B|\zeta|)^{-1/3}$$
$$\sigma_\theta(1 + B|\zeta|)^{1/3} = A\frac{H}{\wp c_p u_*} \tag{4.128}$$

Mas

$$\begin{aligned}
\frac{1}{L} &= -\frac{\kappa g H}{\wp c_p \overline{\Theta} u_*^3} \Rightarrow \\
u_*^3 &= -\frac{\kappa g}{\overline{\Theta}}\frac{H}{\wp c_p}L \Rightarrow \\
u_* &= \left[\frac{\kappa g}{\overline{\Theta}}\right]^{1/3}\left[\frac{H}{\wp c_p}\right]^{1/3}(-L)^{1/3}.
\end{aligned} \tag{4.129}$$

Substituindo-se (4.129) em (4.128):

$$\begin{aligned}
\sigma_\theta(1 + B|\zeta|)^{1/3} &= A\frac{H}{\wp c_p}\left[\frac{\overline{\Theta}}{\kappa g}\right]^{1/3}\left[\frac{\wp c_p}{H}\right]^{1/3}\left[\frac{-1}{L}\right]^{1/3} \\
&= A\left[\frac{H}{\wp c_p}\right]^{2/3}\left[\frac{\overline{\Theta}}{\kappa g z}\right]^{1/3}\left[\frac{-z}{L}\right]^{1/3} \Rightarrow \\
\left[\frac{H}{\wp c_p}\right]^{2/3} &= \frac{\sigma_\theta}{A}(1 + B|\zeta|)^{1/3}\left[\frac{\kappa g z}{\overline{\Theta}}\right]^{1/3}\left[\frac{1}{|\zeta|}\right]^{1/3} \Rightarrow \\
\frac{H}{\wp c_p} &= \left[\left(\frac{\sigma_\theta}{A}\right)^3\left(\frac{\kappa g z}{\overline{\theta}}\right)\left(\frac{1 + B|\zeta|}{|\zeta|}\right)\right]^{1/2}.
\end{aligned} \tag{4.130}$$

Esta é uma equação quase milagrosa, pois ela mostra que é possível calcular H desde que se conheça σ_θ e $|\zeta|$, em condições instáveis. O método é interessante e promissor, e a questão é estendê-lo para outros escalares, e verificar qual é a melhor forma de se estimar ζ: se com a assimetria da própria medição de temperatura, ou se com dados da velocidade média $\overline{U}$ (ver esta última alternativa em Dias et al. (2009)).

4.10 – **Número de Richardson**

Considere a razão dos termos de produção de energia cinética turbulenta por empuxo e por gradiente:

$$R_f \equiv \frac{\frac{g}{\overline{\theta_v}} \overline{w'\theta_v'}}{\overline{u_i' u_k'} \frac{\partial \overline{u_i}}{\partial x_k}} ; \tag{4.131}$$

Se a turbulência é homogênea na horizontal e não há efeitos verticais significativos,

$$R_f = \frac{\frac{g}{\overline{\theta_v}} \overline{w'\theta_v'}}{\overline{w'u'} \frac{\partial \overline{u}}{\partial z} + \overline{w'v'} \frac{\partial \overline{v}}{\partial z}} . \tag{4.132}$$

Esta é a forma usual do *Número de Richardson para fluxos*. Agora, se supusermos que todos os fluxos turbulentos cinemáticos podem ser escritos em termos de uma difusividade turbulenta comum K,

$$\overline{w'\theta_v'} = K \frac{\partial \overline{\theta_v}}{\partial z}, \tag{4.133}$$

$$\overline{w'u'} = K \frac{\partial \overline{u}}{\partial z}, \tag{4.134}$$

$$\overline{w'v'} = K \frac{\partial \overline{v}}{\partial z}, \tag{4.135}$$

o número de Richardson se "transforma" em

$$R_g \equiv \frac{\frac{g}{\overline{\theta_v}} \frac{\partial \overline{\theta_v}}{\partial z}}{\left(\frac{\partial \overline{u}}{\partial z} \right)^2 + \left(\frac{\partial \overline{v}}{\partial z} \right)^2} . \tag{4.136}$$

Esta é a forma usual do *Número de Richardson para gradientes*.

5

Turbulence data processing

5.1 – The separation of the average and the fluctuation

There is no universally accepted methodology for the definition of what represents the "average" $\overline{a}$ and the fluctuation a' of a variable a measured in a turbulent flow. The usual practice is to perform some kind of filtering of the original measured data, $a(t)$, initially producing a component $\overline{a}(t)$, and then to extract the fluctuation $a'(t)$ by (3.14). The problem is that in practice there are many different ways to calculate $\overline{a}(t)$. Figure 5.1-a shows a series of CO_2 concentrations measured at 2 meters above a turf farm in Tijucas do Sul, PR, in 2011-02-17 between 10:30 and 10:40 h. This 10-minute series will be used to illustrate some of the most common averaging procedures in what follows.

Block averages. The block average was defined in (??). As we know, the value $\overline{a}$ calculated remains constant for $-T/2 < t < T/2$. The fluctuation $a'(t)$ is calculated around this constant average. Figure 5.2-a shows the fluctuations of CO_2 density after the extraction of a block average. Essentially, it is the same figure 5.1-a, with the average shifted to zero. Note the pronounced negative asymmetry of ρ_c'.

Running average. This is equation (??): the value of $\overline{a}(t)$ varies continuously over time, and the fluctuation $a'(t)$ is calculated around this variable value. Figure 5.1-b shows the running average calculated with $P = 2\,\text{min.}$. Note that, unless the data of 10 minutes earlier or later are available, is not possible to calculate the running average for $t < 1\,\text{min.}$ or for $t > 9\,\text{min.}$. At these ends, the running average is replaced by the block average of the first 2 minutes and the last 2 minutes.

Figure 5.2-b shows the extracted fluctuations around the mobile averaging.

Linear first-order recursive filter. This is one of the most widely used procedure, perhaps because it is equivalent to analog filtering of a signal using a RC circuit. For a continuous function, the linear first-order recursive filter 1 is the solution of the differential equation

$$\frac{d\overline{a}}{dt} + \frac{1}{P}\overline{a} = \frac{1}{P}a(t). \tag{5.1}$$

In 5.1, P is the filter's "window": in practice, recommendation (??) remains valid also for a recursive filter.
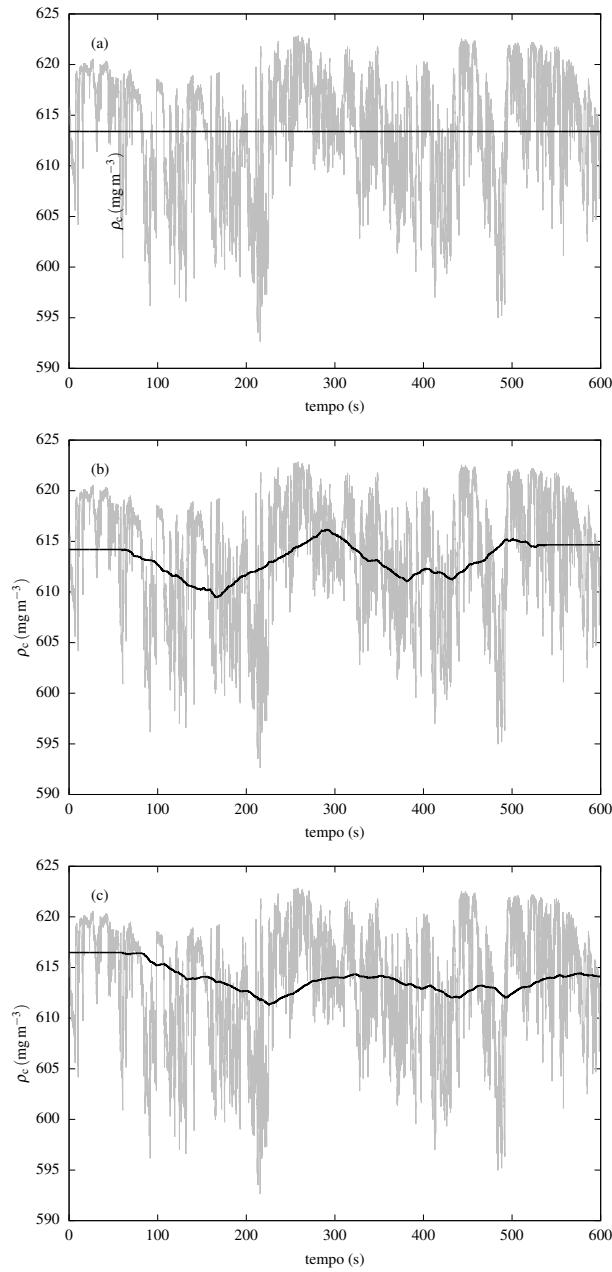
Figure 5.1: 10 minutes of CO_2 concentration measurements over a grass surface in Tijucas do Sul, PR, on 02/17/2011, 10:30 - 10: 40; (a) raw series and block average; (b) Running average with $P = 2\,\text{min}$. (c) Low-pass recursive filter with $P = 2\,\text{min}$..
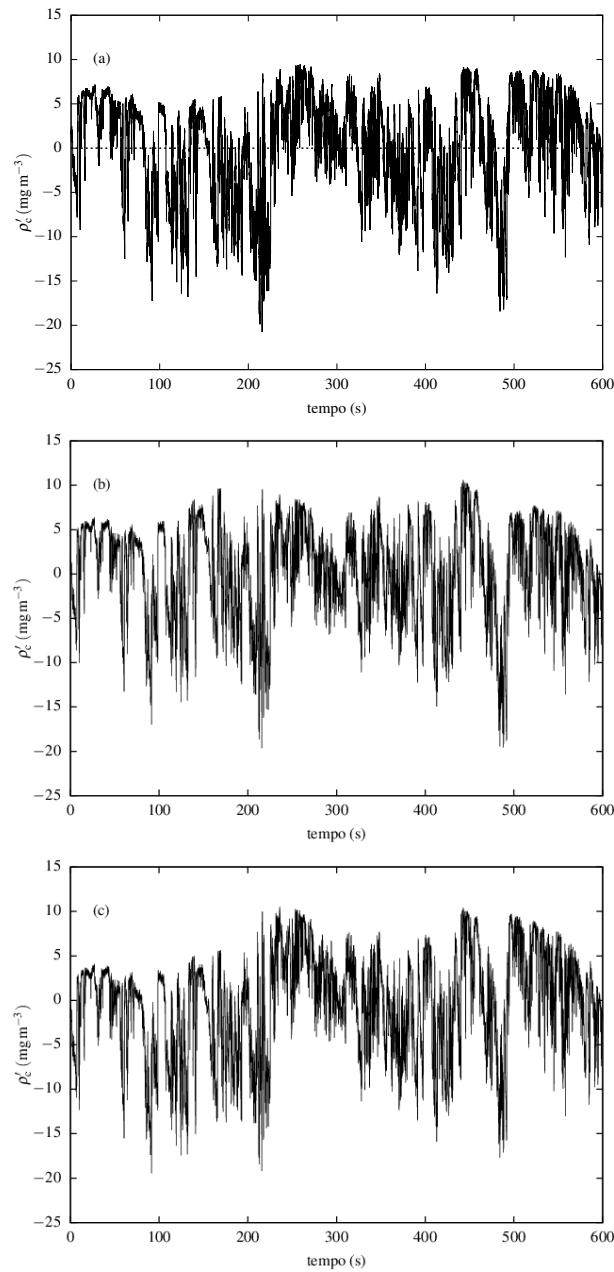
Figure 5.2: Fluctuations of ρ'_c: (a) around a block average; (b) around a running average of 2 minutes; (c) around a low-pass filter of 2 minutes.

Figure 5.1-c shows the resut of applying the recursive filter (low-pass) to the CO_2 series. The first minute is used to "warm up" the filter, with a block average (1 minute), during which the fluctuations are calculated around the constant average. After this time, we apply (5.1) in the discretized form

$$\overline{a}_{n+1} = \frac{\Delta t}{P} a_{n+1} + \left(1 - \frac{\Delta t}{P}\right) \overline{a}_n. \tag{5.2}$$

Figure 5.2-c shows the CO_2 fluctuations around the low-pass filter.

It's important to observe, in figure 5.2, that the fluctuations arising from the the different ways of calculating the average are *different* (although in this case it's hard to notice without close scrutiny). In particular, for the running averag and the low-pass filter, *the sample mean of the fluctuations is no longer identically null.* In these cases, it's common to do additional post-processing, subtracting the residual sample mean from these series.

The calculation of averages is ultimately subjective and the result of a personal decision. Consequently, what is considered "mean" and "fluctuation" varies according to the method used; the corresponding statistics will also vary, as well as turbulent fluxes like $\overline{w'\rho'_c}$.

5.2 – Coordinate rotation

The Monin-Obukhov similarity theory, MOST, assumes a stationary and horizontally homogeneous flow. Under these conditions, it is assumed that the average velocity vector is constant and strictly horizontal, and it is common practice to align the Ox axis with this direction. Therefore, it is usual to write

$$\overline{\boldsymbol{u}} = [\overline{u} \quad 0 \quad 0]^\top \tag{5.3}$$

for the coordinates of the average wind velocity. Horizontal homogeneity also implies that there are no Reynolds shear stresses in the directions xy and yz:

$$\overline{u'v'} = 0, \qquad \overline{v'w'} = 0. \tag{5.4}$$

Under these idealized conditions, the Reynolds tensor simplifies to

$$\boldsymbol{\tau} = \begin{bmatrix} \overline{u'u'} & 0 & \overline{u'w'} \\ 0 & \overline{v'v'} & 0 \\ \overline{u'w'} & 0 & \overline{w'w'} \end{bmatrix}. \tag{5.5}$$

Then, the turbulent stress vector in the horizontal plane whose normal is $\boldsymbol{k}$ is

$$\boldsymbol{t} = \boldsymbol{k}^\top \cdot \boldsymbol{\tau} = \begin{bmatrix} 0 & 0 & 1 \end{bmatrix} \begin{bmatrix} \overline{u'u'} & 0 & \overline{u'w'} \\ 0 & \overline{v'v'} & 0 \\ \overline{u'w'} & 0 & \overline{w'w'} \end{bmatrix} = \begin{bmatrix} \overline{u'w'} \\ 0 \\ \overline{w'w'} \end{bmatrix}. \tag{5.6}$$

Therefore, under ideal conditions, the horizontal component of $\boldsymbol{t}$ is aligned with $\overline{u}$. This makes sense physically, since we expect that the direction of the shear stresse is the same (with the opposite sign) as that of the wind velocity.

Given two successive rotation between the bases

$$E = (\boldsymbol{e}_1, \boldsymbol{e}_2, \boldsymbol{e}_3),$$
$$F = (\boldsymbol{f}_1, \boldsymbol{f}_2, \boldsymbol{f}_3), \qquad \text{e}$$
$$G = (\boldsymbol{g}_1, \boldsymbol{g}_2, \boldsymbol{g}_3),$$

the relations between the vectors of these bases are

$$\boldsymbol{f}_j = C_{ij}\boldsymbol{e}_i, \tag{5.7}$$
$$\boldsymbol{g}_k = D_{jk}\boldsymbol{f}_j = D_{jk}C_{ij}\boldsymbol{e}_i = C_{ij}D_{jk}\boldsymbol{e}_i, \tag{5.8}$$

where C and D are the respective rotation matrices. Therefore, the rotation matrix from E to G is the product

$$\boldsymbol{CD}$$

in this order. In Figure 5.3 we see two successive rotations: the first of an angle $+\alpha$ around z_E in the horizontal plane of basis E which aligns the horizontal wind velocity vector with the axis x_F; the second of a vertical angle β around y_F which aligns the "total" velocity vector of the average wind $\overline{\boldsymbol{u}}$ with the axis x_G.

The equations for the components of the rotation matrices are

$$C_{ij} = (\boldsymbol{e}_i \cdot \boldsymbol{f}_j), \tag{5.9}$$
$$D_{jk} = (\boldsymbol{f}_j \cdot \boldsymbol{g}_k). \tag{5.10}$$

In basis E, the coordinates of the vectors $\boldsymbol{e}_i$ and $\boldsymbol{f}_j$ are:

$$[1, 0, 0]^\top \qquad [0, 1, 0]^\top \qquad [0, 0, 1]^\top,$$
$$[\cos\alpha, \operatorname{sen}\alpha, 0]^\top \quad [-\operatorname{sen}\alpha, \cos\alpha, 0]^\top, \quad [0, 0, 1]^\top.$$

(Note that, in figure 5.3, the angle α is *positive*, because represents a positive rotation around z_E.) Therefore,

$$C = \begin{bmatrix} \cos\alpha & -\operatorname{sen}\alpha & 0 \\ \operatorname{sen}\alpha & \cos\alpha & 0 \\ 0 & 0 & 1 \end{bmatrix} \tag{5.11}$$

In basis F, the coordinates of the vectors $\boldsymbol{f}_j$ and $\boldsymbol{g}_k$ are:

$$[1, 0, 0]^\top \qquad [0, 1, 0]^\top \qquad [0, 0, 1]^\top,$$
$$[\cos\beta, 0, -\operatorname{sen}\beta]^\top \quad [0, 1, 0]^\top, \quad [\operatorname{sen}\beta, 0, \cos\beta]^\top.$$

(Note, in figure 5.3, that the angle β is *negative*, because it represents a negative rotation around y_F.) Therefore,

$$D = \begin{bmatrix} \cos\beta & 0 & \operatorname{sen}\beta \\ 0 & 1 & 0 \\ -\operatorname{sen}\beta & 0 & \cos\beta \end{bmatrix} \tag{5.12}$$

The "total" rotation matrix, given by the product $\boldsymbol{CD}$ will be

$$\begin{bmatrix} \cos\alpha\cos\beta & -\operatorname{sen}\alpha & \cos\alpha\operatorname{sen}\beta \\ \cos\beta\operatorname{sen}\alpha & \cos\alpha & \operatorname{sen}\alpha\operatorname{sen}\beta \\ -\operatorname{sen}\beta & 0 & \cos\beta. \end{bmatrix}$$
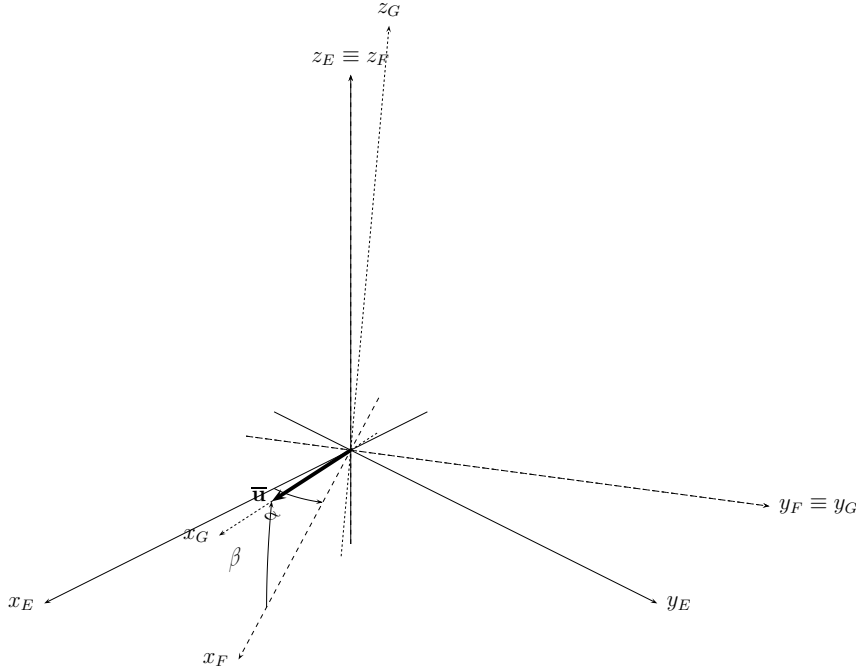
Figure 5.3: 2D coordinate rotation for the alignment of the wind velocity

Finally, the coordinates of the wind velocity vector in basis E, given by $[u, v, w]_E^\intercal$ will be rotated to basis G according to

$$\boldsymbol{u}_G = \boldsymbol{D}^\intercal \boldsymbol{C}^\intercal \boldsymbol{u}_E, \tag{5.13}$$

that is,

$$\begin{bmatrix} u \\ v \\ w \end{bmatrix}_G = \begin{bmatrix} \cos\alpha\cos\beta & \cos\beta\,\text{sen}\,\alpha & -\,\text{sen}\,\beta \\ -\,\text{sen}\,\alpha & \cos\alpha & 0 \\ \cos\alpha\,\text{sen}\,\beta & \text{sen}\,\alpha\,\text{sen}\,\beta & \cos\beta \end{bmatrix} \begin{bmatrix} u \\ v \\ w \end{bmatrix}_E. \tag{5.14}$$

The angles α and β are easily calculated from $\overline{u}$, $\overline{v}$ and $\overline{w}$ measured in basis E: typically, this is the reference system connected to a sonic anemometer installed in the field and carefully leveled, so that the axis z_E is as vertical as possible. These angles are

$$\alpha = +\,\text{arctg2}\left(\overline{v}_E, \overline{u}_E\right), \tag{5.15}$$

$$\beta = -\,\text{arctg2}\left(\overline{w}_E, \sqrt{\overline{u}_E^2 + \overline{v}_E^2}\right) \tag{5.16}$$

(remember that angle β is negative in figure 5.3). The function $\text{arctg2}(y, x)$ gives the angle formed with axis x by a two-dimensional vector (x, y) (notice to the order); in the programming languages C, MATLAB and Python, arctg2 is implemented as `atan2(y,x)`; in FORTRAN, as `ATAN2(Y,X)`.

The scalar fluxes should be rotated similarly. In particular, if η' is a density fluctuation, mixing ratio, temperature, etc., of a scalar, equation (5.14) is almost completely repeated:

$$\begin{bmatrix} \overline{u'\eta'} \\ \overline{v'\eta'} \\ \overline{w'\eta'} \end{bmatrix}_G = \begin{bmatrix} \cos\alpha\cos\beta & \cos\beta\,\text{sen}\,\alpha & -\,\text{sen}\,\beta \\ -\,\text{sen}\,\alpha & \cos\alpha & 0 \\ \cos\alpha\,\text{sen}\,\beta & \text{sen}\,\alpha\,\text{sen}\,\beta & \cos\beta \end{bmatrix} \begin{bmatrix} \overline{u'\eta'} \\ \overline{v'\eta'} \\ \overline{w'\eta'} \end{bmatrix}_E. \tag{5.17}$$

The change of basis for the Reynolds stress tensor is a little more elaborate. Defining the full tensor,

$$\boldsymbol{\tau} \equiv \overline{\boldsymbol{u'} \boldsymbol{u'}^{\mathsf{T}}} = \begin{bmatrix} \overline{u'u'} & \overline{u'v'} & \overline{u'w'} \\ \overline{v'u'} & \overline{v'v'} & \overline{v'w'} \\ \overline{w'u'} & \overline{w'v'} & \overline{w'w'} \end{bmatrix},$$ (5.18)

it follows from (5.13) that

$$\boldsymbol{\tau}_G = \boldsymbol{D}^{\mathsf{T}} \boldsymbol{C}^{\mathsf{T}} \boldsymbol{\tau}_E \boldsymbol{C} \boldsymbol{D}.$$ (5.19)

The coordinate rotations shown in this section form the basis of the data processing of scalar fluxes and momentum measured in micrometeorological experiments. A third rotation is possible, which makes $\overline{v'w'}_G = 0$, but its use is questionable and many authors consider it "non-physical" (Finnigan et al., 2003).

An more recent alternative, the *planar fit method* of Wilczak et al. (2001), decomposes the rotations in a sequence of two, one of them (analogous to the D rotation in this text) being applied to every micrometeorological block available followed by a rotation (analogous to the C rotation in this text) applied separetely to each block, to align the horizontal wind vector with the final x axis. According to the authors, the method minimizes the errors in the calculation of the turbulent shear stresses. The method calculates a mean offset in the vertical axis (typically smaller then the accuracy of the sonic anemometers) with a least squares method, and it has been gaining wide acceptance.

5.2.1 – The WPL correction for the average vertical velocity

A quick inspection of table 2.1 shows that $\rho_c \ll \rho$, and that

$$\rho \approx \rho_d + \rho_v$$ (5.20)

is an excellent approximation. The state equation for air will be (approximately)

$$p = [\rho_d R_d + \rho_v R_v] T.$$ (5.21)

Now, applying the Reynolds decomposition to all of the quantities in (5.21), and neglecting the higher-order products of fluctuations, we have

$$\begin{aligned} \overline{p} + p' &= (\overline{\rho}_d + \rho'_d) R_d (\overline{T} + T') + (\overline{\rho}_v + \rho'_v) R_v (\overline{T} + T') \\ &= (\overline{\rho}_d R_d + \overline{\rho}_v R_v) \overline{T} + \overline{\rho}_d R_d T' + \rho'_d R_d \overline{T} + \overline{\rho}_v R_v T' + \rho'_v R_v \overline{T}. \end{aligned}$$ (5.22)

This allows an obvious interpretation for $\overline{p}$ and p':

$$\overline{p} = (\overline{\rho}_d R_d + \overline{\rho}_v R_v) \overline{T},$$ (5.23)

$$p' = (\overline{\rho}_d R_d + \overline{\rho}_v R_v) T' + \overline{T} (R_d \rho'_d + R_v \rho'_v).$$ (5.24)

Making the observation that, in the surface layer, the pressure fluctuation can be neglected *vis-à-vis* the temperature and density fluctuations (Fleagle and Businger, 1980) (see also the discussion leading to (3.50)),

$$0 = (\overline{\rho}_d R_d + \overline{\rho}_v R_v) T' + \overline{T} (R_d \rho'_d + R_v \rho'_v).$$ (5.25)

Multiplying (5.25) by the vertical velocity fluctuation w', taking a time average average and using Reynolds' postulates, we obtain

$$0 = (\overline{\rho}_d R_d + \overline{\rho}_v R_v)\overline{w'T'} + \overline{T}(R_d\overline{w'\rho'_d} + R_v\overline{w'\rho'_v}). \tag{5.26}$$

Note here a difficulty in this derivation: as already mentioned, strictly speaking, the Reynolds postulates do not apply fully to the block and running averages — see (??) and (??)–(??) — and its approximate validity must be assumed. To the best of our knowledge, a detailed analytical evaluation of the effects of these approximations hasn't been done.

Equation (5.26) plays a central role in the WPL approximation. In fact, applying Reynolds's decomposition to (4.19),

$$\overline{w\rho_d} = \overline{w}\,\overline{\rho_d} + \overline{w'\rho'_d} = 0 \Rightarrow$$
$$\overline{w} = -\frac{\overline{w'\rho'_d}}{\overline{\rho_d}}. \tag{5.27}$$

Note that $\overline{w}$ can be effectively calculated from (5.26)–(5.27), using measurements of $\overline{w'T'}$ and of $\overline{w'\rho'_v}$. A fact rarely mentioned is that the WPL correction stems from the hypothesis of a non-null value of $\overline{w}$; however, in most measurements turbulent fluxes using the eddy covariance method, it is common to apply a coordinate rotation, whose effect is precisely to force $\overline{w} = 0$. This produces an apparent conflict between simultaneous application of the coordinate rotation and the WPL correction (Massman and Lee, 2002; Dias et al., 2007). However, notice also that the vertical velocity value $\overline{w}$ estimated by the WPL correction is *very small*; in fact, it is smaller than the accuracy of the measurements using sonic anemometers (Finnigan, 2009). In practice, therefore, the procedure of first applying a coordinate rotation that makes $\overline{w} = 0$, and *then* applying the WPL correction which is equivalent to stipulate a small value of $\overline{w}$ — too small to be measured with the currently available measuring instruments — is justifiable.

Continuing, now we will calculate the water vapor mass flux taking into account (5.27), this is, taking into account the WPL correction.

For the water vapor mass flux E, start from (4.20) and apply the Reynolds decomposition:

$$E = \overline{w\rho_v} = \overline{w}\,\overline{\rho_v} + \overline{w'\rho'_v}. \tag{5.28}$$

Typically, the eddy covariance method generates the second term in (5.28); the WPL correction consists of calculating, and adding, the first term. For this, we calculate $\overline{w}$ explicitly. From (5.26),

$$\overline{w'\rho'_d} = -\frac{1}{\overline{T}}\left[\overline{\rho_d} + \frac{R_v}{R_d}\overline{\rho_v}\right]\overline{w'T'} - \frac{R_v}{R_d}\overline{w'\rho'_v} \Rightarrow$$
$$\overline{w} = \frac{1}{\overline{\rho_d}}\left\{\frac{1}{\overline{T}}\left[\overline{\rho_d} + \frac{R_v}{R_d}\overline{\rho_v}\right]\overline{w'T'} + \frac{R_v}{R_d}\overline{w'\rho'_v}\right\}. \tag{5.29}$$

Putting $\mu = R_v/R_d$, and taking expression (5.28) to E,

$$
\begin{aligned}
E &= \frac{\overline{\rho_v}}{\overline{\rho_d}} \left\{ \frac{1}{\overline{T}} \left[\overline{\rho_d} + \frac{R_v}{R_d}\overline{\rho_v} \right] \overline{w'T'} + \frac{R_v}{R_d}\overline{w'\rho_v'} \right\} + \overline{w'\rho_v'} \\
&= \overline{\rho_v} \left\{ \left(1 + \mu\frac{\overline{\rho_v}}{\overline{\rho_d}} \right) \frac{\overline{w'T'}}{\overline{T}} \right\} + \frac{\overline{\rho_v}}{\overline{\rho_d}}\mu\overline{w'\rho_v'} + \overline{w'\rho_v'} \\
&= \overline{\rho_v} \left(1 + \mu\overline{r_v} \right) \frac{\overline{w'T'}}{\overline{T}} + \left(1 + \mu\overline{r_v} \right) \overline{w'\rho_v'} \\
&= \left(1 + \mu\overline{r_v} \right) \left[\overline{w'\rho_v'} + \overline{\rho_v}\frac{\overline{w'T'}}{\overline{T}} \right],
\end{aligned}
\tag{5.30}
$$

where

$$
\overline{r_v} = \frac{\overline{\rho_v}}{\overline{\rho_d}}
\tag{5.31}
$$

is the mixing ratio for water vapor. Equation (5.30) is the expression obtained by Webb et al. (1980) for the correction of the water vapor turbulent flux.

Now, proceeding to the case of a greenhouse gas such as CO_2, start from (4.21) and apply the Reynolds decomposition:

$$
\begin{aligned}
F_c &= \overline{w}\,\overline{\rho_c} + \overline{w'\rho_c'} \\
&= \left\{ -\frac{\overline{w'\rho_d'}}{\overline{\rho_d}} \right\} \overline{\rho_c} + \overline{w'\rho_c'} \\
&= -\frac{\overline{\rho_c}}{\overline{\rho_d}} \left\{ -\frac{1}{\overline{T}}(\overline{\rho_d} + \mu\overline{\rho_v})\overline{w'T'} - \mu\overline{w'\rho_v'} \right\} + \overline{w'\rho_c'} \\
&= \overline{r_c} \left[\overline{\rho_d}(1 + \mu\overline{r_v})\frac{\overline{w'T'}}{\overline{T}} + \mu\overline{w'\rho_v'} \right] + \overline{w'\rho_c'} \\
&= \frac{\overline{\rho_c}}{\overline{\rho_d}}\overline{\rho_d}(1 + \mu\overline{r_v})\frac{\overline{w'T'}}{\overline{T}} + \mu\overline{r_c}\,\overline{w'\rho_v'} + \overline{w'\rho_c'} \\
&= \overline{\rho_c}(1 + \mu\overline{r_v})\frac{\overline{w'T'}}{\overline{T}} + \mu\overline{r_c}\,\overline{w'\rho_v'} + \overline{w'\rho_c'},
\end{aligned}
\tag{5.32}
$$

where

$$
\overline{r_c} = \frac{\overline{\rho_c}}{\overline{\rho_d}}
\tag{5.33}
$$

it is the mixing ratio for CO_2.

For measurements of greenhouse gases fluxes, it is essential to apply the WPL correction.

6

Energy fluxes at the surface of the Earth

6.1 – The movement of the Earth

The Earth goes around the Sun in a trajectory that is approximately elliptical. The plane of the trajectory is called the ecliptic plane. In figure 6.1, the distance OA = r_0 is the major semi-axis of the ellipse. It is a unit of length in astronomy: the Astronomical Unit (AU).

The points A, B, C, D, A′, B′, C′ and D′ are outstanding points of the annual movement of the planet around the Sun. A marks the perihelion, the point where the planet is closest to the Sun. By the same token, C marks the afelion, the point where the planet is farthest from the Sun. The dates for these points vary slightly from year to year. Table 6.1, valid for 2020; it has been retrieved from United States Naval Observatory (2022).

The material described here has been collected from several points. Perhaps the most authoritative is the paper by van Flandern and Pulkkinen (1979), and a very detailed guide for the calculation of the Sun's declination and the distance Sun-Earth can be found in Schlyter (2019).

In figure 6.1, the semi-major axis of the ellipse is r_a, and the semi-minor axis is r_b. The distance between the Sun and the Earth at any point in the trajectory is r. The value of r_a is defined in Astronomy as the *Astronomical Unit*, AU. The Sun's *declination* with respect to the Earth is the angle δ between the plane of the Equator and the plane of the Ecliptic, measured perpendicularly to the latter.

Table 6.1: Outstanding days in the Earth's orbit for 2020.

Point	date/time (UTC)	Name
A	January 5, 2020, 07:48	Perihelion
B	April 5, 2020, 19:48	$r/r_a = 1$
C	July 4, 2020, 11:35	Aphelion
D	October 5, 2020,19:48	$r/r_a = 1$
A′	December 21, 2020, 10:02	Winter Solstice
B′	March 20, 2020, 03:50	Spring Equinox
C′	June 20, 2020, 21:44	Summer Solstice
D′	September 22, 2020, 13:31	Autumn Equinox
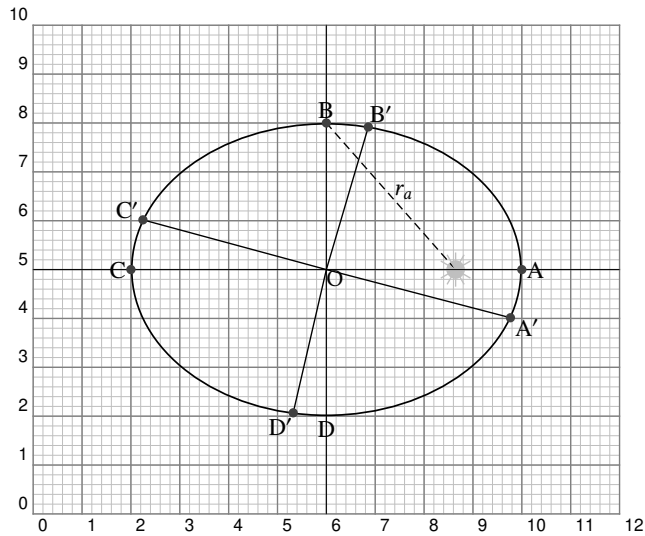
Figure 6.1: The Earth's trajectory around the Sun.
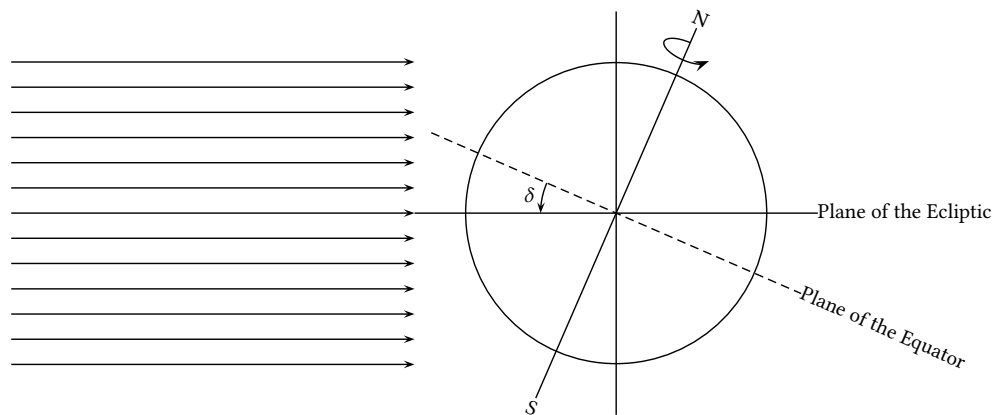
Figure 6.2: The position of the planet Earth with respect to the incidence of the Sun's rays around the Northern Hemisphere Solstice.

The cause for the changing seasons is not the variation in the distance Sun-Earth r, but rather the inclination of the axis of rotation of the planet in relation to the plane of the ecliptic, and the consequent change in the Sun's declination.

For example, figure 6.2 shows the situation of the planet with respect to the incidence of the Sun's rays around the Winter Solstice (Norther Hemisphere). At this point in the planet's trajectory, most of that incidence is on the Southern Hemisphere, where it is the begginning of Summer. The opposite situation will happen around the Summer Solstice (Norther Hemisphere).
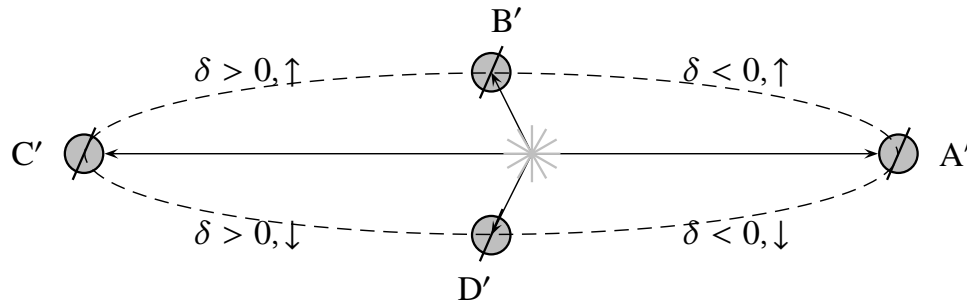
Figure 6.3: The incidence of the rays of the Sun on the Earth around the year. The sign of the Sun's declination δ is indicated between the points A′, B′, C′ and D′, as well as the sign of its rate of change, indicated as positive (↑) or negative (↓).

The situation around the year is shown in Figure 6.3. Note that the figure is not drawn accurately; it does however show the essential elements in terms of how the Sun's rays' incidence changes around the year. The 4 points emphasized are the solstices and the equinoxes. During the solstices, the Sun's rays are at maximum incidence on either hemisphere, and this determines the beginning of Summer and Winter. On the other hand, at the equinoxes, the Sun's rays fall perpendicularly to the Equator (hence their names).

Relatively low precision formulae for the values of δ and r/r_a at a given date are given by van Flandern and Pulkkinen (1979). These formulae are converted into a Python function (ddse) in listing 6.1.

Listing 6.1: `sunearth.py` — Calculation of distance and declination of Sun as a function of date.

```
1   from math import pi, modf, sin, cos, asin, sqrt, atan2
2   TwoPi = 2*pi
3   # -------------------------------------------------------------------
4   # ddse
5   #
6   # version: 2019-05-04T13:46:15
7   #
8   # -------------------------------------------------------------------
9   def ddse(yea,mon,day):
10      '''
11      ddse: declination and distance sun-earth a funcion of
12      (year, month, day)
13
14      based on
15
16      Van Flandern, T. C. and Pulkkinen, K. F. (1979) "Low Precision
17      Formulae for Planetary Positions" - The Astronomical Journal
18      Supplement Series, 41,391:411.
19      '''
20   # -------------------------------------------------------------------
21      assert(isinstance(yea,int))
22      assert(isinstance(mon,int))
23      assert(isinstance(day,int))
24   # -------------------------------------------------------------------
25   # At GMT noon: this is done with purely integer arithmetic
26   # -------------------------------------------------------------------
27      JD = 367 * yea - ( 7 * (yea + (mon + 9) // 12 ) // 4 ) \
28          + ( 275 * mon // 9 + day ) + 1721014
29      # JD = + 367 * yea \
30      #       - 7*(yea + (mon + 9)//12)/4 \
```

```
31     #          - 3*((yea + (mon - 9)//7)//100 + 1)//4 \
32     #          + 275*mon//9 + day + 1721029
33   # -------------------------------------------------------------------
34   # Obtains tee,
35   # TT == thousands of Julian years from 2000
36   # TC == hundreds of Julian years from 1900
37   # -------------------------------------------------------------------
38     tee = float(JD - 2451545.0 + 0.5) ;
39   #   TT = tee/365250.0
40     TC = tee/36525.0 + 1.0 ;
41   #   TC = 10.0*TM + 1.0
42   # -------------------------------------------------------------------
43   # other variables
44   # -------------------------------------------------------------------
45     LS = 0.779072 + 0.00273790931 * tee  # mean longitude, Sun
46     GS = 0.993126 + 0.00273777850 * tee  # mean anomaly, Sun
47     G5 = 0.056531 + 0.00023080893 * tee  # mean anomaly, Jupiter
48     OM = 0.347343 - 0.00014709391 * tee  # longitude of lunar ascending mode
49   # -------------------------------------------------------------------
50   # the eccentricity of the Earth comes from a different source:
51   # http://www.jgiesen.de/kepler/eccentricity.html
52   # -------------------------------------------------------------------
53   # ec = +0.0167086342 - 0.0004203654*TT - 0.0000126734*TT**2 \
54   #      +0.0000001444*TT**3 -0.0000000002*TT**4 + 0.0000000003*TT**5
55   # -------------------------------------------------------------------
56   # extracts fractional part
57   # -------------------------------------------------------------------
58     (LS,ipart) = modf(LS)
59     (GS,ipart) = modf(GS)
60     (G5,ipart) = modf(G5)
61     (OM,ipart) = modf(OM)
62   # -------------------------------------------------------------------
63   # converts to radians
64   # -------------------------------------------------------------------
65     LS = LS * TwoPi
66     GS = GS * TwoPi
67     G5 = G5 * TwoPi
68     OM = OM * TwoPi
69   # -------------------------------------------------------------------
70   # obtains VS
71   # -------------------------------------------------------------------
72     VS = + 0.39785 * sin( LS ) \
73          - 0.01000 * sin( LS - GS ) \
74          + 0.00333 * sin( LS + GS ) \
75          - 0.00021 * TC * sin( LS ) \
76          + 0.00004 * sin( LS + 2.0 * GS ) \
77          - 0.00004 * cos( LS ) \
78          - 0.00004 * sin( OM - LS ) \
79          + 0.00003 * TC * sin( LS - GS )
80   # -------------------------------------------------------------------
81   # obtains US
82   # -------------------------------------------------------------------
83     US = + 1.0 \
84          - 0.03349 * cos( GS ) \
85          - 0.00014 * cos( 2.0 * GS ) \
86          + 0.00008 * TC * cos( GS ) \
87          - 0.00003 * sin( GS - G5 )
88   # -------------------------------------------------------------------
89   # Sun's declination
90   # -------------------------------------------------------------------
91     delta = asin( VS / sqrt(US) ) ;
92   # -------------------------------------------------------------------
93   # distance Sun-Earth in the form (r/a) where a is the length
94   # of the largest semi-axis of the Earth's orbit, i.e.: the equivalent
95   # to one astronomical unit, and r is the Sun-Earth distance
96   # -------------------------------------------------------------------
97     rr = 1.00021 * sqrt( US )
98     return (delta,rr)
99
100  # -------------------------------------------------------------------
101  # sunman
102  #
103  # version of 2019-04-23T09:58:05
```

```
104  # ----------------------------------------------------------------
105  def sunman(yea,mon,day,sec=0.0):
106      '''
107      sunman: only the sun mean anomaly a funcion of (year, month,day)
108
109      based on
110
111      Van Flandern, T. C. and Pulkkinen, K. F. (1979) "Low Precision
112      Formulae for Planetary Positions" - The Astronomical Journal
113      Supplement Series, 41,391:411.
114      '''
115  # ----------------------------------------------------------------
116      assert(isinstance(yea,int))
117      assert(isinstance(mon,int))
118      assert(isinstance(day,int))
119  # ----------------------------------------------------------------
120  # At GMT noon: this is done with purely integer arithmetic
121  # ----------------------------------------------------------------
122      JD = + 367 * yea \
123           - 7*(yea + (mon + 9)/12)/4 \
124           - 3*((yea + (mon - 9)/7)/100 + 1)/4 \
125           + 275*mon/9 + day + 1721029
126  # ----------------------------------------------------------------
127  # trying to get more accuracy by calculating seconds
128  # ----------------------------------------------------------------
129      JD = float(JD + sec/86400.0)
130  # ----------------------------------------------------------------
131  # Obtains tee,
132  # ----------------------------------------------------------------
133      tee = float(JD - 2451545.0) ;
134  # ----------------------------------------------------------------
135  # other variables
136  # ----------------------------------------------------------------
137      GS = 0.993126 + 0.00273777850 * tee  # mean anomaly, Sun
138      (GS,ipart) = modf(GS)
139  # ----------------------------------------------------------------
140  # converts to radians
141  # ----------------------------------------------------------------
142      GS = GS * TwoPi
143      return(GS)
```

6.2 – The declination of the Sun seen from the Earth

Figure 6.4 shows the incidence of the Sun's rays seen from the Earth. The plane of the Equator is Oxy, and Oyz is perpendicular to the plane of the Ecliptic, which is not shown, but contains the line OS connecting the center of the Earth to the center of the Sun: the Sun's declination δ is the angle between the planes of the Ecliptic and the Equator, and is indicated in the figure. Because the Sun is very far away, all rays can be assumed to be parallel. At point P on the surface of the Earth, a ray comes along PS′, and the Sun is effectively seen as in position S′. The position of P is given by the *hour angle h*, which is the angular distance to the solar noon, and the latitude φ.

The vertical through P is given by the unit vector $\boldsymbol{n}$, and the direction towards the Sun at P is given by the unit vector $\boldsymbol{m}$. By definition, the Zenith angle Z is the angle between $\boldsymbol{m}$ and $\boldsymbol{n}$. From figure 6.4, one obtains

$$\boldsymbol{m} = (0, \cos\delta, \sin\delta), \tag{6.1}$$

$$\boldsymbol{n} = (\cos\varphi\sin h, \cos\varphi\cos h, \sin\varphi), \tag{6.2}$$

whence

$$\boldsymbol{m} \cdot \boldsymbol{n} = \cos Z = \cos\delta\cos\varphi\cos h + \sin\delta\sin\varphi. \tag{6.3}$$

Several useful relationships can be derived with the help of (6.3):
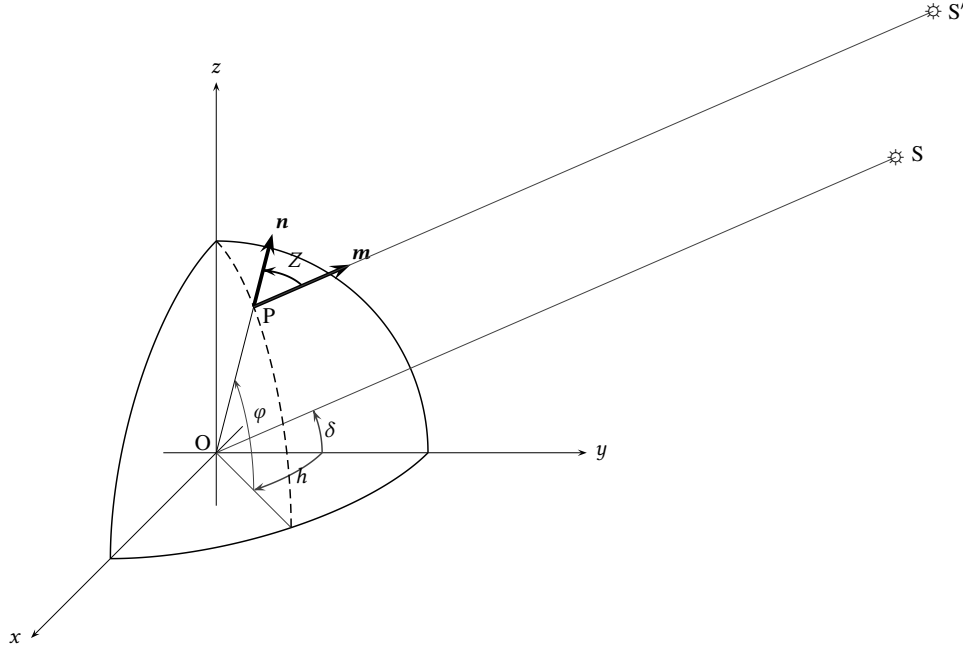
Figure 6.4: The declination of the Sun.

a) The angle H covered between sunrise, when $\boldsymbol{n} \parallel Oxz$ and $\cos Z = 0$, and the solar noon is given by

$$0 = \cos \delta \cos \varphi \cos H + \sin \delta \sin \varphi \;\Rightarrow$$
$$\cos H = -\operatorname{tg} \varphi \operatorname{tg} \delta. \tag{6.4}$$

From (6.4) one obtains the length of daylight in hours, N:

$$\frac{H}{\pi/2} = \frac{N}{12} \qquad \Rightarrow \qquad N = \frac{24H}{\pi}. \tag{6.5}$$

b) The latitude φ_p of the polar night is the point where $H = 0$:

$$\operatorname{tg} \varphi_p = -\cot g\, \delta \qquad \Rightarrow \qquad \varphi_p = \frac{\pi}{2} - \delta. \tag{6.6}$$

c) At the poles,

$$\cos Z = \sin \delta \qquad \Rightarrow \qquad \frac{\pi}{2} - Z = \delta,$$

so that the Sun's elevation is practically constant during the day.

d) The zenith angle at solar noon Z_0, is given by

$$h = 0 \;\Rightarrow\; \cos h = 1,$$
$$\cos Z_0 = \cos \delta \cos \varphi + \sin \delta \sin \varphi$$
$$= \cos(\varphi - \delta) \;\Rightarrow$$
$$Z_0 = \begin{cases} \varphi - \delta, & \varphi > 0, \\ \delta - \varphi, & \varphi < 0. \end{cases} \tag{6.7}$$
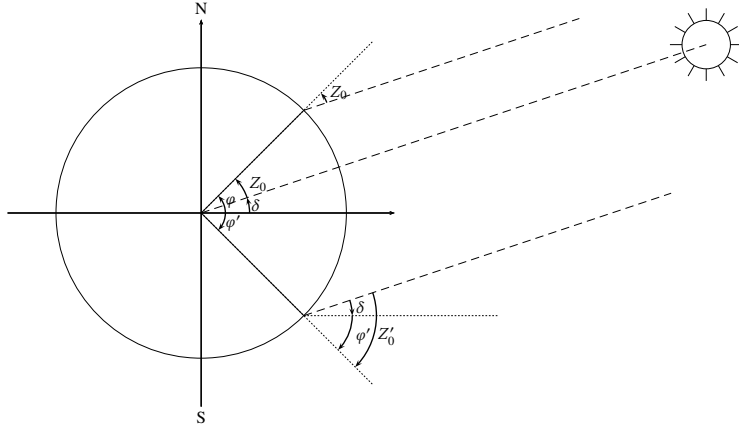
Figure 6.5: The calculation of the zenith angle at solar noon in the Northern and Southern hemispheres.

To understand (6.7), look at figure 6.5. Since $h = 0$, we are now seeing the plane yz of the Earth. All rays coming from the Sun, very far away, are essentially parallel. To fix ideas, we call the latitude and the zenith angle in the Northern hemisphere φ and Z_0, and in the Southern hemisphere φ' and Z_0'. Now straightforward geometry shows that $Z_0 = \varphi - \delta$, and $Z_0' = \delta - \varphi'$, because the latitude $\phi' < 0$ in the Southern hemisphere.

6.3 – Radiaton

The flux of energy per unit area associated with different wavelengths is called *irradiance*, and given in units of W m^{-2} in the SI. The wavelength of the radiation depends on the temperature of the emitting body; at temperature T, a black body emits a spectrum of radiation whose peak is given by Wien's law,

$$\lambda_m = \frac{\alpha}{T}, \tag{6.8}$$

where $\alpha = 2897.0\,\mu\text{m K}$ (Fleagle and Businger, 1980, p. 217).

Solar radiation, emmited by the Sun at a temperature close to $6\,000\,\text{K}$, covers a range of wavelengths $\lambda \sim 0.3\text{–}3\,\mu m$, and reaches the top of the atmosphere of the Earth. The *solar constant* $R_{s0} \approx 1354\,\text{W m}^{-2}$ is the irradiance in the direction of the Sun's rays at a distance of $1\,\text{AU} = r_a$ of the Sun. The irradiance on a direction perpendicular to the top of the Atmosphere at a given day and latitude is the *extra-atmospheric solar irradiance*, and is given by

$$R_{sea} = R_{s0} \left(\frac{r_a}{r}\right)^2 \cos Z. \tag{6.9}$$

The mean value of R_{sea} over 24 hours is a useful quantity, that can later be used to estimate the solar irradiance reaching the surface of the Earth.

$$R_{sea}(t) = R_{s0} \left(\frac{r_a}{r}\right)^2 [\sin\delta\sin\varphi + \cos\delta\cos\varphi\cos h(t)] \,;$$

$$\langle R_{sea} \rangle = \frac{1}{D} \int_0^T R_{sea}(t)\,\mathrm{d}t, \tag{6.10}$$

where $D = 86400\,\mathrm{s}$ is the duration of the day, and T is the duration of sunlight, with time t measured from sunrise to sunset. But

$$D = \frac{2\pi}{\omega}, \tag{6.11}$$

$$\omega\mathrm{d}t = \mathrm{d}h, \tag{6.12}$$

where ω is the angular velocity of Earth, whence

$$\langle R_{sea} \rangle = \int_{-H}^{+H} \frac{\omega}{2\pi} R_{s0} \left(\frac{r_a}{r}\right)^2 [\sin\delta\sin\varphi + \cos\delta\cos\varphi\cos h(t)] \frac{\mathrm{d}h}{\omega}$$

$$= \left(\frac{r_a}{r}\right)^2 \frac{R_{s0}}{\pi} [H\sin\delta\sin\varphi + \cos\delta\cos\varphi\sin H] \,. \tag{6.13}$$

The solar or *short wave* irradiance R_s reaching the surface of the Earth is most of the time less than R_{sea}. Ideally, it should be measured directly with *piranometers*, but historically it has been estimated by measurements of *bright sunshine duration* n (usually in hours), through Prescott's equation (Brutsaert, 1982):

$$\langle R_s \rangle = \langle R_{sea} \rangle \left[a + b\frac{n}{N}\right], \tag{6.14}$$

with $a \sim 0.25$ and $b \sim 0.50$. Note that Prescott's equation is not able to predict values of R_s at a timescale of $\sim 1\,\mathrm{h}$, only at the 24-hour mean, because the duration of bright sunshine is an integrated measurement.

Besides solar radiation, the surface of the Earth also receives radiation emmited by the atmosphere, over wavelengths $\lambda \sim 3$–$100\,\mu m$, due to the fact that the emmiting sources are at temperatures of the order of $300\,\mathrm{K}$. This *longwave* or *atmospheric* irradiance reaching the surface is R_a. Finally, the surface itself re-emits radiation back to the atmosphere; this is the emitted irradiance R_e.

The ratio of the reflected to the incoming solar irradiance is the *albedo* α of the surface; and the ratio of the absorbed to the incoming atmospheric irradiance is the *absortivity/emissivity* ϵ of the surface. The *net* irradiance is the total energy flux per unit area absorbed the the surface:

$$R_n = R_s(1 - \alpha) + \epsilon R_a - R_e. \tag{6.15}$$

6.4 – Atmospheric radiation

The estimation of incoming atmospheric (longwave) irradiance is a complicated business. It is usually split into two parts: the estimation of clear-sky atmospheric irradiance, R_{ac}, and the estimation of the increase due to the presence of clouds. Clear-sky atmospheric irradiance is usually obtained from equations with the form

$$R_{ac} = \epsilon_{ac}\sigma T_a^4. \tag{6.16}$$

(6.16) is obviously inspired by Stefan-Boltzmann's law for a gray body. It appears to have had a strictly empirical origin in the work of Brunt (1932), in the form

$$\epsilon_{ac} = 0.52 + 0.0065\sqrt{e_a} \tag{6.17}$$

(in SI units), but can be obtained from equations for radiative transfer in the atmosphere under certain simplifying assumptions. Perhaps the clearest, and one of the simplest, ways to derive it can be found in Brutsaert (1975). In principle, the longwave radiation reaching the surface can be found by integrating Schwarzschild's equation

$$dI_\lambda = -k_\lambda(I_\lambda - B_\lambda(T)), \tag{6.18}$$

but an alternative that yields a faster analytical result is

$$R_{ac} = \int_0^\infty \sigma T^4 \frac{d\epsilon_f}{du} du. \tag{6.19}$$

Consider now an exponential distribution for the temperature in the atmosphere,

$$T(z) = T_0 \exp\left(-\frac{\gamma z}{T_0}\right) \tag{6.20}$$

with $\gamma = 6.5\,\mathrm{K\,km^{-1}}$ and $T_0 = 288.15\,\mathrm{K}$. To a first approximation,

$$\frac{dT}{dz} = -\gamma, \tag{6.21}$$

so that

$$p = \rho R_d T, \tag{6.22}$$

$$dp = -\rho g dz, \tag{6.23}$$

$$\frac{dp}{p} = \frac{g}{R_d T} dz = \frac{g}{\gamma R_d} \frac{dT}{T}, \tag{6.24}$$

$$\frac{p}{p_0} = \left(\frac{T}{T_0}\right)^{\frac{g}{\gamma R_d}}. \tag{6.25}$$

For water vapor,

$$e_0 = \rho_{v0} R_v T,$$

$$\rho_{v0} = \frac{e_0}{R_v T_0},$$

$$\rho_v(z) = \rho_{v0} \exp(-k_w z), \tag{6.26}$$

with $k_w = 4.4 \times 10^{-4}\,\mathrm{m^{-1}}$. In Brutsaert (1975), the effective emissivity ϵ_f is written as a function of optical path

$$u = \int_0^z \rho_v(\zeta)\left(\frac{p}{p_0}\right)^{1/2} d\zeta \tag{6.27}$$

as

$$\epsilon_f = Aa^m, \tag{6.28}$$

with $A = 0.75$, $m = 1/7$ and

$$a = \frac{u}{\rho_w} \tag{6.29}$$

in cm of equivalent water (with $\rho_w = 1\,\mathrm{g\,cm^{-3}}$). It seems preferable, however, to use a version in which dimensionless factors appear more clearly. Therefore, let us put

$$\epsilon_f = \left(\frac{u}{u_0} \right)^m . \tag{6.30}$$

Then, equating (6.30) to (6.28) with (6.29),

$$u_0 = (0.75)^{-1/7} = 7.491541\,\mathrm{g\,cm^{-2}} = 74.91541\,\mathrm{kg\,m^{-2}}. \tag{6.31}$$

Differentiating (6.30),

$$\frac{\mathrm{d}\epsilon_f}{\mathrm{d}u} = \frac{m}{u_0} \left(\frac{u}{u_0} \right)^{m-1}. \tag{6.32}$$

With (6.32) and (6.19)–(6.20):

$$
\begin{aligned}
R_{ac} &= \int_{u=0}^{\infty} \sigma \left(T_0 e^{-\gamma z/T_0} \right)^4 \frac{m}{u_0} \left(\frac{u}{u_0} \right)^{m-1} \mathrm{d}u \\
&= \int_{z=0}^{\infty} \sigma T_0^4 e^{-4\gamma z/T_0} \frac{m}{u_0} \left(\frac{1}{u_0} \int_{\zeta=0}^{z} \rho_{v0} \left(\frac{p}{p_0} \right)^{1/2} \mathrm{d}\zeta \right)^{m-1} \rho_v \left(\frac{p}{p_0} \right)^{1/2} \mathrm{d}z. \tag{6.33}
\end{aligned}
$$

Now, with (6.20), (6.25) and (6.26):

$$
\begin{aligned}
R_{ac} &= \int_{z=0}^{\infty} \sigma T_0^4 e^{-4\gamma z/T_0} \frac{m}{u_0} \left(\frac{1}{u_0} \int_{\zeta=0}^{z} \rho_{v0} e^{-k_w \zeta} \left(\frac{T}{T_0} \right)^{\frac{g}{2\gamma R_d}} \mathrm{d}\zeta \right)^{m-1} \rho_{v0} e^{-k_w z} \left(\frac{T}{T_0} \right)^{\frac{g}{2\gamma R_d}} \mathrm{d}z \\
&= \int_{z=0}^{\infty} \sigma T_0^4 e^{-4\gamma z/T_0} \frac{m}{u_0} \left(\frac{1}{u_0} \int_{\zeta=0}^{z} \rho_{v0} e^{-\left(k_w + \frac{g}{2R_d T_0}\right)\zeta} \mathrm{d}\zeta \right)^{m-1} \rho_{v0} e^{-\left(k_w + \frac{g}{2R_d T_0}\right)z} \mathrm{d}z \\
&= m \left(\frac{\rho_{v0}}{u_0} \right)^m \sigma T_0^4 \int_{z=0}^{\infty} e^{-\left(\frac{4\gamma}{T_0} + k_w + \frac{g}{2R_d T_0}\right)z} \left(\int_{\zeta=0}^{z} e^{-\left(k_w + \frac{g}{2R_d T_0}\right)\zeta} \mathrm{d}\zeta \right)^{m-1} \mathrm{d}z. \tag{6.34}
\end{aligned}
$$

In order to simplify notation a little bit, let

$$k_1 = \frac{4\gamma}{T_0} + k_2, \tag{6.35}$$

$$k_2 = k_w + \frac{g}{2R_d T_0}; \tag{6.36}$$

then,

$$
\begin{aligned}
R_{ac} &= m \left(\frac{\rho_{v0}}{u_0} \right)^m \sigma T_0^4 \int_{z=0}^{\infty} e^{-k_1 z} \left(\int_{\zeta=0}^{z} e^{-k_2 \zeta} \mathrm{d}\zeta \right)^{m-1} \mathrm{d}z \\
&= m \left(\frac{\rho_{v0}}{u_0 k_2} \right)^m \sigma T_0^4 \int_{z=0}^{\infty} e^{-k_1 z} \left(1 - e^{-k_2 z} \right)^{m-1} k_2\, \mathrm{d}z. \tag{6.37}
\end{aligned}
$$

Now introduce the change of variables

$$t = e^{-k_2 z}, \tag{6.38}$$

$$\mathrm{d}t = -k_2 e^{-k_2 z}\, \mathrm{d}z, \tag{6.39}$$

Table 6.2: Cloudy-sky parameterisations

Parameterization	Experimental site
Jacobs (1978):	Baffin Island (Canada)
$R_a = (1 + 0.26c)R_{ac}$	

to obtain

$$
\begin{aligned}
R_{ac} &= m\left(\frac{\rho_{v0}}{u_0 k_2}\right)^m \sigma T_0^4 \int_{z=\infty}^{0} \left(\mathrm{e}^{-k_2 z}\right)^{\frac{k_1}{k_2}-1} \left(1 - \mathrm{e}^{-k_2 z}\right)^{m-1} k_2 \left(-\mathrm{e}^{-k_2 z}\right)\, \mathrm{d}z \\
&= m\left(\frac{\rho_{v0}}{u_0 k_2}\right)^m \sigma T_0^4 \int_{t=0}^{1} t^{\frac{k_1}{k_2}-1}\left(1 - t\right)^{m-1}\, \mathrm{d}t \\
&= \underbrace{\left[m\left(\frac{e_0}{u_0 k_2 R_v T_0}\right)^m B\left(\frac{k_1}{k_2}, m\right)\right]}_{\epsilon_{ac}} \sigma T_0^4.
\end{aligned}
\tag{6.40}
$$

In SI units, Brutsaert's equation is

$$
\epsilon_{ac} = 0.64 \left(\frac{e_a}{T_a}\right)^{1/7}.
\tag{6.41}
$$

6.5 – Cloudiness effect on atmospheric irradiance

Atmospheric irradiance increases in the presence of clouds. A way to account for that is to write

$$
R_a = \phi R_{ac},
\tag{6.42}
$$

where ϕ is some function of the cloud cover. Bolz's equation, in terms of cloudiness, is

$$
\phi = 1 + 0.22 c^2
\tag{6.43}
$$

where c is cloud cover, between 0 and 1, as reported in manually operated weather stations in *oktas*, or eights of sky clovered by clouds Wikipedia (2019). If c is not available, a surrogate is

$$
c = 1 - n/N,
\tag{6.44}
$$

where n and N have been defined above. Again, (6.44) can only be used with (6.43) to derive daily averages of R_a.

More recent equations have been developed to estimate ϕ, and are shown in table 6.2, obtained from Duarte et al. (2006)

7

Turbulent diffusion

7.1 – Scales in turbulence

In a turbulent flow, it is not always clear what is meant by a "particle". There is a wealth of scales in fully developed turbulent flows, and a way to manage this wide range of scales is to define a few that differ significantly in their sizes. The *integral scale* is defined mathematically in terms of the autocorrelation function $\varrho(x)$ for the longitudinal component of velocity fluctuations:

$$\ell = \int_0^\infty \varrho(x)\,\mathrm{d}x.$$

The autocorrelation function can be expanded in a Taylor series at the origin (Davidson, 2004, p. 326),

$$\varrho(x) = 1 - \frac{x^2}{2\lambda^2} + \dots \tag{7.1}$$

and Taylor's microscale λ is defined in terms of the curvature of $\varrho(x)$ at the origin:

$$-\frac{2}{\lambda} \equiv \left.\frac{\mathrm{d}^2\rho}{\mathrm{d}x^2}\right|_{x=0}.$$

Finally, we have Kolmogorov's microscale:

$$\eta = (v^3/\epsilon)^{1/4}.$$

The classical particles of Fluid Mechanics have to be of size η or smaller: they can only "see" molecular diffusion, and smooth fields around them. On the other hand, "particles" of size λ "see" turbulent diffusion, and a considerably more agitated world around them.

7.2 – Turbulent diffusivity

Let us now define "turbulent diffusivity". If F is the turbulent flux of a scalar whose concentration is c, its turbulent diffusivity K at a point is *defined* as

$$F \equiv -\overline{\rho}K\frac{\mathrm{d}\overline{c}}{\mathrm{d}z}.$$

The overbars on the variables indicate Reynolds (1895) averages. Usually turbulent diffusivity is *modelled* with simple dimensional arguments, such as

$$K = \alpha\sigma_w\ell,$$

where α is a dimensionless constant, and σ_w is a velocity scale (for instance, in this case we are thinking of the standard deviation of vertical velocity). The turbulent flux itself is usually defined by means of Reeynolds averages:

$$F = \overline{\rho w c} \approx \overline{\rho} \, \overline{w'c'},$$

as long as c is a mass concentration.

7.3 – Turbulent diffusion theory

Let us proceed to Taylor (1921)' s turbulent diffusion theory. We do it by following a particle (in Kolmogorov's sense) using a *Lagrangian* description of the flow:

$$Z(t) = Z(0) + \int_0^t W(t') \, \mathrm{d}t'. \tag{7.2}$$

Without loss of generality, assume $Z(0) \equiv 0$ (always), and

$$\overline{Z(t)} = 0. \tag{7.3}$$

Our averages now need also to be considered from a Lagrangian point of view, as averages over a large number of particles. If $Z_i(t)$ is the position of the $i^{\underline{\text{th}}}$ particle and we are emitting a large number N of particles,

$$\overline{Z(t)} = \frac{1}{N} \sum_{i=1}^N Z_i(t).$$

Consider now the mean square deviation of $Z(t)$ with respect to the origin. Clearly, this is a measure of how the particles will "disperse" around it. We are interested in the quantities

$$\overline{Z^2(t)}, \qquad \frac{\mathrm{d}}{\mathrm{d}t}\left[\overline{Z^2(t)}\right].$$

Proceeding,

$$\frac{\mathrm{d}}{\mathrm{d}t}\left[\overline{Z^2(t)}\right] = 2\overline{Z(t)\frac{\mathrm{d}Z}{\mathrm{d}t}}.$$

But

$$W(t) = \frac{\mathrm{d}Z}{\mathrm{d}t}; \tag{7.4}$$

Therefore,

$$\frac{\mathrm{d}}{\mathrm{d}t}\left[\overline{Z^2(t)}\right] = 2\overline{Z(t)W(t)}$$

$$= 2\overline{\left[\int_{t'=0}^t W(t') \, \mathrm{d}t'\right] W(t)}$$

$$= 2\int_0^t \overline{W(t')W(t)} \, \mathrm{d}t'.$$

Now if $W(t)$ is a *stationary* stochastic process,

$$\overline{W(t')W(t)} = \overline{W(0)W(t - t')} \Rightarrow$$

$$\frac{\mathrm{d}}{\mathrm{d}t}\left[\overline{Z^2(t)}\right] = 2\int_0^t \overline{W(0)W(t - t')} \, \mathrm{d}t'.$$

To proceed further, we define the *Lagrangian autocorrelation function*,

$$\varrho_L(\tau) \equiv \frac{1}{\overline{W^2}} \overline{W(t)W(t+\tau)},$$

where we are assuming that $\overline{W^2}$, differently from $\overline{Z^2(t)}$, does not depend on t (which is the stationarity hypothesis for $W(t)$). With that,

$$\frac{\mathrm{d}}{\mathrm{d}t}\left[\overline{Z^2(t)}\right] = 2\overline{W^2}\int_0^t \varrho_L(\tau)\,\mathrm{d}\tau;$$

$$\overline{Z^2(t)} = 2\overline{W^2}\int_0^t \int_0^{t'} \varrho_L(\tau)\,\mathrm{d}\tau\mathrm{d}t'.$$

We now integrate by parts:

$$f(t') \equiv \int_0^{t'} \varrho_L(\tau)\,\mathrm{d}\tau;$$

$$\int_0^t f(t')\,\mathrm{d}t' = t'f(t')\Big|_0^t - \int_0^t t'\varrho_L(t')\,\mathrm{d}t';\Rightarrow$$

$$\overline{Z^2(t)} = 2\overline{W^2}\left[t\int_0^t \varrho_L(t')\,\mathrm{d}t' - \int_0^t t'\varrho_L(t')\,\mathrm{d}t'\right]$$

$$= 2\overline{W^2}t\int_0^t \left(1 - \frac{t'}{t}\right)\varrho_L(t')\,\mathrm{d}t'. \tag{7.5}$$

At this point, we want to introduce the *Lagrangian integral scale*:

$$\mathscr{T}_L \equiv \int_0^\infty \varrho_L(\tau)\,\mathrm{d}\tau, \tag{7.6}$$

but does it exist? The safest bet seems to be to assume that $\varrho_L(t)$ belongs to the space L_1; this means to assume that

$$\int_0^\infty |\varrho_L(t)|\,\mathrm{d}t < \infty. \tag{7.7}$$

Assuming (7.7) ensures that $\mathscr{T}_L$ in (7.6) exists. We now change variables to

$$\tau = \frac{t'}{\mathscr{T}_L}, \tag{7.8}$$

$$\tau_L = \frac{t}{\mathscr{T}_L}, \tag{7.9}$$

$$\varrho_L^*(\tau) \equiv \varrho_L(\tau\mathscr{T}_L), \tag{7.10}$$

so that (7.5) becomes

$$\overline{Z^2(t)} = 2\overline{W^2(t)}\mathscr{T}_L t\int_{\tau=0}^{\tau_L} \left(1 - \frac{\tau}{\tau_L}\right)\varrho_L^*(\tau)\,\mathrm{d}\tau. \tag{7.11}$$

Proceed with an *asymptotic analysis*: suppose that $\tau_L \ll 1$; then, there isn't enough "time" for $\varrho_L^*(\tau)$ to decrease very much from 1, and

$$\varrho_L(\tau) \approx 1 \implies$$

$$\overline{Z^2(t)} \approx 2\overline{W^2(t)}\mathscr{T}_L t \int_0^{\tau_L} (1 - \frac{\tau}{\tau_L})\, \mathrm{d}\tau$$

$$= 2\overline{W^2(t)}\mathscr{T}_L t \times \frac{1}{2}\tau_L$$

$$= \overline{W^2}t^2 \quad \blacksquare \tag{7.12}$$

Consider now the case $\tau_L \gg 1$. The objective is to obtain a suitable approximation for the integral in (7.11). First, note that if (7.7) holds, then obviously

$$\int_0^\infty |\varrho_L^*(\tau)|\, \mathrm{d}\tau < \infty. \tag{7.13}$$

Next, a standard interpretation in stochastic processes is that under reasonable assumptions such as stationarity and ergodicity, a process becomes effectively decorrelated from itself in two integral time scales (Tennekes and Lumley, 1972, p. 213–214). This means that it is reasonable to expect ϱ_L^* to decrease to zero relatively fast from $\tau_L = 1$ onwards.

In the literature, in obtaining an approximation for (7.11), this is not always discussed at length. Pope (2000)'s presentation of this subject can be found in Chapter 12, p. 498–499, but there is no deep justification for his equation (12.154). Monin and Yaglom (1971) (Ch. 5, p. 543–544) do better. We quote from them:

> Let us now make the natural assumption that the Lagrangian correlation function $R_{ii}^{(L)}(s)$ approaches zero when $s \to \infty$, *and so rapidly that the following correlation time will exist* (...)

There is also some justification in Tennekes and Lumley (1972) (Ch. 6, Eqs. (6.4.11–6.4.12)). It is clear that Taylor's expression for large times (which we will obtain soon) is by no means only a mathematical derivation, but rather a result that requires "reasonable" assumptions that cannot be proved *a priori*.

Therefore, to proceed, *some* additional assumption is needed on $\varrho_L^*(\tau)$. From the foregoing discussion, an assumption as good as any is that there exists $g(\tau) = \tau^{-m}$ with $m > 1$ and such that $|\varrho_L^*(\tau)| \le g(\tau)$, $\tau \ge 1$ (note that $|\varrho_L^*(\tau)| \le 1$ always). Then, for $\tau_L \gg 1$,

$$\overline{Z^2(t)} \approx \lim_{\tau_L \to \infty} 2\overline{W^2(t)}\mathscr{T}_L t \int_0^{\tau_L} \left(1 - \frac{\tau}{\tau_L}\right)\varrho_L^*(\tau)\, \mathrm{d}\tau$$

$$= 2\overline{W^2(t)}\mathscr{T}_L t \left[\int_0^\infty \varrho_L^*(\tau)\, \mathrm{d}\tau - \lim_{\tau_L \to \infty} \int_0^{\tau_L} \frac{\tau}{\tau_L}\varrho_L^*(\tau)\, \mathrm{d}\tau\right] \tag{7.14}$$

The first integral in the brackets is equal to 1; for the second, we split the integration interval beteween $\tau \in [0, 1)$ and $\tau \in [1, \infty)$. We have

$$\lim_{\tau_L \to \infty} \int_0^1 \frac{\tau}{\tau_L}\varrho_L^*(\tau)\, \mathrm{d}\tau = 0 \tag{7.15}$$

and

$$\left| \lim_{\tau_L \to \infty} \int_1^{\tau_L} \frac{\tau}{\tau_L} \varrho_L^*(\tau)\, \mathrm{d}\tau \right| \leq \lim_{\tau_L \to \infty} \int_1^{\tau_L} \left| \frac{\tau}{\tau_L} \varrho_L^*(\tau) \right| \mathrm{d}\tau$$

$$\leq \lim_{\tau_L \to \infty} \frac{1}{\tau_L} \int_1^{\tau_L} \tau g(\tau)\, \mathrm{d}\tau$$

$$= \lim_{\tau_L \to \infty} \frac{1}{\tau_L} \int_1^{\tau_L} \tau^{-m+1}\, \mathrm{d}\tau. \tag{7.16}$$

For $m \neq 2$,

$$\lim_{\tau_L \to \infty} \frac{1}{\tau_L} \int_1^{\tau_L} \tau^{-m+1}\, \mathrm{d}\tau = \lim_{\tau_L \to \infty} \frac{1}{\tau_L} \left[\frac{1}{-m+2} \tau^{-m+2} \right]_1^{\tau_L}$$

$$= \lim_{\tau_L \to \infty} \frac{1}{(-m+2)} \frac{1}{\tau_L} \left[\tau_L^{-m+2} - 1 \right] = 0. \tag{7.17}$$

For $m = 2$,

$$\lim_{\tau_L \to \infty} \frac{1}{\tau_L} \int_1^{\tau_L} \tau^{-m+1}\, \mathrm{d}\tau = \lim_{\tau_L \to \infty} \frac{1}{\tau_L} \left[\ln(\tau) \right]_1^{\tau_L}$$

$$= \lim_{\tau_L \to \infty} \frac{1}{\tau_L} \ln(\tau_L) = 0. \tag{7.18}$$

Together, (7.14)–(7.18) give

$$\lim_{\tau_L \to \infty} \int_0^{\tau_L} \frac{\tau}{\tau_L} \varrho_L^*(\tau)\, \mathrm{d}\tau = 0 \tag{7.19}$$

and the desired expression for $\overline{Z^2(t)}$ for $\tau_L \gg 1$ is

$$\overline{Z^2(t)} \approx 2\overline{W^2(t)} \mathcal{T}_L t. \tag{7.20}$$

In short, our results for the root mean square values of $Z(t)$ are

$$Z^{\mathrm{rms}} = W^{\mathrm{rms}} t, \qquad\qquad\qquad t \ll \mathcal{T}_L; \tag{7.21}$$

$$Z^{\mathrm{rms}} = W^{\mathrm{rms}} \sqrt{2 \mathcal{T}_L t}, \qquad\qquad t \gg \mathcal{T}_L. \tag{7.22}$$

7.4 – The Lagrangian concentration field

Let us change focus to the path of the Lagrangian particles. Each particle has a function of position in the form

$$x = X(\xi, t),$$

where ξ is the position of the particle at $t = 0$, so that

$$\xi = X(\xi, 0).$$

Therefore, at $t = 0$, X is the identity. In the absence of diffusion, the transport equation for a scalar whose concentration is c is

$$\frac{\mathrm{D}c}{\mathrm{D}t} = \frac{\partial c}{\partial t} + \sum_{i=1}^3 u_i \frac{\partial c}{\partial x_i} = 0,$$

with solution

$$c(X(\xi, t), t) = c(\xi, 0).$$

We need to introduce the probability density function (pdf) $f_c(x, t|\xi)$, which gives the probability density that, starting from ξ at $t = 0$, a particle reaches x at time t. The expected value of the concentration in (x, t) is

$$\overline{c}(x, t) = \int_{\xi \in \mathbb{R}^3} c(\xi, 0) f_c(x, t|\xi) \mathrm{d}^3\xi.$$

In particular, if all mass M of the scalar is concentrated at $\xi = 0$,

$$c(\xi, 0) = M\delta(\xi);$$

$$\overline{c}(x, t) = \int_{\xi \in \mathbb{R}^3} M\delta(\xi) f_c(x, t|\xi) \mathrm{d}^3\xi$$

$$= M f_c(x, t|0).$$

In one dimension, we just saw (7.2). Let us interpret (7.2) with the help of the Central Limit Theorem for an integral (Tennekes and Lumley, 1972, Sec. 6.5). We will take $Z(t)$ to be a random variable produced by the "sum" of a large number of random variables $W(t') \, \mathrm{d}t'$: the Central Limit Theorem predicts that $Z(t)$ is normally distributed. Since we know that its mean is $\overline{Z(t)} = 0$ (c.f. (7.3)) and the standard deviation can be obtained from (7.21)–(7.22), we just use the large-time limit for Z^{rms} and obtain

$$Z^{\mathrm{rms}} = \sigma_Z = \sigma_w \sqrt{2\mathscr{T}_L t}. \tag{7.23}$$

Then, we immediately find that

$$\overline{c}(z, t) = \frac{M}{A\sqrt{2\pi}\sigma_Z} \exp\left[-\frac{z^2}{2\sigma_Z^2}\right]. \tag{7.24}$$

This can be readily generalized to three dimensions:

$$\overline{c}(x, y, z, t) = \frac{M}{(2\pi)^{3/2}\sigma_X\sigma_Y\sigma_Z} \exp\left[-\frac{x^2}{2\sigma_X^2}\right] \exp\left[-\frac{y^2}{2\sigma_Y^2}\right] \exp\left[-\frac{z^2}{2\sigma_Z^2}\right]. \tag{7.25}$$

7.5 – The Eulerian concentration field

7.5.1 – One-dimensional solution of the diffusion equation

The same problem can be approached from the Eulerian point of view, as the solution to the *diffusion equation*

$$\frac{\partial \overline{c}}{\partial t} = K_{zz} \frac{\partial^2 \overline{c}}{\partial z^2}; \qquad c(z, 0) = \frac{M}{A}\delta(z); \qquad \lim_{z \to \pm\infty} \overline{c}(z, t) = 0, \tag{7.26}$$

which is (Dias, 2017, Example 15.6)

$$\overline{c}(z, t) = \frac{M}{A\sqrt{4K_{zz}\pi t}} \exp\left[-\frac{z^2}{4K_{zz}t}\right]. \tag{7.27}$$

Note that formally it is the same as the lagrangian solution! By equating (7.24) and (7.27), we immediately obtain

$$2\sigma_Z^2 = 4K_{zz}t, \tag{7.28}$$

$$4\overline{W^2}\,\mathscr{T}_L t = 4K_{zz}t \tag{7.29}$$

$$K_{zz} = \overline{W^2}\,\mathscr{T}_L \quad\blacksquare \tag{7.30}$$

7.5.2 – Two- and three-dimensional solutions of the diffusion equation

The generalization of (7.26) to 3 dimensions is

$$\frac{\partial \overline{c}}{\partial t} = K_{xx}\frac{\partial^2 \overline{c}}{\partial x^2} + K_{yy}\frac{\partial^2 \overline{c}}{\partial y^2} + K_{zz}\frac{\partial^2 \overline{c}}{\partial z^2}; \tag{7.31}$$

$$c(z, 0) = M\delta(x)\delta(y)\delta(z); \tag{7.32}$$

$$\lim_{x,y,z\to\pm\infty} \overline{c}(x, y, z, t) = 0, \tag{7.33}$$

Let us try a solution by means of separation of variables, of the type

$$c(x, y, z, t) = X(x, t)Y(y, t)Z(z, t); \tag{7.34}$$

substitution in (7.31) produces

$$YZ\frac{\partial X}{\partial t} + XZ\frac{\partial Y}{\partial t} + XY\frac{\partial Z}{\partial t} = YZK_{xx}\frac{\partial^2 X}{\partial x^2} + XZK_{yy}\frac{\partial^2 Y}{\partial y^2} + XYK_{zz}\frac{\partial^2 Z}{\partial z^2};$$

$$X(x, 0)Y(y, 0)Z(z, 0) = M\delta(x)\delta(y)\delta(z),$$

$$X(\pm\infty, t)Y(\pm\infty, t)Z(\pm\infty, t) = 0.$$

This immediately yields 3 separate problems:

$$\frac{\partial X}{\partial t} = K_{xx}\frac{\partial^2 X}{\partial x^2}; \qquad X(x, 0) = M^{1/3}\delta(x); \qquad X(\pm\infty) = 0; \tag{7.35}$$

$$\frac{\partial Y}{\partial t} = K_{yy}\frac{\partial^2 Y}{\partial y^2}; \qquad Y(y, 0) = M^{1/3}\delta(y); \qquad Y(\pm\infty) = 0; \tag{7.36}$$

$$\frac{\partial Z}{\partial t} = K_{zz}\frac{\partial^2 Z}{\partial z^2}; \qquad Z(z, 0) = M^{1/3}\delta(z); \qquad Z(\pm\infty) = 0. \tag{7.37}$$

Note that each one of (7.35)–(7.36) is the same as (7.26); therefore,

$$\begin{aligned} c(x, y, z, t) &= \frac{M^{1/3}}{\sqrt{4K_{xx}\pi t}}\exp\left[-\frac{x^2}{4K_{xx}t}\right] \\ &\times \frac{M^{1/3}}{\sqrt{4K_{yy}\pi t}}\exp\left[-\frac{y^2}{4K_{yy}t}\right] \\ &\times \frac{M^{1/3}}{\sqrt{4K_{zz}\pi t}}\exp\left[-\frac{z^2}{4K_{zz}t}\right] \\ &= \frac{M}{8(\pi t)^{3/2}(K_{xx}K_{yy}K_{zz})^{1/2}}\exp\left[-\frac{x^2}{4K_{xx}t} - \frac{y^2}{4K_{yy}t} - \frac{z^2}{4K_z t}\right]. \tag{7.38} \end{aligned}$$

7.6 – The advection-diffusion case

Let us now modify the diffusion equation and add an advection term. In most cases, it is enough to add advection in the x-direction, *and rotate the mean wind into the x axis.* The equation is

$$\frac{\partial \overline{c}}{\partial t} + \overline{u}\frac{\partial \overline{c}}{\partial x} = K_{xx}\frac{\partial^2 \overline{c}}{\partial x^2},$$

$$\overline{c}(x, 0) = \frac{M}{A}\delta(x),$$

where $[\![A]\!]$ = YZ. It turns out that we can return to a purely diffusive problem by means of the change of variables

$$x' = x - \overline{u}t,$$

$$t' = t.$$

In the new coordinates, the solution will be

$$\chi(x', t') = \overline{c}(x, t) = \overline{c}(x' + ut', t'). \tag{7.39}$$

Then,

$$\frac{\partial \chi}{\partial t'} = \frac{\partial \overline{c}}{\partial t}\frac{\partial t}{\partial t'} + \frac{\partial \overline{c}}{\partial x}\frac{\partial x}{\partial t'},$$

$$= \frac{\partial \overline{c}}{\partial t} + \overline{u}\frac{\partial \overline{c}}{\partial x};$$

$$\frac{\partial \chi}{\partial x'} = \frac{\partial \overline{c}}{\partial x}\frac{\partial x}{\partial x'} = \frac{\partial \overline{c}}{\partial x};$$

$$\frac{\partial^2 \chi}{\partial x'^2} = \frac{\partial}{\partial x}\left[\frac{\partial \chi}{\partial x'}\right]\frac{\partial x}{\partial x'} = \frac{\partial}{\partial x}\left[\frac{\partial \overline{c}}{\partial x}\right]\frac{\partial x}{\partial x'} = \frac{\partial^2 \overline{c}}{\partial x^2}.$$

This brings us back to the diffusion equation

$$\frac{\partial \overline{\chi}}{\partial t} = K_{xx}\frac{\partial^2 \overline{\chi}}{\partial x'^2},$$

$$\overline{\chi}(x', 0) = \overline{c}(x, 0) = \frac{M}{A}\delta(x')$$

with solution

$$\overline{\chi}(x', t') = \frac{M}{A\sqrt{4K_{xx}\pi t'}}\exp\left[-\frac{(x')^2}{4K_{xx}t'}\right]; \Rightarrow$$

$$\overline{c}(x, t) = \frac{M}{A\sqrt{4K_{xx}\pi t}}\exp\left[-\frac{(x - \overline{u}t)^2}{4K_{xx}t}\right].$$

Can we solve

$$\frac{\partial c}{\partial t} + u\frac{\partial c}{\partial x} = K_{xx}\frac{\partial^2 c}{\partial x^2} + K_{yy}\frac{\partial^2 c}{\partial y^2} + K_{zz}\frac{\partial^2 c}{\partial z^2}, \tag{7.40}$$

$$c(x, y, z, 0) = M\delta(x)\delta(y)\delta(z)? \tag{7.41}$$

Obviously we can. This time the change of variables is

$$x' = x - ut, \tag{7.42}$$
$$y' = y, \tag{7.43}$$
$$z' = z, \tag{7.44}$$
$$t' = t. \tag{7.45}$$

Put, as before,

$$\chi(x', y', z', t') = c(x, y, z, t) = c(x' + ut', y', z', t').$$

Then,

$$\frac{\partial \chi}{\partial t'} = \frac{\partial c}{\partial t}\frac{\partial t}{\partial t'} + \frac{\partial c}{\partial x}\frac{\partial x}{\partial t'} = \frac{\partial c}{\partial t} + u\frac{\partial c}{\partial x}, \tag{7.46}$$

$$\frac{\partial^2 \chi}{\partial x'^2} = \frac{\partial^2 c}{\partial x^2}, \tag{7.47}$$

$$\frac{\partial^2 \chi}{\partial y'^2} = \frac{\partial^2 c}{\partial y^2}, \tag{7.48}$$

$$\frac{\partial^2 \chi}{\partial z'^2} = \frac{\partial^2 c}{\partial z^2}. \tag{7.49}$$

Substituting back, we obtain the purely diffusive equation

$$\frac{\partial \chi}{\partial t} = K_{xx}\frac{\partial^2 \chi}{\partial x^2} + K_{yy}\frac{\partial^2 \chi}{\partial y^2} + K_{zz}\frac{\partial^2 \chi}{\partial z^2}, \tag{7.50}$$

$$\chi(x', y', z', 0) = c(x, z, z, 0) = M\delta(x')\delta(y')\delta(z'). \tag{7.51}$$

On account of (7.38), the solution is

$$c(x, y, z, t) = \frac{M}{8(\pi t)^{3/2}(K_{xx}K_{yy}K_{zz})^{1/2}}\exp\left[-\frac{(x - ut)^2}{4K_{xx}t} - \frac{y^2}{4K_{yy}t} - \frac{z^2}{4K_z t}\right]. \tag{7.52}$$

7.6.1 – Steady-state diffusion problems

Let us build a series of solutions to atmospheric dispersion problems based on the general ideas introduced in the previous sections Our first adaptation will be the *steady* one-dimensional problem

$$\bar{u}\frac{\partial \bar{c}}{\partial x} = K_{zz}\frac{\partial^2 \bar{c}}{\partial z^2}. \tag{7.53}$$

Formally, this is a diffusion equation completely similar to (7.26), but with t replaced by $x/\bar{u}$. Our initial condition now needs to be specified at $x = 0$, and modified to the right physical dimensions. It will be, accordingly, (Kumar and Sharan, 2010, eq. (2.5))

$$\bar{c}(x = 0, z) = \frac{q}{L\bar{u}}\delta(z),$$

with L indicating a length scale in the y direction: $[\![L]\!] = \mathsf{Y}$. The solution for a continuous injection of pollutant mass q ($[\![q]\!] = \mathsf{M}_p\mathsf{T}^{-1}$) is recovered from direct substitution:

$$\bar{c}(x,z) = \frac{q}{L\bar{u}\sqrt{4\pi K_{zz}(x/\bar{u})}}\exp\left[-\frac{\bar{u}}{x}\left(\frac{z^2}{4K_{zz}}\right)\right]$$

$$= \frac{q}{L\sqrt{4\pi K_{zz}\bar{u}x}}\exp\left[-\frac{\bar{u}}{x}\left(\frac{z^2}{4K_{zz}}\right)\right]. \tag{7.54}$$

This is a very useful expression for dispersion studies, which are usually made by analyzing 1-hour periods each of which is assumed to be a steady-state problem. Let us now extend this to y and z, in the form

$$\bar{u}\frac{\partial\bar{c}}{\partial x} = K_{yy}\frac{\partial^2\bar{c}}{\partial y^2} + K_{zz}\frac{\partial^2\bar{c}}{\partial z^2}, \tag{7.55}$$

$$\bar{c}(x=0,y,z) = \frac{q}{\bar{u}}\delta(y)\delta(z) \tag{7.56}$$

As before, we try *separation of variables*:

$$\bar{c}(x,y,z) = Y(x,y)Z(x,z), \tag{7.57}$$

which produces:

$$\bar{u}\frac{\partial\bar{c}}{\partial x} = \bar{u}\left[Z\frac{\partial Y}{\partial x} + Y\frac{\partial Z}{\partial x}\right]; \tag{7.58}$$

$$K_{yy}\frac{\partial^2\bar{c}}{\partial y^2} = ZK_{yy}\frac{\partial^2 Y}{\partial y^2}; \tag{7.59}$$

$$K_{zz}\frac{\partial^2\bar{c}}{\partial z^2} = YK_{zz}\frac{\partial^2 Y}{\partial y^2}. \tag{7.60}$$

Grouped together, these equations are

$$\bar{u}\left[Z\frac{\partial Y}{\partial x} + Y\frac{\partial Z}{\partial x}\right] = ZK_{yy}\frac{\partial^2 Y}{\partial y^2} + YK_{zz}\frac{\partial^2 Y}{\partial y^2}, \tag{7.61}$$

$$Y(0,y)Z(0,z) = \left[\frac{q}{\bar{u}}\right]^{1/2}\delta(y)\left[\frac{q}{\bar{u}}\right]^{1/2}\delta(z) \tag{7.62}$$

This can quite obviously be dismembered into a pair of problems:

$$\bar{u}\frac{\partial Y}{\partial x} = K_{yy}\frac{\partial^2 Y}{\partial y^2}; \qquad Y(y,0) = \left[\frac{q}{\bar{u}}\right]^{1/2}\delta(y); \qquad Y(\pm\infty) = 0; \tag{7.63}$$

$$\bar{u}\frac{\partial Z}{\partial x} = K_{zz}\frac{\partial^2 Z}{\partial z^2}; \qquad Z(z,0) = \left[\frac{q}{\bar{u}}\right]^{1/2}\delta(z); \qquad Z(\pm\infty) = 0. \tag{7.64}$$

so that now

$$c(x,y,z) = Y(x,y)Z(x,z)$$

$$= \left[\frac{q}{\bar{u}}\right]^{1/2}\frac{1}{\sqrt{4\pi K_{yy}(x/\bar{u})}}\exp\left[-\frac{\bar{u}}{x}\left(\frac{y^2}{4K_{yy}}\right)\right]$$

$$\times\left[\frac{q}{\bar{u}}\right]^{1/2}\frac{1}{\sqrt{4\pi K_{zz}(x/\bar{u})}}\exp\left[-\frac{\bar{u}}{x}\left(\frac{z^2}{4K_{zz}}\right)\right]$$

$$= \frac{q}{4\pi x\sqrt{K_{yy}K_{zz}}}\exp\left[-\frac{\bar{u}}{4x}\left(\frac{y^2}{K_{yy}} + \frac{z^2}{K_{zz}}\right)\right]. \tag{7.65}$$

8

The last lectures

Atmospheric standards relate to some of the most common atmospheric pollutants, and their accepted maximum values. Here are some Brazilian standards.

Através da Portaria Normativa IBAMA nº 348, de 14/03/90 e Resolução CONAMA nº 03/90 foram estabelecidos os padrões nacionais de qualidade do ar. O Secretário de Estado do Meio Ambiente confirmou estes padrões através da Resolução SEMA nº 06/92. Portanto, os padrões paranaenses são os mesmos que os nacionais. Ficaram assim estabelecidos para todo território do Estado do Paraná padrões primários e secundários de qualidade do ar para os seguintes parâmetros:

1. Partículas Totais em Suspensão (PTS)

2. Fumaça

3. Partículas Inaláveis (PI), (também denominadas PM10)

4. Dióxido de Enxofre (SO2)

5. Monóxido de Carbono (CO)

6. Ozônio (O3)

7. Dióxido de Nitrogênio (NO2)

O padrão primário de qualidade do ar define legalmente as concentrações máximas de um componente atmosférico. O padrão primário pode ser entendido como o nível máximo tolerável de concentração de poluentes atmosféricos. Em situações de poluição atmosférica, portanto, a primeira meta a ser atingida é a obediência destes padrões. Entretanto, o padrão primário não garante que animais, plantas e construções não sofrerão danos devidos à poluição atmosférica. Ele tem o objetivo apenas de estabelecer um nível mínimo de proteção à saúde humana.

Para uma proteção maior existe o padrão secundário. O padrão secundário de qualidade do ar define legalmente as concentrações abaixo das quais se prevê — com base no conhecimento científico atual — o mínimo efeito adverso sobre o bem-estar da população, assim como o mínimo dano à fauna e flora, aos materiais e ao meio ambiente em geral, podendo ser entendido como nível desejado de concentração de poluentes, e constituindo-se em meta de longo prazo.

Table 8.1: Padrões primários e secundários de poluentes atmosféricos no Paraná (Resolução CONAMA 03/90, SEMA n⁰ 06/92)

Poluente	Tempo de amostragem	Padrão primário $(\mu g\,m^{-3})^{(1)}$	Padrão secundário $(\mu g\,m^{-3})^{(1)}$
Partículas Totais em Suspensão (PTS)	24 horas	$240^{(3)}$	$150^{(3)}$
	1 ano$^{(2)}$	80	60
Fumaça	24 horas	$150^{(3)}$	$100^{(3)}$
	1 ano$^{(2)}$	60	40
Partículas Inaláveis (PI)	24 horas	$150^{(3)}$	$150^{(3)}$
	1 ano$^{(2)}$	50	50
Dióxido de Enxofre (SO2)	24 horas	$365^{(3)}$	$100^{(3)}$
	1 ano$^{(2)}$	80	40
Monóxido de Carbono (CO)	1 hora	$40.000^{(3)}$	$40.000^{(3)}$
	8 horas	$10.000^{(3)}$	$10.000^{(3)}$
Ozônio (O3)	1 hora	$160^{(3)}$	$160^{(3)}$
Dióxido de Nitrogênio (NO2)	1 hora	320	190
	1 ano$^{(2)}$	100	100

Notas:

1. Ficam definidas como condições de referência a temperatura de 25°C e a pressão de 101,32 kPa

2. Média geométrica para PTS, para as restantes substâncias as médias são aritméticas

3. não deve ser excedida mais de uma vez por ano

Table 8.2: Critérios para episódios agudos de poluição do ar (Resolução CONAMA 03/90, SEMA nº 06/92)

Poluente	Tempo de amostragem	Nível de atenção $\mu g\,m^{-3}$	Nível de alerta $\mu g\,m^{-3}$	Nível de emergência $\mu g\,m^{-3}$
Partículas Totais em Suspensão (PTS)	24 horas	375	625	875
Fumaça	24 horas	250	420	500
Partículas Inaláveis (PI)	24 horas	250	420	500
Dióxido de Enxofre (SO2)	24 horas	800	1.600	2.100
Monóxido de Carbono (CO)	8 horas	17.000 [1]	34.000 [2]	46.000 [3]
Ozônio (O3)	1 hora	400	800	1.000
Dióxido de Nitrogênio (NO2)	1 hora	1.130	2.260	3000

Notas:

1. corresponde a uma concentração volumétrica de 15 ppm

2. corresponde a uma concentração volumétrica de 30 ppm

3. corresponde a uma concentração volumétrica de 40 ppm

Os padrões regulamentados pela Resolução SEMA nº 06/92 e os respectivos tempos de amostragem estão listados na tabela 8.1. Há para todos poluentes um padrão de curto prazo (horas) e outro de longo prazo, exceto no caso do Ozônio. Os padrões de curto prazo consideram os efeitos irritantes e agudos dos poluentes enquanto que os de longo prazo são estabelecidos para proteção contra os efeitos cumulativos. Os efeitos de curto prazo geralmente são reversíveis, enquanto os de longo prazo não são.

O padrão (primário ou secundário) que deve ser respeitado depende da Classe da área em questão. A Resolução CONAMA nº 05/89 estabeleceu três Classes (I, II e III). Áreas de Classe I são áreas de preservação, lazer e turismo onde se deve manter as concentrações nos níveis mais próximos possíveis dos verificados sem a intervenção antropogênica, e portanto abaixo dos níveis do padrão secundário. Nas áreas da Classe II se aplica o padrão secundário e naquelas da Classe III o padrão menos rígido, o primário. Cabe ao estado a definição das áreas de Classe I, II e III. Enquanto esta definição não for feita serão adotados os padrões primários de qualidade do ar. Esta classificação ainda não é feita no Paraná e por isso aplica-se em geral o padrão primário.

Para episódios agudos de poluição do ar ficam estabelecidos os níveis de Atenção, Alerta e Emergência conforme a tabela 8.2.

Remember Richardson's number!

$$\mathrm{Ri} = \frac{g}{\overline{\theta}} \frac{\mathrm{d}\overline{\theta}/\mathrm{d}z}{(\mathrm{d}\overline{u}/\mathrm{d}z)^2}.$$

and Pasquill's stability classes:

$\overline{u}$ (10 m) m s^{-1}	Solar irradiance			Cloud cover	
	> 700 W m^{-2}	350 – 700 W m^{-2}	< 350W m^{-2}	≥ 4/8	< 3/8
< 2	A	A-B	B		
2 − 3	A-B	B	C	E	F
3 − 5	B	B-C	C	D	E
5 − 6	C	C-D	D	D	D
> 6	C	D	D	D	D

Stability classes have been empirically related to Obukhov's length:

$$\frac{1}{L_O} = a + b \log z_0,$$

and

Condição	Classe de Pasquill	a	b
Muito instável	A	−0.096	0.029
Moderadamente instável	B	−0.037	0.029
Levemente instável	C	−0.002	0.018
Neutra	D	0	0
Levemente estável	E	+0.004	−0.018
Moderadamente estável	F	+0.035	−0.036

The standard deviations σ_Z and σ_Y can also be "recovered" empirically from stability classes, *viz.*

$$\sigma = \exp\left[I + J(\ln x) + K(\ln x)^2\right]$$

Classe	para obter σ_z			para obter σ_y		
	I	J	K	I	J	K
A	6,035	2,1097	0,2770	5,357	0,8828	-0,0076
B	4,694	1,0629	0,0136	5,058	0,9024	-0,0096
C	4,110	0,9201	-0,0020	4,651	0,9181	-0,0076
D	3,414	0,7371	-0,0316	4,230	0,9222	-0,0087
E	3,057	0,6794	-0,0450	3,922	0,9222	-0,0064
F	2,621	0,6564	-0,0540	3,533	0,9191	-0,0070

8.1 – Exemplo

Calcule a concentração dos poluentes num receptor localizado ao nível do solo, no eixo da pluma de dispersão a uma distância $x = 1500$ m da chaminé.

A tabela a seguir lista dados meteorológicos medidos a cada 3 horas. Os valores representam médias horárias.

tempo (h)	direção	$u(\text{m s}^{-1})$	$T_a(\text{K})$	$R_s(\text{W m}^{-2})$
3	0.0	1.8	291.2	0
6	0.0	0.9	291.3	0
9	0.0	1.3	291.7	134
12	0.0	2.7	294.0	405
15	22.5	2.2	296.6	210
18	0.0	2.7	293.3	2
21	0.0	2.2	292.3	0
24	22.5	0.9	292.0	0

Dados de emissão:

temperatura de saída do gás	400 K
velocidade de saída do gás	$6.0 \, \text{m s}^{-1}$
diâmetro da chaminé	2.0 m
altura da chaminé acima do solo	50.0 m
altura do anemômetro	10.0 m
tipo de terreno	rural

Fluxos de poluentes na chaminé:

poluente	emissão (g s^{-1})
MP	10.69
NOx	7.54
SOx	1.07

Agora calcula-se a classe de estabilidade de Pasquill para cada período de uma hora de medição:

Classes de estabilidade para cada período de medição:

tempo (h)	$R_s(\text{W m}^{-2})$	$u(10 \, \text{m})(\text{m s}^{-1}S)$	classe
3	0	1.8	E
6	0	0.9	E
9	134	1.3	B
12	405	2.7	B
15	210	2.2	C
18	2	2.7	C
21	0	2.2	E
24	0	0.9	E

Parâmetro de estabilidade de Briggs:

$$s = \left(\frac{g}{T_a}\right)\frac{d\theta}{dz},$$

onde:

s parâmetro de estabilidade (s^{-1})

g $9,807 \, \text{m s}^{-1}$

T_a temperatura ambiente do ar

$d\theta/dz$ gradiente vertical de temperatura potencial

Relação entre classes de estabilidade e estratificação da temperatura potencial

classe	$d\theta/dz(\text{K m}^{-1})$
A	< -0.009
B	-0.008
C	-0.006
D	0.000
E	0.015
F	> 0.025

Com as classes de estabilidade obtidas acima, nós encontramos os seguintes valores para $d\theta/dz$ e s:

tempo (h)	classe	$d\theta/dz(\text{K m}^{-1})$	temperatura (K)	$s(\text{s}^{-2})$
3	E	0.015	291.2	0.000505
6	E	0.015	291.3	0.00505
9	B	-0.008	291.7	-0.000269
12	B	-0.008	294.0	-0.000267
15	C	-0.006	296.6	-0.000198
18	C	-0.006	293.3	-0.000201
21	E	0.015	292.3	0.000503
24	E	0.015	292.0	0.000504

Fator de flutuação de Briggs

$$F = g v_s r^2 \frac{T_s - T_a}{T_s}$$

onde:

F fator de flutuação de Briggs ($\text{m}^4\,\text{s}^{-3}$)

g $9,807\text{m}PerSSq$

v_s velocidade de saída do gás (m s^{-1})

T_a temperatura do ar ambiente (K)

T_s temperatura de saída do gás (K)

r raio da chaminé (m)

Distância da chaminé até o ponto máximo de elevação da pluma:

$$x_f = 119F^{0.40} \quad \text{para} \quad F \geq 55\text{m}^4\text{s}^{-3}$$

e

$$x_f = 49F^{0.625} \quad \text{para} \quad F < 55\text{m}^4\text{s}^{-3}$$

tempo (h)	temperatura (K)	$F(\text{ m}^4\text{s}^{-3})$	$x_f(m)$
3	291,2	16,01	277,24
6	291,3	15,99	277,08
9	291,7	15,93	276,44
12	294,0	15,59	272,76
15	296,6	15,21	268,56
18	293,3	15,70	273,88
21	292,3	15,84	275,49
24	292,0	15,89	275,96

Relação entre velocidade do vento e altura:

$$u(z) = u_a \left(z/z_a\right)^n$$

onde:

$u(z)$ velocidade do vento na altura z

u_a velocidade do vento a altura do anemômetro z_a

n expoente em função da classe de estabilidade

Expoente de conversão da velocidade do vento

classe	n
A	0,10
B	0,15
C	0,20
D	0,25
E	0,25
F	0,30

Equações de Briggs para a altura de curvatura da pluma
Classes de estabilidade de Pasquill A, B, C, D:

$$\Delta h = 1.6F^{1/3}x^{2/3}u^{-1}, \;\; \text{para} \;\; x < x_f$$

e

$$\Delta h = 1.6F^{1/3}x_f^{2/3}u^{-1}, \;\; \text{para} \;\; x \geq x_f$$

Classes de estabilidade de Pasquill E, F:
Quando $1.84us^{-1/2} \geq x_f \implies$

$$\Delta h = 1.6F^{1/3}x^{2/3}u^{-1}, \;\; \text{para} \;\; x < x_f$$

e

$$\Delta h_{\max} = 1.6F^{1/3}x_f^{2/3}u^{-1}, \;\; \text{para} \;\; x \geq x_f$$

Quando $1.84us^{-1/2} < x_f \implies$

$$\Delta h = 1.6F^{1/3}x^{2/3}u^{-1}, \;\; \text{para} \;\; x < 1.84us^{-1/2}$$

e

$$\Delta h_{\max} = 2.4\left(F/us\right)^{1/3}, \;\; \text{para} \;\; x \geq 1.84us^{-1/2}$$

Altura efetiva de emissão:

$$H_e = h_s + \Delta h$$

Onde:

h_s altura da chaminé

Δh altura de curvatura da pluma

tempo (h)	classe	$u(10\,\text{m})$	n	$u(50\,\text{m})$	$1.84us^{-1/2}(\text{m})$	$\Delta h(\text{m})$	$H_e(\text{m})$
3	E	1,8	0,25	2,69	220,35	54,62	104,62
6	E	0,9	0,25	1,35	110,39	68,70	118,70
9	B	1,3	0,15	1,65	—	103,54	153,54
12	B	2,7	0,15	3,44	—	48,87	98,87
15	C	2,2	0,20	3,04	—	54,28	104,28
18	C	2,7	0,20	3,73	—	45,30	95,30
21	E	2,2	0,25	3,29	269,83	50,96	100,96
24	E	0,9	0,25	1,35	110,33	68,60	118,60

Desvios-padrão:

$$\sigma = \exp\left[I + J(\ln x) + K(\ln x)^2\right]$$

onde:

σ coeficiente de dispersão rural (m)

x distância do receptor (km)

Constantes de McMullen para obtenção dos coeficientes de dispersão rural

Classe	para obter σ_z			para obter σ_y		
	I	J	K	I	J	K
A	6,035	2,1097	0,2770	5,357	0,8828	-0,0076
B	4,694	1,0629	0,0136	5,058	0,9024	-0,0096
C	4,110	0,9201	-0,0020	4,651	0,9181	-0,0076
D	3,414	0,7371	-0,0316	4,230	0,9222	-0,0087
E	3,057	0,6794	-0,0450	3,922	0,9222	-0,0064
F	2,621	0,6564	-0,0540	3,533	0,9191	-0,0070

tempo (h)	classe	H_e(m)	$u(H_e)$(m)	σ_z(m)	σ_y(m)
3	E	104,62	3,24	27,80	73,32
6	E	118,70	1,67	27,80	73,32
9	B	153,54	1,96	168,55	226,40
12	B	98,87	3,81	168,55	226,40
15	C	104,28	3,52	88,48	151,72
18	C	95,30	4,24	88,48	151,72
21	E	100,96	3,92	27,80	73,32
24	E	118,60	1,67	27,80	73,32

Concentração das emissões da chaminé usando a equação de dispersão gaussiana generalizada; a dependência com x entra via σ_z e σ_y:

$$C(x,y,z) = \frac{Q}{(2\pi u \sigma_z \sigma_y)} \exp\left(-\frac{y^2}{2\sigma_y^2}\right)\left[\exp\left(-\frac{(z-H_e)^2}{2\sigma_z^2}\right) + \exp\left(-\frac{(z+H_e)^2}{2\sigma_z^2}\right)\right]$$

$$(8.1)$$

onde:

C concentração das emissões (μgm^{-3}) localizada

Q taxa de emissão da chaminé (μgs^{-1})

u velocidade do vento (m s^{-1})

σ_z desvio-padrão vertical (m)

σ_y desvio-padrão transversal (m)

H_e altura efetiva de emissão (m)

tempo (h)	concentrações (μgm^{-3})		
	MP	NOx	SOx
3	0.4	0.3	0.0
6	0.1	0.1	0.0
9	30.1	21.2	3.0
12	19.7	13.9	2.0
15	36.0	25.4	3.6
18	33.5	23.6	3.4
21	0.6	0.4	0.1
24	0.1	0.1	0.0

8.2 – Explanation of 8.1

Start from (7.65), and substitute

$$\sigma_y^2 = 2K_{yy}t,$$
$$\sigma_z^2 = 2K_{zz}t,$$
$$t = \frac{x}{\overline{u}};$$

then,

$$K_{yy} = \frac{\sigma_y^2 \overline{u}}{2x},$$
$$K_{zz} = \frac{\sigma_z^2 \overline{u}}{2x}.$$

Plugging those expresions in (7.65), we obtain

$$\sqrt{K_{yy}K_{zz}} = \frac{\overline{u}}{2x}\sigma_y\sigma_z,$$

$$-\frac{\overline{u}}{4x}\left(\frac{y^2}{K_{yy}} + \frac{z^2}{K_{zz}}\right) = -\frac{\overline{u}}{4x}\frac{2x}{\overline{u}}\left(\frac{y^2}{\sigma_y^2} + \frac{z^2}{\sigma_z^2}\right)$$

$$= -\frac{1}{2}\left(\frac{y^2}{\sigma_y^2} + \frac{z^2}{\sigma_z^2}\right).$$

Putting everything together, (7.65) becomes

$$\overline{c}(x, y, z) = \frac{q}{2\pi\overline{u}\sigma_y\sigma_z}\exp\left[-\frac{1}{2}\left(\frac{y^2}{\sigma_y^2} + \frac{z^2}{\sigma_z^2}\right)\right].$$

Next we adjust the emission height to $z = H_e$, and obtain the intermediate expression

$$\overline{c}(x, y, z) = \frac{q}{2\pi\overline{u}\sigma_y\sigma_z}\exp\left[-\frac{1}{2}\left(\frac{y^2}{\sigma_y^2} + \frac{(z - H_e)^2}{\sigma_z^2}\right)\right]. \tag{8.2}$$

The problem with (8.2) is that it is valid for an *infinite* domain, and predicts concentrations below ground level, *i.e.*, for $z < 0$.

A conservative approach to estimate pollutant concentrations is to put a barrier at $z = 0$, and force the vertical mass flux to zero at this height. This is equivalent to

$$-K_{zz}\frac{\partial \overline{c}(x,y,0)}{\partial z} = 0.$$

This condition now can be obtained by the *method of images*: we place a second source "upside down" at $z - (-H_e)$. The result is that all pollutant mass flux that crosses the plane $z = 0$ will be compensated by an equal flux with the opposite sign coming from *below*. In this way, no mass will be lost to $z < 0$. This is as simple as summing this second source, so that now

$$\overline{c}(x,y,z) = \frac{q}{2\pi\overline{u}\sigma_y\sigma_z}\exp\left[-\frac{1}{2}\left(\frac{y^2}{\sigma_y^2} + \frac{(z-H_e)^2}{\sigma_z^2}\right)\right]$$
$$+ \frac{q}{2\pi\overline{u}\sigma_y\sigma_z}\exp\left[-\frac{1}{2}\left(\frac{y^2}{\sigma_y^2} + \frac{(z+H_e)^2}{\sigma_z^2}\right)\right]. \quad (8.3)$$

Of course, (8.3) is the same as (8.1). We leave to the reader, as an exercise, to show from (8.3) that

$$\frac{\partial \overline{c}(x,y,0)}{\partial z} = 0.$$

8.3 – Modernamente!

Os modelos de pluma gaussiana têm sido substituídos por modelos mais detalhados, que são capazes de levar em conta a evolução horária dos parâmetros meteorológicos, a topografia do terreno, etc..

Nos EUA, duas gerações desse tipo de modelo foram o ISC3 e, atualmente, o AERMOD. Ver:

https://www.epa.gov/scram/air-quality-dispersion-modeling-preferred-and-recommended-models█

Uma das partes mais legais do AERMOD é a sua capacidade de acompanhar terreno.

9

A camada de mistura

9.1 – A espiral de Ekman

A notação deste documento está, neste momento, uma grande bagunça. Mas isto é incontornável por enquanto. Vamos começar com uma rápida revisão das equações para uma camada-limite atmosférica na forma

$$\frac{\partial \overline{U}_i}{\partial t} + \overline{U}_k \frac{\partial \overline{U}_i}{\partial x_k} + \frac{\partial (\overline{u_i u_k})}{\partial x_k} = \frac{\overline{\delta \wp}}{\wp_s} g_i - \frac{1}{\wp_s} \frac{\partial \overline{\delta P}}{\partial x_i} + f_c \epsilon_{ik3} \overline{U}_k + \nu \frac{\partial^2 \overline{U}_i}{\partial x_k \partial x_k}. \tag{9.1}$$

Uma questão na qual não vou me aprofundar agora é até que ponto esta equação vale para *toda* a camada de mistura. As equações para o vento geostrófico são

$$\frac{1}{\wp_S} \frac{\partial \overline{\delta P}}{\partial x_i} = f_c \epsilon_{ik3} U_{Gk}, \tag{9.2}$$

de modo que a equação de *momentum* pode ser escrita com as componentes do vento geostrófico substituindo os gradientes horizontais de pressão:

$$\frac{\partial \overline{U}_i}{\partial t} + \overline{U}_k \frac{\partial \overline{U}_i}{\partial x_k} + \frac{\partial (\overline{u_i u_k})}{\partial x_k} = \frac{\overline{\delta \wp}}{\wp_s} g_i + f_c \epsilon_{ik3} \left(\overline{U}_k - U_{Gk} \right) + \nu \frac{\partial^2 \overline{U}_i}{\partial x_k \partial x_k}. \tag{9.3}$$

Para o caso estacionário e horizontalmente homogêneo, as equações tornam-se

$$\frac{\partial (\overline{uw})}{\partial z} = f_c (\overline{V} - V_G), \tag{9.4}$$

$$\frac{\partial (\overline{vw})}{\partial z} = -f_c (\overline{U} - U_G). \tag{9.5}$$

Use um modelo de fechamento muito simples, com uma difusividade turbulenta K:

$$\overline{uw} = -K \frac{\partial \overline{U}}{\partial z}, \tag{9.6}$$

$$\overline{vw} = -K \frac{\partial \overline{V}}{\partial z}. \tag{9.7}$$

Evidentemente, a única variável independente é z, e passaremos a utilizar derivadas ordinárias em lugar de derivadas parciais:

$$K \frac{d^2 \overline{U}}{dz^2} = f_c (V_G - \overline{V}), \tag{9.8}$$

$$K \frac{d^2 \overline{V}}{dz^2} = -f_c (U_G - \overline{U}). \tag{9.9}$$

Neste ponto, introduza as variáveis complexas

$$w \equiv \overline{U} + \mathrm{i}\overline{V}; \qquad w_G \equiv U_G + \mathrm{i}V_G; \tag{9.10}$$

o sistema de equações diferenciais ordinárias torna-se

$$\begin{aligned}
K\frac{d^2w}{dz^2} &= K\left(\frac{d^2\overline{U}}{dz^2} + \mathrm{i}\frac{d^2\overline{V}}{dz^2}\right) \\
&= f_c(V_G - \overline{V}) - \mathrm{i}f_c(U_G - \overline{U}) \\
&= -\mathrm{i}f_c\left[(U_G + \mathrm{i}V_G) - (\overline{U} + \mathrm{i}\overline{V})\right] \\
&= -\mathrm{i}f_c\left[w_g - w\right].
\end{aligned} \tag{9.11}$$

O problema reduz-se, então, à solução da equação diferencial complexa

$$K\frac{d^2w}{dz^2} - \mathrm{i}f_c w = -\mathrm{i}f_c w_G. \tag{9.12}$$

As condições de contorno são

$$w(0) = 0, \tag{9.13}$$

$$\lim_{z \to \infty} w(z) = w_G. \tag{9.14}$$

Portanto, este é um problema de valor de contorno. Por inspeção, $w_p = w_G$ é uma solução particular; a equação característica é

$$\lambda^2 - \frac{\mathrm{i}f_c}{K} = 0, \tag{9.15}$$

com raízes

$$\lambda_{1,2} = \sqrt{\frac{\mathrm{i}f_c}{K}} = \sqrt{\frac{|f_c|}{K}}\sqrt{\mathrm{sinal}(f_c)\mathrm{i}}. \tag{9.16}$$

A solução agora deve depender do sinal de

$$f_c = 2\Omega \operatorname{sen}\varphi, \tag{9.17}$$

onde Ω é a velocidade angular da terra, e φ é a latitude. No Hemisfério Norte, $f_c > 0$, enquanto que no Hemisfério Sul, $f_c < 0$.

9.1.1 – Hemisfério Norte

Procura-se $\sqrt{\mathrm{i}}$:

$$w^2 = r^2 e^{2(\mathrm{i}\theta)} = e^{\mathrm{i}\left(\frac{\pi}{2} + 2\pi\right)}, \tag{9.18}$$

$$r = 1, \tag{9.19}$$

$$\theta = \frac{\pi}{4} + \pi \tag{9.20}$$

Os dois valores possíveis para $\sqrt{\mathrm{i}}$ são

$$w_1 = \frac{\sqrt{2}}{2}(1 + \mathrm{i}), \tag{9.21}$$

$$w_2 = -\frac{\sqrt{2}}{2}(1 + \mathrm{i}). \tag{9.22}$$

A solução geral, portanto, é

$$w(z) = w_G + c_1 \exp\left(w_1 \sqrt{\frac{f_c}{K}} z\right) + c_2 \exp\left(w_2 \sqrt{\frac{f_c}{K}} z\right). \tag{9.23}$$

Para atender às condições de contorno (9.13)–(9.14), $c_1 = 0$ e $c_2 = -w_G$. A solução é

$$w(z) = w_G \left[1 - \exp\left(-(1+\mathrm{i})\sqrt{\frac{f_c}{2K}} z\right)\right], \tag{9.24}$$

$$= w_G \left[1 - \exp\left(-\sqrt{\frac{f_c}{2K}} z\right)\left(\cos\sqrt{\frac{f_c}{2K}} z - \mathrm{i}\operatorname{sen}\sqrt{\frac{f_c}{2K}} z\right)\right]. \tag{9.25}$$

Agora, se alinharmos o vetor vento geostrófico com o eixo x, ou seja, se $V_G = 0$, a solução para a velocidade média na camada-limite atmosférica é

$$\overline{U}(z) = U_G \left[1 - \exp\left(-\sqrt{\frac{f_c}{2K}} z\right)\cos\sqrt{\frac{f_c}{2K}} z\right], \tag{9.26}$$

$$\overline{V}(z) = U_G \left[\exp\left(-\sqrt{\frac{f_c}{2K}} z\right)\operatorname{sen}\sqrt{\frac{f_c}{2K}} z\right]. \tag{9.27}$$

9.1.2 – Hemisfério Sul

Procura-se $\sqrt{-\mathrm{i}}$:

$$w^2 = r^2 e^{2(\mathrm{i}\theta)} = e^{\mathrm{i}(-\frac{\pi}{2}+2\pi)}, \tag{9.28}$$

$$r = 1, \tag{9.29}$$

$$\theta = -\frac{\pi}{4} + \pi \tag{9.30}$$

Os dois valores possíveis para $\sqrt{\mathrm{i}}$ são

$$w_3 = \frac{\sqrt{2}}{2}(1 - \mathrm{i}), \tag{9.31}$$

$$w_4 = \frac{\sqrt{2}}{2}(-1 + \mathrm{i}). \tag{9.32}$$

A solução geral agora será

$$w(z) = w_G + c_3 \exp\left(w_3 \sqrt{\frac{f_c}{K}} z\right) + c_4 \exp\left(w_4 \sqrt{\frac{f_c}{K}} z\right). \tag{9.33}$$

Para atender às condições de contorno (9.13)–(9.14), $c_3 = 0$ e $c_4 = -w_G$. A solução é

$$w(z) = w_G \left[1 - \exp\left((-1+\mathrm{i})\sqrt{\frac{f_c}{2K}} z\right)\right], \tag{9.34}$$

$$= w_G \left[1 - \exp\left(-\sqrt{\frac{f_c}{2K}} z\right)\left(\cos\sqrt{\frac{f_c}{2K}} z + \mathrm{i}\operatorname{sen}\sqrt{\frac{f_c}{2K}} z\right)\right]. \tag{9.35}$$

Agora, se alinharmos o vetor vento geostrófico com o eixo x, ou seja, se $V_G = 0$, a solução para a velocidade média na camada-limite atmosférica é

$$\overline{U}(z) = U_G \left[1 - \exp\left(-\sqrt{\frac{f_c}{2K}}\, z\right) \cos \sqrt{\frac{f_c}{2K}} z \right], \tag{9.36}$$

$$\overline{V}(z) = -U_G \left[\exp\left(-\sqrt{\frac{f_c}{2K}}\, z\right) \text{sen} \sqrt{\frac{f_c}{2K}} z \right]. \tag{9.37}$$

Note que a diferença entre a solução (9.26)–(9.27) obtida anteriormente para o Hemisfério Norte, e (9.36)–(9.37) obtida agora para o Hemisfério Sul, é que $\overline{V}$ muda de sinal, ou seja: o vetor velocidade do vento "gira" para a esquerda no Hemisfério Norte, e para a direita no Hemisfério Sul.

Neste modelo simplificado, é fácil calcular o ângulo total de giro da espiral:

$$\lim_{z \to 0} \frac{\overline{V}}{\overline{U}} = \pm 1, \tag{9.38}$$

onde o sinal de menos se aplica ao Hemisfério Sul. Portanto, o giro total é de $\pi/4$ radianos (45°).

9.2 – Similaridade de Rossby e *Asymptotic Matching*

(Extraído de H. Tennekes, "Similarity relations, scaling laws and spectral dynamics")

Suponha uma atmosfera neutra, $|L_O| = +\infty$ sobre uma superfície horizontalmente homogênea. Nela, o vetor velocidade horizontal do vento é

$$\overline{\boldsymbol{u}} = \overline{u}\, \boldsymbol{i} + \overline{v}\, \boldsymbol{j}, \tag{9.39}$$

de tal forma que no topo da camada-limite atmosférica:

$$|\overline{\boldsymbol{u}}| \to \sqrt{u_g^2 + v_g^2} \equiv G, \tag{9.40}$$

onde u_g e v_g são as componentes do vento geostrófico. As duas escalas de comprimento possíveis para o nosso problema são z_0 (a rugosidade da superfície para quantidade de movimento) e G/f, onde f é o parâmetro de Coriolis. Note que

$$\frac{G}{f} \sim L_p \quad \text{com} \quad \frac{\partial \overline{p}}{\partial x} \sim \frac{\Delta \overline{p}}{L_p}. \tag{9.41}$$

A razão entre estas duas escalas produz o *Número de Rossby de rugosidade*:

$$R_o = \frac{G}{f z_0}. \tag{9.42}$$

As equações médias de Reynolds para um problema homogêneo na horizontal e permanente são

$$f(\overline{v} - v_g) = \frac{\partial}{\partial z}(\overline{w'u'}), \tag{9.43}$$

$$f(u_g - \overline{u}) = \frac{\partial}{\partial z}(\overline{w'v'}) \tag{9.44}$$

Para tornar (9.43)–(9.44) adimensionais, divida por $f u_*$: nós vamos supor que dentro da CLA porém ainda suficientemente "longe" da superfície, os perfis de vento dependem do número adimensional zf/u_* de acordo com

$$\frac{\overline{v} - v_g}{u_*} \;=\; \frac{\partial(\overline{w'u'})}{\partial z f u_*} \;=\; F_y(\frac{zf}{u_*}), \tag{9.45}$$

$$\frac{\overline{u} - ug}{u_*} \;=\; -\frac{\partial(\overline{w'v'})}{\partial z f u_*} \;=\; F_x(\frac{zf}{u_*}) \tag{9.46}$$

Devido à eq. (9.40), no topo da CLA onde $z = z_i$ [1] devemos ter:

$$F_x(\frac{zf}{u_*}) = F_y(\frac{zf}{u_*}) = 0 \tag{9.47}$$

Ambas as funções adimensionais F_x e F_y devem possuir a mesma raiz, que denominaremos aqui e^A para facilitar a manipulação algébrica posterior; a constante A efetivamente *define* a espessura da CLA dinamicamente:

$$\frac{z_i f}{u_*} \equiv e^{-A} \Rightarrow z_i = \frac{e^{-A} u_*}{f} \tag{9.48}$$

Crítica: esta definição não funciona no equador, onde $f = 0$; na prática, aparentemente a similaridade de Rossby que estamos estudando não funciona muito bem em lugar nenhum, devido a diversos complicadores; mesmo assim, nós a estamos estudando aqui por seu interesse matemático.

Agora, sabemos que a adimensionalização proposta por (9.45)–(9.46) *não* vai funcionar à medida em que nos aproximarmos da superfície. Por exemplo, próximo de $z = 0$ a previsão de (9.45) é

$$-\frac{v_g}{u_*} = \frac{1}{f u_*}\frac{d\,\overline{w'u'}}{dz}; \tag{9.49}$$

mas $\overline{w'u'} = 0$ em $z = 0$; em alturas verticais próximas da rugosidade z_0 a contribuição viscosa para o fluxo de quantidade de movimento é significativa, e o termo de viscosidade teria que ser incluído nas equações de Reynolds para médias.

Uma alternativa, que nós já utilizamos quando estudamos os perfis de vento na sub-camada dinâmica, é tentar re-escrever as equações utilizando a rugosidade z_0; utilizando o número de Rossby de rugosidade, obtemos:

$$\frac{z_0 f}{G}\frac{G}{u_*}\frac{\overline{v} - v_g}{u_*} \;=\; \frac{d\,\overline{w'u'}/u_*^2}{dz/z_0} \tag{9.50}$$

$$\frac{z_0 f}{G}\frac{G}{u_*}\frac{\overline{u} - u_g}{u_*} \;=\; -\frac{d\,\overline{w'u'}/u_*^2}{dz/z_0} \tag{9.51}$$

Ora, o número de Rossby de rugosidade é necessariamente um número muito grande; quando $R_o \to \infty$, é razoável supor que

$$\left|\frac{G(\overline{v} - v_g)}{u_*^2}\right| < \infty \;\text{ e }\; \left|\frac{G(\overline{u} - u_g)}{u_*^2}\right| < \infty \;;$$

---

[1]Note que apesar de eu estar usando o símbolo z_i, cuja origem é "altura de inversão", a definição da espessura da CLA utilizada aqui é *totalmente dinâmica*, e não tem nada a ver com a altura da inversão do perfil de temperatura potencial

já que u_* deve crescer com G, enquanto que $\overline{u} \sim G$ e $\overline{v} \sim G$ (no máximo). Portanto, quando $R_o \to \infty$, o lado esquerdo tende a zero, e consequentemente o lado direito também:

$$\lim_{R_o \to \infty} \frac{d\,\overline{w'u'}\,/u_*^2}{dz/z_0} = 0, \tag{9.52}$$

$$\lim_{R_o \to \infty} \frac{d\,\overline{w'v'}\,/u_*^2}{dz/z_0} = 0. \tag{9.53}$$

Então, ao orientarmos os eixos x e y de tal forma que em $z = 0$, $\overline{v} = 0$ e $\overline{w'v'} = 0$, obtemos:

$$\overline{w'u'} \;=\; u_*^2 \;=\; \text{cte} \tag{9.54}$$
$$\overline{w'v'} \;=\; 0 \tag{9.55}$$

Ambas as equações acima devem valer numa "camada superficial" dinamicamente definida por

$$1 \ll |z/z_0| < \infty.$$

Agora cabe fazer o *matching* propriamente dito. Nossos resultados até agora são:

1. Na "camada superficial":

$$\frac{u}{u_*} = g(z/z_0) \tag{9.56}$$

2. Na "camada-limite atmosférica":

$$\frac{\overline{u} - u_g}{u_*} \;=\; F_x\left(\frac{zf}{u_*}\right) \tag{9.57}$$

$$\frac{\overline{v} - v_g}{u_*} \;=\; F_y\left(\frac{zf}{u_*}\right) \tag{9.58}$$

O *matching* em si consiste em tentar "casar" estas equações quando $zf/u_* \to 0$ e $z/z_0 \to \infty$. Além disso, segundo Tennekes, eu *derivo* ambas as relações de similaridade, e faço o "casamento" para $\partial \overline{u}/\partial z$ e $\partial \overline{v}/\partial z$. Para $\overline{u}$:

$$\frac{\partial \overline{u}}{\partial z} = \frac{u_*}{z_0}\frac{\partial g}{\partial \xi}, \quad \text{onde} \quad \xi = \frac{z}{z_0} \tag{9.59}$$

$$\frac{\partial \overline{u}}{\partial z} = u_*\frac{\partial F_x}{\partial z} = f\frac{\partial F_x}{\partial \eta}, \quad \text{onde} \quad \eta = \frac{zf}{u_*} \tag{9.60}$$

Agora, quando $\xi \to \infty$ e $\eta \to 0$, devemos ter:

$$\frac{u_*}{z_0}\frac{\partial g}{\partial \xi} \;=\; f\frac{\partial F_x}{\partial \eta} \;\Rightarrow \tag{9.61}$$

$$\xi\frac{\partial g}{\partial \xi} = \eta\frac{\partial F_x}{\partial \eta} \tag{9.62}$$

Numa analogia com o método de separação de variáveis, cada um dos lados de (9.62) deve ser igual a uma constante *na região do casamento*:

$$\frac{z}{u_*}\frac{\partial \overline{u}}{\partial z} = \frac{1}{\kappa}, \tag{9.63}$$

onde a constante assintótica κ é a própria constante de von Kármán; integrando,

$$\frac{\kappa}{u_*}\left(\overline{u}_2 - \overline{u}_1\right) = \ln\frac{z_2}{z_1}. \tag{9.64}$$

Na camada superficial, escolho $\overline{u}_1 = 0$ em $z_1 = z_0$ e obtenho o bem-conhecido perfil logaritmico

$$\frac{u}{u_*} = \frac{1}{\kappa}\ln(\frac{z}{z_0}). \quad (z/z_0 \gg 1) \tag{9.65}$$

Se, por outro lado, eu tomar $\overline{u}_1$ como a velocidade dentro da CLA e $\overline{u}_2 = u_g$:

$$\frac{\kappa}{u_*}\left(u_g - \overline{u}\right) = \ln\frac{z_i}{z}, \tag{9.66}$$

$$\frac{\kappa}{u_*}\left(\overline{u} - u_g\right) = \ln\frac{zf}{u_*}\frac{u_*}{z_i f}. \tag{9.67}$$

usando (9.48):

$$\frac{\kappa}{u_*}\left(\overline{u} - u_g\right) = \ln\frac{zf}{u_*} + A \tag{9.68}$$

isto é:

$$\frac{\overline{u} - u_g}{u_*} = \frac{1}{\kappa}\left(\ln\left(\frac{zf}{u_*}\right) + A\right) \quad (zf/u_* \ll 1) \tag{9.69}$$

Eliminando-se agora $\overline{u}$ entre (9.65) e (9.68), obtém-se uma *relação de arrasto*,

$$\frac{u_g}{u_*} = \frac{1}{\kappa}\left(\ln\frac{u_*}{fz_0} - A\right) \tag{9.70}$$

Para $\overline{v}$, em $1 \ll z/z_0 < \infty$,

$$\overline{v} = 0, \tag{9.71}$$

enquanto que em $1 \gg (zf)/u_* \to 0$:

$$\frac{-v_g}{u_*} = F_y(0) = \frac{B}{\kappa}, \tag{9.72}$$

onde a segunda igualdade é a *definição* da constante B de forma análoga a A. Combinando-se (9.70) e (9.72):

$$\frac{G}{u_*} = \frac{1}{\kappa}\left\{\left[\ln\left(\frac{u_*}{fz_0}\right) - A\right]^2 + B^2\right\}^{1/2}. \tag{9.73}$$

10

O processamento de dados micrometeorológicos

10.1 – Médias probabilísticas, e os postulados de Reynolds

As medições eulerianas realizadas rotineiramente ou em modo de campanha em estações micro-, agro-, ou simplesmente "meteorológicas" podem ser compreendidas em termos de suas escalas temporais à luz da decomposição de Reynolds, via (**??**).

A decomposição de Reynolds, ela mesma, baseia-se fortemente na idéia de que a turbulência atmosférica é um processo estocástico superposto a uma "média" determinística:

$$U(\omega, t) = \langle U \rangle (t) + u(\omega, t). \tag{10.1}$$

Estritamente falando, (10.1) e, principalmente, os "postulados de Reynolds" que em geral se seguem, valem para médias *probabilísticas* (em Inglês, *ensemble averaging*). Vamos defini-los todos sucintamente. Sejam $U(\omega, t)$ e $V(\omega, t)$ dois processos estocásticos, não necessariamente estacionários, que representam duas grandezas atmosféricas quaisquer. O valor esperado de U é a sua integral em relação à medida de probabilidade P do espaço amostral (Billingsley, 1986, cap. 3, seção 21):

$$\langle U \rangle (t) \equiv \int_{\omega \in \Omega} U(\omega, t) dP(\omega). \tag{10.2}$$

Esta definição é extremamente sofisticada, e requer pelo menos alguma idéia do que significa, em termos matemáticos, uma "medida de probabilidade". É possível torná-la um pouco mais palatável. Considere aqui um conjunto Ω, o "espaço amostral". Em termos simples, Ω é o conjunto do qual serão sorteados elementos ω. Um problema matemático gigantesco é *definir* o significado de uma integral sobre Ω quando as probabilidades de ocorrência de cada elemento ω não são finitas, mas sim infinitesimais. Suponhamos então que seja possível postular uma densidade de probabilidade para cada ω, de tal maneira que a probabilidade de ocorrência de um subconjunto $A \subset \Omega$ seja:

$$P(A) = \int_{\omega \in A} p(\omega) d\omega. \tag{10.3}$$

Esta, entretanto, é normalmente interpretada como uma integral "de Riemman". Em lugar de "fatiar" o eixo ω, é possível "fatiar" o eixo P, e escrever:

$$P(A) = \int_{\omega \in A} dP(\omega). \tag{10.4}$$

A integral mais antiga com este jeito é a integral de Stieljes. Com integrais deste tipo, integrais de Stieljes e de Lesbegue, a forma elegante de definir $\langle U \rangle (t)$ é (10.2). Segue-se que

$$u(\omega, t) = U(\omega, t) - \int_{\xi \in \Omega} U(\xi, t) dP(\xi),$$

$$\langle u(\omega, t) \rangle = \int_{\omega \in \Omega} \left[U(\omega, t) - \int_{\xi \in \Omega} U(\xi, t) dP(\xi) \right] dP(\omega)$$

$$= \int_{\omega \in \Omega} U(\omega, t) dP(\omega) - \int_{\omega \in \Omega} \int_{\xi \in \Omega} U(\xi, t) dP(\xi) dP(\omega)$$

$$= \int_{\omega \in \Omega} U(\omega, t) dP(\omega) - \int_{\xi \in \Omega} \underbrace{\left[\int_{\omega \in \Omega} dP(\omega) \right]}_{=1} U(\xi, t) dP(\xi)$$

$$= 0 \tag{10.5}$$

Portanto, u tem média probabilística zero.

Visto desta forma, $\langle U \rangle (t)$ é uma função determinística (e não aleatória), porque a aleatoriedade, representada pela dependência com ω, foi integrada. Os demais "postulados" se seguem:

$$\langle \langle U \rangle u \rangle = \int_{\omega \in \Omega} \langle U \rangle u \, dP$$

$$= \langle U \rangle \int_{\omega \in \Omega} u \, dp$$

$$= 0, \tag{10.6}$$

$$\langle \langle U \rangle V \rangle = \int_{\omega \in \Omega} \left[\langle U \rangle \left(\langle V \rangle + v \right) \right] dP$$

$$= \langle U \rangle \langle V \rangle + \langle U \rangle \int_{\omega \in \Omega} v \, dP$$

$$= \langle U \rangle \langle V \rangle, \tag{10.7}$$

e

$$\langle UV \rangle = \int_{\omega \in \Omega} \left[\left(\langle U \rangle + u \right) \left(\langle V \rangle + v \right) \right] dP$$

$$= \langle U \rangle \langle U \rangle + \int_{\omega \in \Omega} u(\omega, t) v(\omega, t) \, dP(\omega)$$

$$\langle U \rangle \langle V \rangle + \langle uv \rangle. \tag{10.8}$$

Finalmente, as derivadas temporais e espaciais e seus valores esperados comutam; por exemplo, no caso da derivada temporal,

$$\frac{\partial}{\partial t} \langle U \rangle = \frac{\partial}{\partial t} \int_{\omega \in \Omega} U(\omega, t) \, dP(\omega)$$

$$= \int_{\omega \in \Omega} \frac{\partial U(\omega, t)}{\partial t} \, dP(\omega)$$

$$= \left\langle \frac{\partial U}{\partial t} \right\rangle. \tag{10.9}$$

10.2 – Outras médias

Além da média probabilística, outras possibilidades existem. Por exemplo, a média temporal simples

$$\langle U(\omega, t)\rangle_{\mathrm{T}} = \langle U\rangle_{\mathrm{T}}(\omega) \equiv \frac{1}{T}\int_0^T U(\omega, t)\,dt. \tag{10.10}$$

Observe que $\langle U\rangle_{\mathrm{T}}(\omega)$ é, como a notação indica, apenas uma função de ω, e que portanto as derivadas em relação a t não comutam:

$$\frac{\partial}{\partial t}\left[\langle U\rangle_{\mathrm{T}}(\omega)\right] = 0 \neq \left\langle\frac{\partial U(\omega, t)}{\partial t}\right\rangle_{\mathrm{T}}. \tag{10.11}$$

Mesmo assim, uma propriedade desejável destas médias é que a média da flutuação é zero. Para ver como, estabeleça uma "decomposição de Reynolds" da forma

$$U(\omega, t) = \langle U(\omega, t)\rangle_{\mathrm{T}} + u(\omega, t), \tag{10.12}$$

mas agora $u(\omega, t)$ possui um significado *diferente* daquele de (10.1)! Mesmo assim, é evidente que vale

$$\begin{aligned}
\langle u(\omega, t)\rangle_{\mathrm{T}} &= \frac{1}{T}\int_0^T u(\omega, t)\,dt \\
&= \frac{1}{T}\int_0^T \left[U(\omega, t) - \langle U(\omega, t)\rangle_{\mathrm{T}}\right]\,dt \\
&= \langle U(\omega, t)\rangle_{\mathrm{T}}(\omega) - \langle U(\omega, t)\rangle_{\mathrm{T}}(\omega) = 0 \;\blacksquare
\end{aligned} \tag{10.13}$$

Médias temporais, entretanto, servem para definir a *ergodicidade* de um processo; um processo é *ergódico* quando

$$\lim_{T\to\infty}\frac{1}{T}\int_0^T U(\omega, t)\,dt = \langle U\rangle(t). \tag{10.14}$$

Mas haverá alguma estranheza nesta relação? Sim: o lado esquerdo é (no caso mais geral) função de ω, enquanto que o lado direito é, no caso mais geral, função de t; portanto, nossa definição de ergodicidade implica

$$\langle U\rangle_{\mathrm{T}}(\omega) = \langle U\rangle(t) \iff \langle U\rangle_{\mathrm{T}} = \langle U\rangle = \text{constante}. \tag{10.15}$$

Um processo em que $\langle U\rangle = $ constante é dito *estacionário na média*; de forma mais geral, um processo estocástico é estacionário quando a distribuição conjunta de probabilidade de

$$(U(\omega, t_1 + h), U(\omega, t_2 + h), \ldots, U(\omega, t_n + h))$$

(para qualquer enupla $(t_1, t_2, \ldots, t_n)$ imaginável!) é independente de h (Cram?r and Leadbeter, 2004). Valendo a estacionariedade, segue-se que, *para qualquer momento de ordem n,*

$$\begin{aligned}
\langle U^n(\omega, t + h)\rangle &= \langle U^n(\omega, t)\rangle\,; \\
\langle U^n(\omega, t + h)\rangle - \langle U^n(\omega, t)\rangle &= 0; \\
\lim_{h\to 0}\frac{\langle U^n(\omega, t + h)\rangle - \langle U^n(\omega, t)\rangle}{h} &= 0; \\
\frac{\partial\langle U^n(\omega, t)\rangle}{\partial t} &= 0 \;\blacksquare
\end{aligned} \tag{10.16}$$

Nem todo processo estacionário é ergódico; porém, como vimos, a estacionariedade é uma condição *necessária* para a ergodicidade.

A "extração da média" de um registro de dados turbulentos tende a ser mais complicada do que a exposição acima para os postulados de Reynolds, *porque a dependência funcional com ω é desconhecida para dados observacionais*. A rigor, ela é uma hipótese; porém, trata-se de uma hipótese não-verificável. Para dados observacionais de turbulência atmosférica, algumas médias "empíricas" sobre os dados são tradicionalmente empregadas. A esperança costuma ser que as flutuações $u(t)$ extraídas pelo processo sejam representativas de um processo estocástico estacionário.

As formas mais comuns de se extrair médias $\langle U(t) \rangle_?$ e flutuações $u(t)$ em micrometeorologia são as seguintes:

1. "Médias de bloco" (*block averages*).

2. "Remoção linear de tendência" (*linear detrending*).

3. "Filtragens" (*filtering*).

Médias de bloco são o equivalente discreto de (10.10). Se o *array* U é

$$U = (U_0, U_1, \ldots, U_{n-1}),$$

$$\overline{U} = \frac{1}{n} \sum_{k=0}^{n-1} U_k, \tag{10.17}$$

$$u_k = U_k - \overline{U}. \tag{10.18}$$

Em um caso muito comum, o tempo de medição é de 30 minutos, e a frequência de medição é de 20 Hz, donde $n = 30 \times 60 \times 20 = 36000$.

No caso de remoção linear de tendência, ajusta-se uma reta de mínimos quadrados à variável tempo, na forma

$$\overline{U}_k = ak + b \tag{10.19}$$

de forma a minimizar

$$\sum_{i=k}^{n-1} \left[\overline{U}_k - U_k \right]^2.$$

O modelo contínuo equivalente para a média de tendência linear é o seguinte: dado $U(t)$ deseja-se obter a função

$$\langle U \rangle_{\mathrm{T}} (t) = at + b \tag{10.20}$$

tal que

$$S = \frac{1}{T} \int_0^T [U(t) - (at + b)]^2 \, dt$$

seja mínimo. Uma condição necessária (e neste caso também suficiente) para a minimização é

$$\frac{\partial S}{\partial a} = \frac{\partial S}{\partial b} = 0,$$

que leva a

$$\frac{1}{T}\int_0^T \left[U(t) - (at+b)\right] t \, dt = 0, \tag{10.21}$$

$$\frac{1}{T}\int_0^T \left[U(t) - (at+b)\right] = 0. \tag{10.22}$$

A equação (10.22) mostra que, se definirmos a decomposição

$$U(t) = \langle U \rangle_{\mathrm{T}}(t) + u(t) = [at+b] + u(t), \tag{10.23}$$

então segue-se que

$$\langle u(t) \rangle_{\mathrm{T}} = \frac{1}{T}\int_0^T u(t)\,dt = \frac{1}{T}\int_0^T \left[U(t) - (at+b)\right]\,dt = 0, \tag{10.24}$$

que é análogo ao postulado de Reynolds (10.5). Além disto,

$$\begin{aligned}
\langle \langle U \rangle_{\mathrm{T}} u \rangle_{\mathrm{T}} &= \frac{1}{T}\int_0^T [at+b]\left[U(t) - (at+b)\right]\,dt \\
&= a\underbrace{\frac{1}{T}\int_0^T t\left[U(t) - (at+b)\right]\,dt}_{=0} + b\underbrace{\frac{1}{T}\int_0^T \left[U - (at+b)\right]\,dt}_{=0} = 0,
\end{aligned}$$
$$\tag{10.25}$$

em que os dois colchetes são nulos em virtude de (10.20)–(10.21), e que é análogo ao postulado de Reynolds (10.6).

Nesta altura algumas características desejáveis da remoção linear de tendência ficam evidentes: ela parece propiciar uma média que evolui no tempo tal que, dada a decomposição (10.23), um conjunto de teoremas para as médias temporais análogo aos postulados de Reynolds (10.5)–(10.9) pode ser deduzido.

Vale a pena verificar se isto é mesmo verdade para os postulados restantes, (10.7)–(10.9). Suporemos portanto que obtivemos tendências lineares por mínimos quadrados,

$$\langle U \rangle_{\mathrm{T}}(t) = at + b,$$
$$\langle V \rangle_{\mathrm{T}}(t) = ct + d$$

e verificaremos:

$$\begin{aligned}
\langle \langle U \rangle_{\mathrm{T}} V \rangle_{\mathrm{T}} &= \frac{1}{T}\int_0^T [at+b]V(t)\,dt \\
&= \text{constante} \\
&\neq [at+b][ct+d] = \langle U \rangle_{\mathrm{T}} \langle V \rangle_{\mathrm{T}}. \tag{10.26}
\end{aligned}$$

Além disto,

$$\begin{aligned}
\langle UV \rangle_{\mathrm{T}} &= \langle (\langle U \rangle_{\mathrm{T}} + u)(\langle V \rangle_{\mathrm{T}} + v) \rangle_{\mathrm{T}} \\
&= \langle \langle U \rangle_{\mathrm{T}} \langle V \rangle_{\mathrm{T}} \rangle_{\mathrm{T}} + \langle \langle U \rangle_{\mathrm{T}} v \rangle_{\mathrm{T}} + \langle u \langle V \rangle_{\mathrm{T}} \rangle_{\mathrm{T}} + \langle uv \rangle_{\mathrm{T}}. \tag{10.27}
\end{aligned}$$

Portanto, não há analogia entre os postulados de Reynolds (10.7)–(10.8) com as médias temporais respectivas (10.26)–(10.27) utilizando remoção linear de tendência.

O último postulado a ser verificado é

$$
\begin{aligned}
\left\langle \frac{\partial U}{\partial t} \right\rangle_{\mathrm{T}} &= \frac{1}{T} \int_0^T \frac{\partial U}{\partial t}\, dt \\
&= \frac{1}{T} \int_0^T \left[a + \frac{\partial u}{\partial t} \right] dt \\
&= a + \frac{1}{T} \left[u(T) - u(0) \right] \neq a = \frac{\partial \langle U \rangle_{\mathrm{T}}}{\partial t}.
\end{aligned}
\tag{10.28}
$$

Neste caso, apesar da desigualdade estrita, vale entretanto o resultado assintótico:

$$
\lim_{T \to \infty} \left\langle \frac{\partial U}{\partial t} \right\rangle_{\mathrm{T}} = a = \frac{\partial \langle U \rangle_{\mathrm{T}}}{\partial t}.
\tag{10.29}
$$

Além disto, integrando-se (10.21)–(10.22) obtém-se o sistema

$$
I_0 = \frac{1}{T} \int_0^T U(t)\, dt = \frac{aT}{2} + b,
\tag{10.30}
$$

$$
I_1 = \frac{1}{T} \int_0^T t U(t)\, dt = \frac{aT^2}{3} + \frac{bT}{2},
\tag{10.31}
$$

cuja solução é

$$
a = \frac{12 I_1 - 6 I_0 T}{T^2}, \qquad b = \frac{4 I_0 T - 6 I_1}{T}.
$$

No caso das médias por filtragem, gera-se alguma função (do tempo) sucedânea de uma média que evolui também no tempo. Talvez o procedimento mais comum seja usar um filtro auto-recursivo de passa-baixa, com uma janela de tempo $T_L = L\Delta t$, onde $n = (\Delta t)^{-1}$ é a frequencia de aquisição.

Novamente, dado o vetor de dados $\boldsymbol{U}$, aplica-se inicialmente um procedimento auto-recursivo aos valores de U_k:

$$
U_k^< = \frac{U_k + (L - 1) U_{k-1}^<}{L}.
\tag{10.32}
$$

A série $U_k^<$ possui escalas de tempo características longas (ou seja: baixas frequências), e desempenha o papel de uma média que evolui no tempo deterministicamente. As flutuações serão associadas com o componente de alta frequência, e são extraídas em dois passos. Inicialmente, extrai-se as altas frequências por meio de

$$
U_k^> = U_k - U_k^<.
\tag{10.33}
$$

Este procedimento, por si, não garante que a média dos $U_k^>$'s seja nula. Portanto, faz-se, ainda

$$
u_k = U_k^> - \frac{1}{N} \sum_{k=1}^N U_k^>
\tag{10.34}
$$

para extrair a (pequena) média residual dos $U_k^>$'s.

É comum adotar-se $\Delta t \ll T_L \ll T$, onde $T = N\Delta t$. Valores típicos de T_L são da ordem de uns poucos minutos. Rannik and Vesala (1999) observaram que valores adequados de T_L para impedir a subestimativa de fluxos e variâncias são da ordem de 1/4 de T. Cada uma das equações (10.32)–(10.34) tem suas definições e razões de ser a seguir: $U^<$ é a componente filtrada de baixa frequência: ela é um sucedâneo do sinal que seria obtido por um sensor lento com constante de tempo T_L, que seria incapaz de "ver" as flutuações turbulentas. Por definição, a componente de alta frequência $U^>$ é a diferença entre o sinal bruto e a componente de baixa frequência. $U^>$ tem uma aparência muito próxima das flutuações turbulentas desejadas, mas sua média, embora em geral pequena em relação a $\overline{U}$, não é exatamente igual a zero.

Em última análise, a sequência de operações (10.32)–(10.34) tem o objetivo de tentar remover, pelo menos em parte, a não-estacionariedade de U na camada-limite atmosférica devida ao ciclo diário da radiação líquida na superfície. De fato, suponha que U fosse um processo estacionário; então, para (a escolha óbvia) $U^< = 0$, $U^> = U$, a série de dados brutos poderia ser diretamente decomposta em média e flutuações que atenderiam por definição aos postulados de Reynolds.

O filtro auto-recursivo de passa-baixa (10.32) é o equivalente numérico a uma operação de convolução de U com o núcleo

$$G(t) = H(t)e^{-t/T_L}/T_L, \tag{10.35}$$

onde $H(t)$ é a função de Heaviside (Dias, 1994). Grosso modo, ele remove componentes com escalas de tempo da ordem de, ou maiores que, T_L.

Considere agora a transformada de Fourier de $G(t)$,

$$\widehat{G}(n) = \int_{-\infty}^{+\infty} G(t)e^{-2\pi int}\, dt = \frac{1}{1 + 2\pi inT_L}; \tag{10.36}$$

pelo teorema da convolução, a operação de filtragem é então equivalente ao produto $\widehat{G}(n)\widehat{U}(n)$ no domínio da frequência. Embora $\widehat{G}(n)$ seja uma função complexa que não pode ser visualizada em duas dimensões, é possível avaliar seu efeito sobre $\widehat{U}$ plotando a função real $|\widehat{G}(n)|$. Isto é feito na figura 10.1: note que a aplicação do filtro afeta fortemente frequências muito *menores* que T_L^{-1}: por exemplo, a intensidade de $\widehat{U}$ na frequência $0,1T_L$ é reduzida em 30%! Já um filtro ideal de passa-baixa (também mostrado em 10.1 para comparação),

$$\widehat{G}^<_{\mathrm{id}}(n) = \begin{cases} 1, & n < T_L^{-1} \\ 0, & n > T_L^{-1} \end{cases}, \tag{10.37}$$

deixa passar sem amortecimento todas as frequências menores que $1/T_L$, e aniquila todas as frequências maiores que este valor. Da mesma forma, um filtro ideal de passa-alta é

$$\widehat{G}^>_{\mathrm{id}}(n) = \left(1 - \widehat{G}^<_{\mathrm{id}}(n)\right). \tag{10.38}$$

O mesmo teorema da convolução proporciona uma sistemática simples de filtragem no domínio da frequência. Dada a série de dados brutos $\boldsymbol{U}$ de um *run*, considere uma única transformada de Fourier numérica dada por

$$\widehat{U}_m = \Delta t \sum_{k=0}^{N-1} U_k \exp\left[\frac{-2\pi ikm}{N}\right]. \tag{10.39}$$
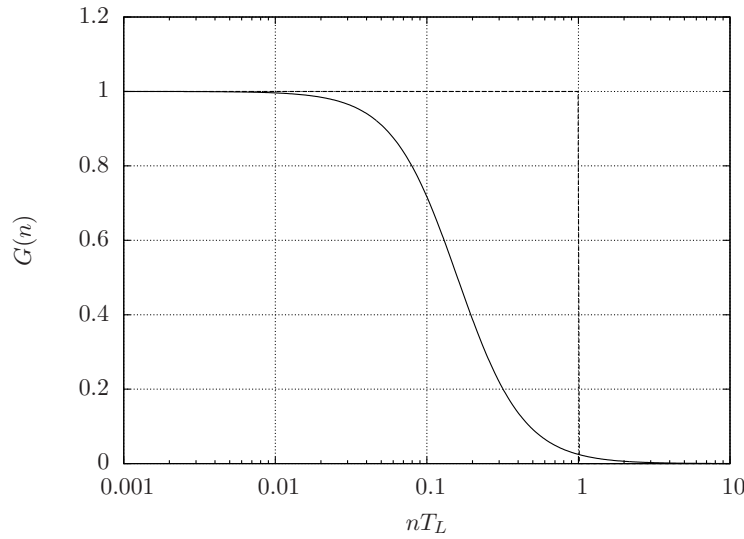
Figure 10.1: Módulo da função de transferência espectral $\widehat{G}(n)$ do filtro de passa-baixa (10.32) (linha sólida) e de um filtro ideal (linha pontilhada)

Para $m \leq N/2$, $\widehat{U}_m$ é a componente de Fourier associada à frequência $n = m/(N\Delta t)$. A partir deste ponto, há um "dobramento" da transformada de Fourier em torno da frequência de Nyquist,

$$n_c = \frac{2}{N\Delta t} \tag{10.40}$$

(vide Bendat and Piersol, 1986, p. 381–382, fig. 11.3), de tal modo que

$$\widehat{U}_m = \widehat{U}_{N-m}^*, \tag{10.41}$$

onde $(\cdot)^*$ significa o conjugado complexo.

Este sinal pode ser agora filtrado *no domínio da frequência*, como se segue. Suponha que desejamos eliminar todas as frequências menores que n_b, ou seja, realizar uma operação de filtragem de *passa-alta*; basta então anular os componentes com frequências inferiores a n_b:

$$\widehat{U}_m = 0, \qquad\qquad \frac{m}{N\Delta t} \leq n_b, \tag{10.42}$$

$$\widehat{U}_m = 0, \qquad\qquad \frac{N-m}{N\Delta t} \leq n_b, \tag{10.43}$$

onde (10.43) é consequência de (10.41), e então voltar ao domínio do tempo por meio de uma transformada de Fourier inversa. A série resultante não conterá mais nenhum harmônico de frequência inferior a n_b. Isto elimina naturalmente tendências de não-estacionariedade da média.

Nós agora vamos dar um exemplo de ambos os filtros [Nota: apenas o filtro no domínio do tempo foi feito. Um bom trabalho para este curso seria fazer uma aplicação de filtro espectral, para completar o exemplo] com medições em alta frequência de densidades de vapor d'água; nós vamos escolher um período particularmente interessante, que são as medições realizadas no Lago de Furnas durante 30 minutos terminando em 2003-06-04T14:00:00.00. Para uma descrição do experimento, veja Dias et al. (2007). A decomposição de Reynolds é

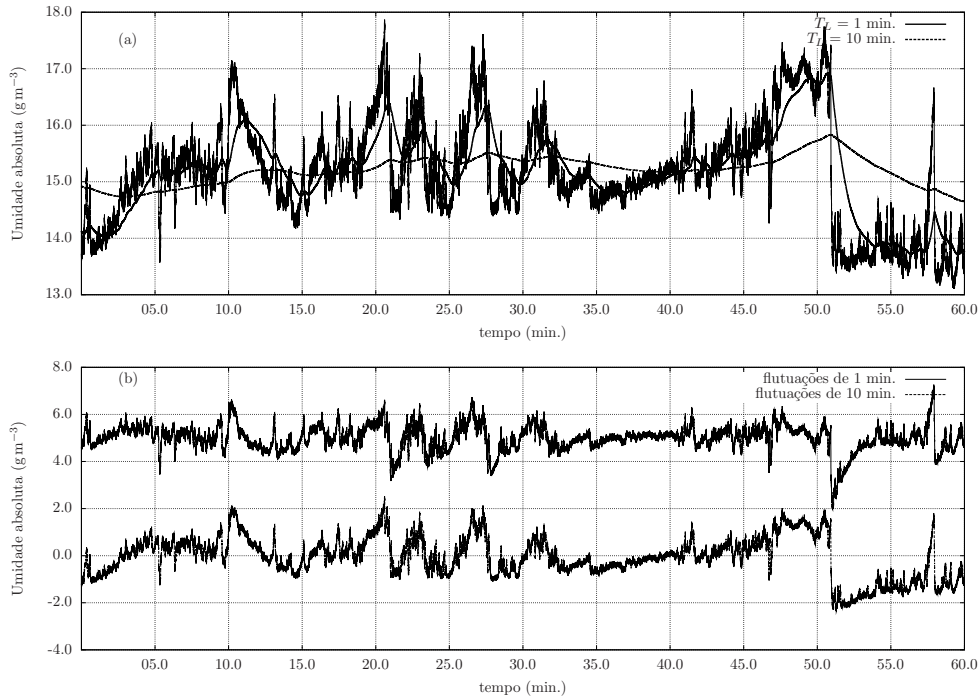$$\wp_v = \langle \wp_v \rangle + \rho_v. \tag{10.44}$$

Figure 10.2: (a): filtro recursivo de passa-baixa com "janelas" T_L = 1 minuto e T_L = 10 minutos; (b): flutuações turbulentas de 1 minuto (deslocadas de +5g m^{-3}) e de 10 minutos

A figura 10.2 mostra os dados de densidade de vapor d'água medidos, a operação de filtragem de passa-baixa, e as séries de flutuações resultantes das filtragens de 1 minuto e 10 minutos. É importante observar que a escolha da "janela" T_L do filtro *modifica* a série de flutuações (neste caso, ρ_v) resultantes.

10.3 – Correlação temporal

Para processos estocásticos estacionários, é possível definir diversas estatísticas de dependência e memória. A mais clássica é a função de autocovariância (muitos autores a chamam simplesmente de função de autocorrelação); para um processo geral (não necessariamente estacionário), a função de autocovariância é uma função de *duas* variáveis:

$$R(t_1, t_2) \equiv \langle u(\omega, t_1) u(\omega, t_2) \rangle . \tag{10.45}$$

Agora, se o processo for estacionário, $R(t_1, t_2)$ deve ser invariante sob uma translação qualquer no tempo. Em particular,

$$R(t_1, t_2) = R(0, t_2 - t_1) = \langle u(\omega, 0) u(\omega, t_2 - t_1) \rangle , \tag{10.46}$$

ou

$$R(\tau) \equiv \langle u(\omega, 0) u(\omega, \tau) \rangle , \tag{10.47}$$

que é a definição que vamos usar para a função de autocovariância de processos estacionários. Uma outra função igualmente importante é a *função de estrutura*:

$$D(\tau) \equiv \left\langle [u(\omega, \tau) - u(\omega, 0)]^2 \right\rangle , \tag{10.48}$$

que desempenha um papel fundamental na Teoria de turbulência de Kolmogorov de 1941 (Kolmogorov, 1991). Em processos estocásticos estacionários, as duas são equivalentes:

$$\begin{aligned}
\left\langle \left[u(\omega, \tau) - u(\omega, 0) \right]^2 \right\rangle &= \left\langle u^2(\omega, \tau) - 2u(\omega, \tau)u(\omega, 0) + u(\omega, 0) \right\rangle \\
&= \left\langle u^2(\omega, \tau) \right\rangle + \left\langle u^2(\omega, 0) \right\rangle - 2 \left\langle (\omega, \tau)u(\omega, 0) \right\rangle \\
&= 2R(0) - 2R(\tau) \\
&= 2[R(0) - R(\tau)] \; \blacksquare
\end{aligned} \tag{10.49}$$

Um estimador para a função de autocovariância a partir de dados amostrais contidos em um vetor de dados de flutuações $\boldsymbol{u} = (u_0, u_1, \ldots, u_{N-1})$ é

$$\widehat{R}(k\Delta t) = \widehat{R}_k = \frac{1}{N-k} \sum_{i=0}^{N-k} u_i u_{i+k}. \tag{10.50}$$

Seguimos agora para covariâncias cruzadas. Estas são definidas por

$$R_{i,j}(\tau) \equiv \left\langle u_i(\omega, 0)u_j(\omega, \tau) \right\rangle. \tag{10.51}$$

Note que $R_{i,j}(0)$ é o fluxo (cinemático) de Reynolds:

$$R_{i,j}(0) = \left\langle u_i(\omega, 0)u_j(\omega, 0) \right\rangle \tag{10.52}$$

O estimador óbvio para dados discretos é

$$\widehat{R}_{i,j}(k\Delta t) = \frac{1}{N-k} \sum_{l=0}^{N-k} u_{il} u_{j_{l+k}}. \tag{10.53}$$

Note a dificuldade notacional com os índices.

10.4 – Transformadas de Fourier

O par $f(x)$ e sua transformada de Fourier de $\widehat{f}(k_1)$ são definidos como

$$\widehat{f}(k_1) = \frac{1}{2\pi} \int_{-\infty}^{+\infty} f(x)e^{-ik_1 x} \, dx, \tag{10.54}$$

$$f(x) = \int_{-\infty}^{\infty} \widehat{f}(k_1)e^{+ik_1 x} \, dk_1. \tag{10.55}$$

A transformada de Fourier inversa da delta de Dirac é

$$\int_{-\infty}^{+\infty} \delta(k_1)e^{+ik_1 x} \, dk_1 = e^{ik_1 x} \Big|_{k_1=0} = 1. \tag{10.56}$$

Portanto, formalmente temos

$$\mathscr{F}\{1\} = \frac{1}{2\pi} \int_{-\infty}^{+\infty} e^{-ik_1 x} \, dx = \delta(k_1). \tag{10.57}$$

Em particular,

$$\delta(0) = \frac{1}{2\pi} \int_{-\infty}^{+\infty} dx. \tag{10.58}$$

Nesta forma, estes resultados são um pouco abstratos. Considere então a versão finita,

$$\frac{1}{2\pi} \int_{-L}^{+L} [\cos k_1 x - i \operatorname{sen} k_1 x] \, dx. \tag{10.59}$$

A parte imaginária do integrando é uma função ímpar de x, cuja integral de $-L$ a $+L$ se anula. Ficamos com

$$\begin{aligned}
\frac{1}{2\pi k_1} \int_{-L}^{+L} \cos k_1 x k_1 dx &= \frac{1}{2\pi k_1} \operatorname{sen} k_1 x \Big|_{-L}^{+L} \\
&= \frac{1}{2\pi k_1} \left[\operatorname{sen} k_1 L - \operatorname{sen}(-k_1 L) \right] \\
&= \frac{\operatorname{sen} k_1 L}{\pi k_1}.
\end{aligned} \tag{10.60}$$

As duas propriedades mais importantes da delta de Dirac são

$$\int_{-\infty}^{+\infty} \delta(k_1) \, dk_1 = 1, \tag{10.61}$$

$$\int_{-\infty}^{+\infty} \delta(k_1) \widehat{f}(k_1) \, dk_1 = \widehat{f}(0). \tag{10.62}$$

(Na verdade, a primeira é um caso particular da segunda). A função que obtivemos, $\operatorname{sen} k_1 L / \pi k_1$, atende a ambas:

$$\int_{-\infty}^{+\infty} \frac{\operatorname{sen} k_1 L}{\pi k_1} \, dk_1 = 1, \qquad \forall L; \tag{10.63}$$

e

$$\begin{aligned}
\lim_{L \to \infty} \int_{-\infty}^{+\infty} \widehat{f}(k_1) \frac{\operatorname{sen} k_1 L}{\pi k_1} \, dk_1 &= \lim_{L \to \infty} \int_{-\infty}^{+\infty} \widehat{f}(\frac{k_1 L}{L}) \frac{\operatorname{sen} k_1 L}{\pi (k_1 L)} \, d(k_1 L) \\
&= \lim_{L \to \infty} \int_{u=-\infty}^{+\infty} \widehat{f}(\frac{u}{L}) \frac{\operatorname{sen} u}{\pi u} \, du \\
&= \int_{-\infty}^{+\infty} \widehat{f}(0) \frac{\operatorname{sen} u}{\pi u} \, du \\
&= \widehat{f}(0) \int_{-\infty}^{+\infty} \frac{\operatorname{sen} u}{\pi u} \, du = \widehat{f}(0). \tag{10.64}
\end{aligned}$$

Vale a pena "ver" a cara desta particular encarnação (entre infinitas outras possíveis) de $\delta(k_1)$, na figura 10.3. O resultado (10.58) pode ser visualizado de forma mais concreta utilizando também a versão "finita":

$$\delta(k_1) \approx \frac{\operatorname{sen} k_1 L}{\pi k_1} = \frac{L}{\pi} \frac{\operatorname{sen} k_1 L}{k_1 L}; \tag{10.65}$$

$$\lim_{k_1 \to 0} \delta(k_1) = \frac{L}{\pi} = \frac{1}{2\pi} \int_{-L}^{+L} dx. \tag{10.66}$$

Portanto, $\delta(0)$ é somente uma maneira sofisticada de escrever L/π.
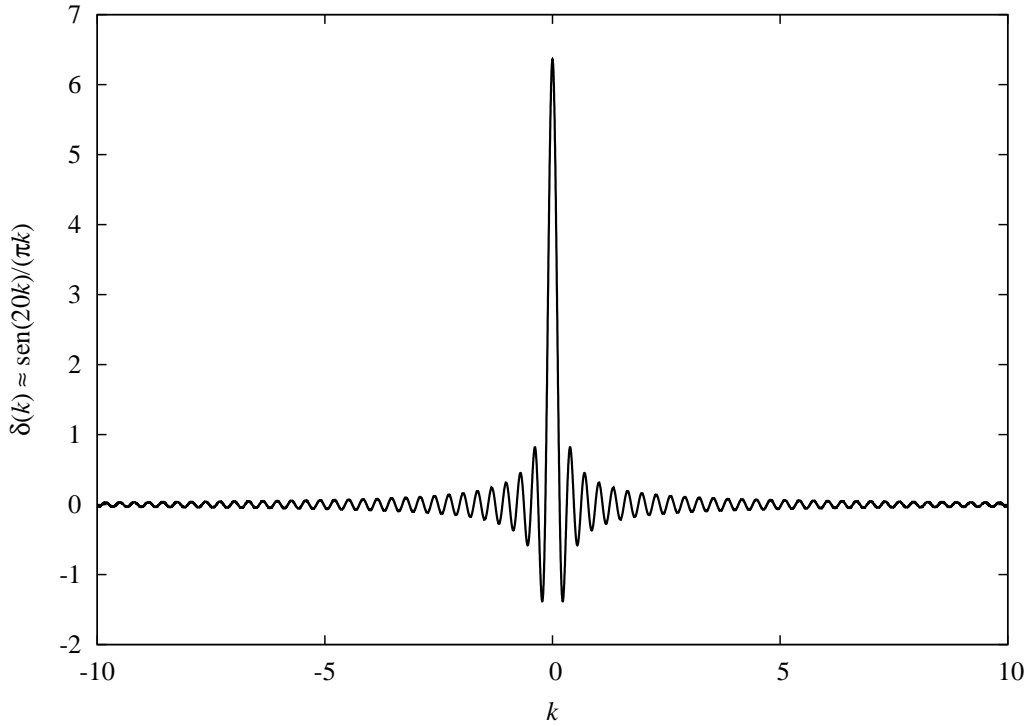
Figure 10.3: Uma representação aproximada de $\delta(k_1)$

10.5 – Espectros

Dado um processo estocástico $u_i(x)$, a função de covariância cruzada é definida como

$$R_{i,j}(r) \equiv \left\langle u_i(x)u_j(x+r) \right\rangle \tag{10.67}$$

Define-se o espectro cruzado entre u_i e u_j como

$$F_{i,j}(k_1) \equiv \frac{1}{2\pi} \int_{-\infty}^{+\infty} R_{i,j}(r)e^{-\mathrm{i}k_1 r}\,dr, \tag{10.68}$$

ou seja: $\phi_{i,j} = \widehat{R}_{ij}$. Agora, vale o seguinte teorema:

$$F_{i,j}(k_1) = \frac{1}{\delta(0)} \left\langle \widehat{u}_i^* \widehat{u}_j \right\rangle. \tag{10.69}$$

A prova é relativamente simples, mas há algumas sutilezas:

$$
\begin{aligned}
\left\langle \widehat{u}_i^* \widehat{u}_j \right\rangle &= \left\langle \left(\frac{1}{2\pi} \right)^2 \int_{x=-\infty}^{+\infty} u_i(x)e^{+\mathrm{i}k_1 x}\,dx \int_{y=-\infty}^{+\infty} u_j(y)e^{-\mathrm{i}k_1 y}\,dy \right\rangle \\
&= \left(\frac{1}{2\pi} \right)^2 \int_{x=-\infty}^{+\infty} \int_{y=-\infty}^{+\infty} \left\langle u_i(x)u_j(y) \right\rangle e^{-\mathrm{i}k_1(y-x)}\,dx\,dy
\end{aligned}
\tag{10.70}
$$

Seja agora a mudança de variáveis

$$r = x, \qquad\qquad\qquad x = r, \tag{10.71}$$

$$s = y - x, \qquad\qquad\qquad y = r + s, \tag{10.72}$$

cujo jacobiano é

$$\frac{\partial(x,y)}{\partial(s,r)} = \begin{vmatrix} \frac{\partial x}{\partial r} & \frac{\partial x}{\partial s} \\ \frac{\partial y}{\partial r} & \frac{\partial y}{\partial x} \end{vmatrix} = \begin{vmatrix} 1 & 0 \\ 1 & 1 \end{vmatrix} = 1. \tag{10.73}$$

A integral (10.70) fica agora

$$
\begin{aligned}
\left\langle \widehat{u_i^*}\widehat{u_j} \right\rangle &= \left(\frac{1}{2\pi}\right)^2 \int_{r=-\infty}^{+\infty} \int_{s=-\infty}^{+\infty} \left\langle u_i(x)u_j(y) \right\rangle e^{-ik_1 s} \frac{\partial(x,y)}{\partial(s,r)} \, ds \, dr \\
&= \left[\frac{1}{2\pi} \int_{-\infty}^{+\infty} dr\right] \left[\frac{1}{2\pi} \int_{s=\infty}^{+\infty} R_{i,j}(s) e^{-ik_1 s} \, ds\right] \\
&= \delta(0) F_{i,j}(k_1). \tag{10.74}
\end{aligned}
$$

Um resultado importante é que a integral do espectro cruzado é igual à covariância. Pelo teorema da transformada inversa, a inversa de (10.68) é

$$R_{i,j}(r) = \int_{k_1=-\infty}^{+\infty} F_{i,j}(k_1) e^{ik_1 r} \, dk_1,$$

$$\left\langle u_i u_j \right\rangle = R_{i,j}(0) = \int_{k_1=-\infty}^{+\infty} F_{i,j}(k_1) \, dk_1 \ \blacksquare \tag{10.75}$$

Agora, se $R_{i,j}(r)$ é uma função real, é evidente que

$$F_{i,j}(k_1) = \text{Co}_{i,j}^F(k_1) + i\,\text{Qu}_{i,j}^F(k_1) \tag{10.76}$$

é uma função complexa de k_1. Em (10.76), $\text{Co}_{i,j}^F$ é o *co-espectro*, e $\text{Qu}_{i,j}^F$ é o *espectro de quadratura*. Além disso, é trivial que

$$F_{i,j}(-k_1) = F_{i,j}^*(k_1). \tag{10.77}$$

Portanto, $\text{Co}_{i,j}^F(k_1)$ é uma função par de k_1, e $\text{Qu}_{i,j}^F(k_1)$ é uma função ímpar de k_1. Segue-se imediatamente que

$$\int_{-\infty}^{+\infty} \text{Qu}_{i,j}^F(k_1) \, dk_1 = 0, \tag{10.78}$$

$$\int_{-\infty}^{+\infty} F_{i,j}(k_1) = \int_{-\infty}^{+\infty} \text{Co}_{i,j}^F(k_1) \, dk_1. \tag{10.79}$$

Portanto,

$$\left\langle u_i u_j \right\rangle = \int_{-\infty}^{+\infty} \text{Co}_{i,j}^F(k_1) \, dk_1. \tag{10.80}$$

10.6 – Espectros eulerianos

Seja agora uma medição euleriana, $u_i(t)$. A sua transformada de Fourier é

$$\widehat{u_i}(\omega) = \frac{1}{2\pi} \int_{-\infty}^{+\infty} u_i(t) e^{-i\omega t} \, dt \tag{10.81}$$

Note que ω é uma frequência *angular*; para passar para a frequência cíclica, faça

$$2\pi n = \omega; \tag{10.82}$$

$$\widehat{u_i}(n) \equiv \int_{t=-\infty}^{+\infty} u_i(t) e^{-i2\pi n t} \, dt = 2\pi \widehat{u_i}(\omega). \tag{10.83}$$

Note a ausência do fator $1/2\pi$ na *definição* de $\widehat{u}_i(n)$! Isto é porque, com o fator 2π como argumento da exponencial, a inversa é

$$u_i(t) = \int_{n=-\infty}^{+\infty} \widehat{u}_i(n)e^{+\text{i}2\pi nt}\, dn. \tag{10.84}$$

A relação (10.83) entre $\widehat{u}_i(n)$ e $\widehat{u}_i(\omega)$ deve ser cuidadosamente observada.

No domínio do tempo,

$$S_{i,j}(n) = \int_{t=-\infty}^{+\infty} R_{i,j}(t)e^{-\text{i}2\pi nt}\, dt. \tag{10.85}$$

é o espectro cruzado na variável frequência cíclica n; novamente, o teorema da inversa de Fourier produz

$$R_{i,j}(t) = \int_{t=-\infty}^{+\infty} S_{i,j}(n)e^{+\text{i}2\pi nt}\, dt. \tag{10.86}$$

Não há necessidade de repetir tudo de novo: teremos

$$\begin{aligned}\langle u_i u_j \rangle &= \int_{n=-\infty}^{+\infty} S_{i,j}(n)\, dn \\ &= \int_{n=-\infty}^{+\infty} \text{Co}_{i,j}^S(n)\, dn = \int_{k_1=-\infty}^{+\infty} \text{Co}_{i,j}^F(k_1)\, dk_1 = \int_{k_1=-\infty}^{+\infty} F_{i,j}(k_1)\, dk_1. \end{aligned} \tag{10.87}$$

O principal ponto aqui é transitar entre espectros no espaço e no tempo, usando a *hipótese de turbulência congelada de Taylor* (Lumley and Panofksy, 1964, p. 56):

$$k_1 = \frac{2\pi}{\lambda} = \frac{2\pi}{\overline{U}\,\mathscr{T}} = \frac{2\pi n}{\overline{U}}, \tag{10.88}$$

onde λ é o comprimento de onda, e $\mathscr{T}$ é o período. Substituindo-se (10.88) em (10.87),

$$\frac{2\pi}{\overline{U}}\, \text{Co}_{i,j}^F\left(\frac{2\pi n}{\overline{U}}\right) = \text{Co}_{i,j}^S(n) \tag{10.89}$$

proporciona a conversão de co-espectros entre frequência cíclica n e número de onda k_1. De forma um pouco mais geral,

$$\frac{2\pi}{\overline{U}}F_{i,j}\left(\frac{2\pi n}{\overline{U}}\right) = S_{i,j}(n). \tag{10.90}$$

10.7 – Espectros tridimensionais

Finalmente, precisamos estudar brevemente os espectros tridimensionais da turbulência e suas relações com os espectros unidimensionais. A transformada de Fourier tridimensional do campo de velocidade $u_i(\boldsymbol{x})$ é

$$\mathscr{F}[u_i] = \widehat{u}_i = \frac{1}{(2\pi)^3} \int_{\boldsymbol{x}\in\mathbb{R}^3} u_i(\boldsymbol{x})\text{e}^{-\text{i}(\boldsymbol{k}\cdot\boldsymbol{x})}\, d^3\boldsymbol{x}. \tag{10.91}$$

Isto é tudo o que precisamos para definir o espectro trimensional de forma totalmente análoga à usada anteriormente para espectros unidimensionais:

$$\Phi_{i,j}(\boldsymbol{k}, t) \equiv \frac{1}{\delta(\boldsymbol{0})}\, \langle \widehat{u}_i^*\widehat{u}_j \rangle. \tag{10.92}$$

Espectros unidimensionais são médias sobre cascas esféricas:

$$E_{i,j}(k) \equiv \int_{|\boldsymbol{k}|=k} \Phi_{i,j}(\boldsymbol{k})\, d^2\boldsymbol{k}. \tag{10.93}$$

Finalmente, nós recuperamos os espectros unidimensionais da seção anterior integrando sobre todos os k_2 e k_3:

$$F_{i,j}(k_1) \equiv \int_{k_2 \in \mathbb{R}, k_3 \in \mathbb{R}} \Phi_{i,j}(k_1, k_2, k_3)\, dk_2\, dk_3. \tag{10.94}$$

Diversas integrais agora são iguais à covariância $\langle u_i u_j \rangle$:

$$\langle u_i u_j \rangle = \int_{\boldsymbol{k} \in \mathbb{R}^3} \Phi_{i,j}(\boldsymbol{k})\, d^3\boldsymbol{k} = \int_{k=0}^{\infty} E_{i,j}(k)\, dk = \int_{k_1=-\infty}^{+\infty} F_{i,j}(k_1)\, dk_1. \tag{10.95}$$

11

Additional stuff

11.1 – Theoretical background

The autocovariance function and the (isotropic) three-dimensional spectrum are related by Lawrence and Strohbehn (1970)

$$C_{n,n}(r) = \langle n(r_1)n(r_1 + r)\rangle = \frac{4\pi}{r}\int_0^\infty \Phi_{n,n}(k)k\sin(kr)\,dk. \tag{11.1}$$

Setting $r \to 0$ and using the well-known limit $\lim_{x\to 0}\sin(x)/x = 1$, produces the variance

$$\sigma_{n,n}^2 = C_{n,n}(0) = 4\pi\int_0^\infty \Phi_{n,n}(k)k^2\,dk. \tag{11.2}$$

Of course, $4\pi k^2\Phi_{n,n}(k)$ is none other than the shell-averaged spectrum. A careful review of spectra and related definitions is in order.

Let $\widehat{u}_i$ be the Fourier transform of turbulence variable $u_i(\boldsymbol{x}, t)$. The three-dimensional spectrum is

$$\Phi_{i,j}(\boldsymbol{k}, t) \equiv \frac{1}{\delta(\boldsymbol{0})}\left\langle \widehat{u}_i^*\widehat{u}_j\right\rangle. \tag{11.3}$$

The *one-dimensional* shell average $E_{i,j}(k, t)$ is

$$E_{i,j}(k, t) \equiv \int_{|\boldsymbol{k}|=k}\Phi_{i,j}(\boldsymbol{k}, t)\,d^2\boldsymbol{k}. \tag{11.4}$$

Put $\Phi_{i,j}$ in spherical coordinates: $\Phi_{i,j}(k, \vartheta, \varphi)$. If turbulence is isotropic, the two last dependences (angles in space) drop and we have: $\Phi_{i,j}(k)$. We then have

$$E_{i,j}(k, t) \equiv \int_{\varphi=0}^{2\pi}\int_{\vartheta=0}^{\pi}\Phi_{i,j}(k, t)k^2\sin\vartheta\,d\vartheta\,d\varphi = 4\pi k^2\Phi_{i,j}(k, t). \tag{11.5}$$

In particular, the TKE spectrum is

$$E_e(k, t) = 4\pi k^2\frac{\Phi_{ii}(k, t)}{2}, \tag{11.6}$$

where the summation convention applies. The K41 prediction for the inertial subrange is

$$E_e(k) = \alpha_e\epsilon_e^{2/3}k^{-5/3}. \tag{11.7}$$

Notice that the Kolmogorov constant is used here for the TKE spectrum, which is also the spectrum of velocity modulus *semi*-variance. We bear this point in mind as we deal with scalar spectra.

Now take $E_{i,j}(k) = E_{\theta,\theta}$ to be the temperature spectrum in the inertial subrange; according to the Kolmogorov-Corrsin theory, $E_{\theta,\theta} \sim k^{-5/3}$, whence $\Phi_{\theta,\theta} \sim k^{-11/3}$. More precisely, if

$$\frac{E_{\theta,\theta}}{2} = \alpha_{\theta,\theta}\epsilon_{\theta,\theta}\epsilon_e^{-1/3}k^{-5/3}, \tag{11.8}$$

then

$$\frac{\Phi_{\theta,\theta}}{2} = \frac{\alpha_{\theta,\theta}}{4\pi}\epsilon_{\theta,\theta}\epsilon_e^{-1/3}k^{-11/3}. \tag{11.9}$$

This is Equation (1) in Hill and Clifford (1978). It is important to stress, once and for all, that in (11.8) and in (11.9), ϵ_e is the rate of dissipation of turbulence kinetic energy (TKE); accordingly, $\epsilon_{\theta,\theta}$ is the rate of dissipation of temperature *semi*-variance:

$$\epsilon_e \approx \nu_u \left\langle \frac{\partial u_i}{\partial x_k}\frac{\partial u_i}{\partial x_k} \right\rangle, \tag{11.10}$$

$$\epsilon_{\theta,\theta} = \nu_\theta \left\langle \frac{\partial \theta}{\partial x_k}\frac{\partial \theta}{\partial x_k} \right\rangle. \tag{11.11}$$

Notice that we never measure any of these. What we do measure are the one-dimensional spectra $F_{i,j}(k_1)$ or $G_{i,j}(k_1)$ defined by

$$F_{i,j}(k_1) = \int_{k_2=-\infty}^{+\infty} \int_{k_3=-\infty}^{+\infty} \Phi_{i,j}(k_1, k_2, k_3)\, dk_2\, dk_3 \tag{11.12}$$

$$G_{i,j}(k_1) \equiv 2F_{i,j}(k_1), \qquad k_1 \geq 0. \tag{11.13}$$

Under isotropy, the relationship between $G_{\theta,\theta}(k_1)$ and $E_{\theta,\theta}(k)$ is

$$G_{\theta,\theta}(k_1) = \int_{k_1}^{\infty} \frac{E_{\theta,\theta}}{k}\, dk \tag{11.14}$$

(Monin and Yaglom, 1975, Eqn. 12.13), so we can "recover" the isotropic spectra from line measurements. Notice how dependent we are on the isotropy assumption!

Using (11.8),

$$\frac{G_{\theta,\theta}(k_1)}{2} = \frac{3}{5}\alpha_{\theta,\theta}\epsilon_{\theta,\theta}\epsilon_e^{-1/3}k_1^{-5/3}. \tag{11.15}$$

11.2 – The structure functions in the dissipation subrange

Let us remember a few important points about Kolmogorov's theory. Kolmogorov's first similarity hypothesis reads (Monin and Yaglom, 1975, p. 347):

> *In the case of turbulence with a sufficiently large Reynolds number, the multi-dimensional probability distributions for the relative velocities $\Delta u(r, \tau) = u(x_0 + r, t_0 + \tau) - u(x_0, t_0)$, in a space-time region G in which the turbulence is locally isotropic, are unambiguously defined by the values of ϵ_e and ν_u.*

Let us explain:

- "Locally" means that the the hypothesis concerns only small scales, much smaller than those at which turbulence is produced by shear, buoancy, etc.

- Reynolds'decomposition is

$$U_i = \langle U_i \rangle + u_i. \tag{11.16}$$

- ϵ_e is the rate of dissipation of TKE, given by

$$\epsilon_e = 2\nu_u \langle s_{ij} s_{ij} \rangle, \quad s_{ij} = \frac{1}{2}\left(\frac{\partial u_i}{\partial x_j} + \frac{\partial u_j}{\partial x_i}\right). \tag{11.17}$$

Proceed: in isotropic turbulence, there is an important result which is not so easy to derive (Tennekes and Lumley (1972), for example, do not derive it in their book):

$$\epsilon_e = 15\nu_u \left\langle \left(\frac{\partial u_1}{\partial x_1}\right)^2 \right\rangle = \frac{15}{2}\nu_u \left\langle \left(\frac{\partial u_1}{\partial x_2}\right)^2 \right\rangle. \tag{11.18}$$

With ϵ_e and ν_u, one can form the famous Kolmogorov microscales:

$$\eta_u = (\nu_u^3/\epsilon_e)^{1/4}, \qquad \upsilon_u = (\nu_u \epsilon_e)^{1/4}, \qquad \tau_u = (\nu_u/\epsilon_e)^{1/2}. \tag{11.19}$$

Here, ν_u is a *length* scale; υ_u is a *velocity* scale; and τ_u is a *time* scale.

Let us now look at the *longitudinal structure function*

$$D_{11}(r_1) \equiv \left\langle [u_1(x_1 + r_1, x_2, x_3) - u_1(x_1, x_2, x_3)]^2 \right\rangle \tag{11.20}$$

There is a lot about the structure function *tensor*, and tensor isotropic relations, that I am not discussing. Notice that D_{11} is relatively easy to measure in a micrometeorological tower with the help of Taylor's hypothesis.

Now the big plunge: if $r \ll \eta$, the flow is *locally laminar*, very smooth and therefore

$$u_1(x_1 + r_1, x_2, x_3) - u_1(x_1, x_2, x_3) \approx \frac{\partial u_1}{\partial x_1} r,$$

$$D_{11}(r_1) \approx \left\langle \left(\frac{\partial u_1}{\partial x_1}\right)^2 \right\rangle r^2 = \frac{\epsilon_e}{15\nu_u} r^2. \tag{11.21}$$

Very much like the velocity field, we can establish a Reynolds decomposition,

$$\Theta = \langle \Theta \rangle + \theta, \tag{11.22}$$

define the rate of dissipation of temperature semi-variance (Tennekes and Lumley, 1972, Eqns. (3.4.3) and (3.4.4)):

$$\epsilon_{\theta\theta} = \nu_\theta \left\langle \frac{\partial \theta}{\partial x_k} \frac{\partial \theta}{\partial x_k} \right\rangle = 3\nu_\theta \left\langle \left(\frac{\partial \theta}{\partial x_1}\right)^2 \right\rangle, \tag{11.23}$$

from which we can write a Kolmogorov temperature microscale

$$\eta_\theta = (\nu_\theta^3/\epsilon_e)^{1/4}. \tag{11.24}$$

The factor 3 in the equation is found by assuming isotropy. This is not too difficult (in comparison with the result for ϵ_e): see (Tennekes and Lumley, 1972, p. 96).

So we see that we have *two* microscales now, η_u and η_θ, and we must proceed with caution. A (longitudinal) temperature structure function can be defined in just the same way that the velocity structure function was defined, namely

$$D_{\theta,\theta}(r_1) \equiv \left\langle [\theta(x_1 + r_1, x_2, x_3) - \theta(x_1, x_2, x_3)]^2 \right\rangle. \tag{11.25}$$

Suppose $r \ll \max(\eta_u, \eta_\theta)$; then we can, as before, admit a Taylor expansion

$$\theta(x_1 + r_1, x_2, x_3) - \theta(x_1, x_2, x_3) = \frac{\partial \theta}{\partial x_1} r_1,$$

$$D_{\theta,\theta}(r_1) \approx \left\langle \left(\frac{\partial \theta}{\partial x_1} \right)^2 \right\rangle r_1^2 = \frac{\epsilon_{\theta,\theta}}{3\nu_\theta} r_1^2. \tag{11.26}$$

11.3 – The structure function in the inertial-convective subrange

For scales $r \gg \max(\eta_u, \eta_\theta)$, the best-known result of Kolmogorov's turbulence theory is

$$D_{1,1}(r_1) = \frac{9}{10} \Gamma\left(\frac{1}{3}\right) (2\alpha_e) \epsilon_e^{2/3} r_1^{2/3} = \mathscr{C}_{1,1}^2 r_1^{2/3}, \tag{11.27}$$

$$D_{\theta,\theta}(r_1) = \frac{9}{10} \Gamma\left(\frac{1}{3}\right) (2\alpha_{\theta,\theta}) \epsilon_e^{-1/3} \epsilon_{\theta,\theta} r_1^{2/3} = \mathscr{C}_{\theta,\theta}^2 r_1^{2/3}. \tag{11.28}$$

The equations above define the *structure parameters* $\mathscr{C}_{1,1}^2$ and $\mathscr{C}_{\theta,\theta}^2$. There is a lot of confusion in the value of the constants, because the Kolmogorov 5/3 law can be written both for the three-dimensional spectra $E_e(k)$ and $E_{\theta,\theta}(k)$, and for the one-dimensional spectra $F_{1,1}(k_1)$ and $F_{\theta,\theta}(k_1)$. The constants α_e and $\alpha_{\theta,\theta}$ above are those for the 3D-spectra. Taking (11.28) into (11.9),

$$\Phi_{\theta,\theta}(k) = \frac{2\alpha_{\theta,\theta}}{4\pi} \epsilon_e^{-1/3} \epsilon_{\theta,\theta} k^{-11/3} = \frac{10}{9\Gamma(1/3) \times 4\pi} \mathscr{C}_{\theta,\theta}^2 k^{-11/3} = B\mathscr{C}_{\theta,\theta}^2 k^{-11/3}, \tag{11.29}$$

with $B = 0.033005$. This is to stay in line with what is traditional in scintillometry. This equation will later be compared with (A).

11.4 – The inner scale

We are now ready for the inner scale definition. By equating the formulae (11.26) and (11.28) for $D_{\theta,\theta}$ in the dissipation and the inertial-convective subranges, one finds

$$\frac{\epsilon_{\theta,\theta}}{3\nu_\theta} \ell_0^2 = \frac{9}{10} \Gamma(1/3)(2\alpha_{\theta,\theta}) \epsilon_e^{-1/3} \epsilon_{\theta,\theta} \ell_0^{2/3}$$

$$\frac{\ell_0^{4/3}}{3\nu_\theta} = \frac{9}{10} \Gamma(1/3)(2\alpha_{\theta,\theta}) \epsilon_e^{-1/3}$$

$$\ell_0^{4/3} = \frac{27}{10} \Gamma(1/3)(2\alpha_{\theta,\theta}) \frac{\nu_\theta}{\nu_u} [\nu_u \epsilon_e^{-1/3}]$$

$$\frac{\ell_0}{\eta_u} = \left[\frac{54}{10\text{Pr}} \Gamma(1/3) \alpha_{\theta,\theta} \right]^{3/4} \tag{11.30}$$

For Pr = 0.72 (air) and $\alpha_{\theta,\theta} = 0.72$ (a convenient choice within the values reported in the literature), one finds

$$\frac{\ell_0}{\eta_u} = 7.417668, \tag{11.31}$$

which is Eqn (7) of Hill and Clifford (1978).

11.5 – The regions of the temperature spectrum

For a velocity field *not affected by the temperature field*, the classical wisdom is to divide the turbulent scales into 3 regions:

energy-containing or production subrange: Where $k \sim 2\pi/L_u$, L_u being the integral, or production, scale.

the inertial subrange : $2\pi/L_u \ll k \ll 2\pi/\eta_u$.

the viscous or dissipation subrange : $2\pi/\eta_u \ll k$.

(*Notice that it is not clear to which range $2\pi/\eta_u$ belongs!*)

The temperature, whowever, is *advected* by the velocity field, so its spectrum/structure function must be affected by both η_u and η_θ microscales. To that effect it is useful to remember the definition of the molecular Prandtl number,

$$\mathrm{Pr} \equiv \frac{\nu_u}{\nu_\theta}. \tag{11.32}$$

As for the temperature spectrum, now, we must analyze no less than 3 cases before defining sub-ranges. Here we go:

Case 1: $\mathrm{Pr} \ll 1$, with

$$\frac{\nu_u}{\nu_\theta} \ll 1 \qquad \text{and} \qquad \frac{\eta_u}{\eta_\theta} \ll 1.$$

The expected temperature spectrum in this case is depicted in figure 11.1. There are four regions:

energy-containing or production subrange: Where $k \sim 2\pi/L_\theta$, L_θ being the integral, or production, scale.

inertial-convective subrange: $2\pi/L_\theta \ll k \ll 2\pi/\eta_\theta$. This is essentially analogous to the inertial subrange, in that scales are still much larger than both η_u and η_θ and are therefore not directly influenced by them.

inertial-diffusive subrange: $2\pi/\eta_\theta \ll k \ll 2\pi/\eta_u$. Note how the name has been carefully crafted: in this range, the kinematic viscosity ν_u (and by the same token η_u) is too small to influence the velocity field, which is "turbulent" and strongly advects temperature fluctuations. However, the molecular difusivity of heat ν_θ (and η_θ) is large enough to dampen the temperature fluctuations, whose field is smoother.

no name usually assigned: $k \gg 2\pi/\eta_u$. This is however clearly a *diffusive-viscous subrange*, where viscosity comes last in the name because its effects appear after the effects of heat diffusion. It appears that in measurements it would be extremely difficult to indentify this subrange separately from the inertial-diffusive subrange.

Figure 11.1: The temperature spectra for $Pr \ll 1$. The log-log axes are depicted in a 2:1 horizontal to vertical scale.

Figure 11.2: The temperature spectra for $Pr \sim 1$. The log-log axes are depicted in a 2:1 horizontal to vertical scale.

Case 2: $Pr \sim 1$, with

$$\frac{\nu_u}{\nu_\theta} \sim 1 \qquad \text{and} \qquad \frac{\eta_u}{\eta_\theta} \sim 1.$$

The expected temperature spectrum in this case is depicted in figure 11.2. There are only three regions:

energy-containing or production subrange: Where $k \sim 2\pi/L_\theta$, L_θ being the integral, or production, scale.

inertial-convective subrange: $2\pi/L_\theta \ll k \ll 2\pi/\eta_\theta$. This is essentially analogous to the inertial subrange, in that scales are still much larger than both η_u and η_θ and are therefore not directly influenced by them.

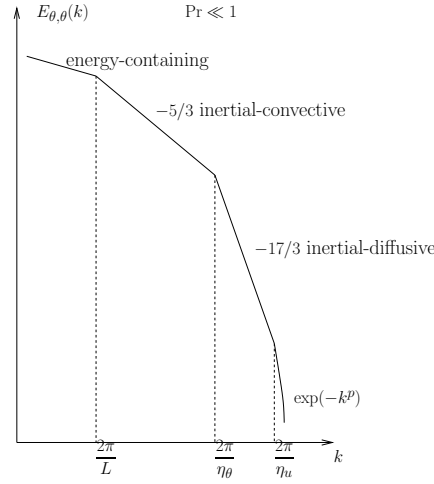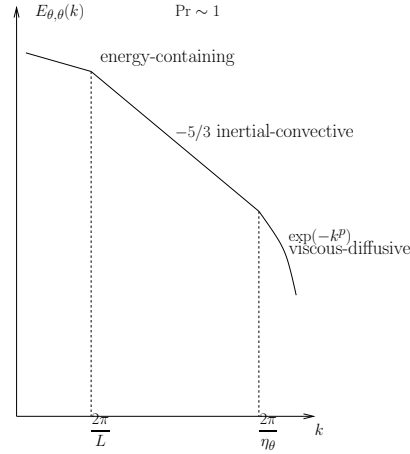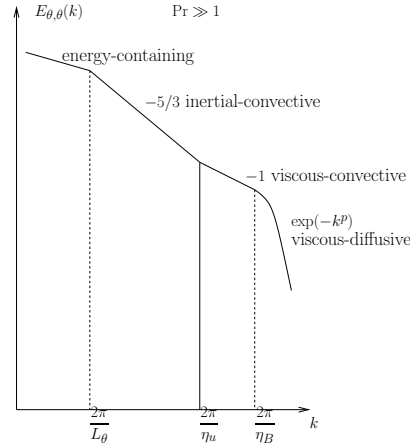**viscous-diffusive subrange:** $k \gg 2\pi/\eta_\theta$.

Figure 11.3: The temperature spectra for $\mathrm{Pr} \gg 1$. The log-log axes are depicted in a 2:1 horizontal to vertical scale.

Case 2: $\mathrm{Pr} \gg 1$, with

$$\frac{\nu_u}{\nu_\theta} \gg 1 \qquad \text{and} \qquad \frac{\eta_u}{\eta_\theta} \gg 1.$$

The expected temperature spectrum in this case is depicted in figure 11.3. There are again four regions:

energy-containing or production subrange: Where $k \sim 2\pi/L_\theta$, L_θ being the integral, or production, scale.

inertial-convective subrange: $2\pi/L_\theta \ll k \ll 2\pi/\eta_\theta$. This is essentially analogous to the inertial subrange, in that scales are still much larger than both η_u and η_θ and are therefore not directly influenced by them.

viscous-convective: $2\pi/\eta_u \ll k \ll 2\pi/\eta_\theta$. Note how the name has been carefully crafted: in this range, the molecular diffusivity ν_θ (and by the same token η_θ) is too small to influence the temperature temperature field, which is advected by a locally "laminar" (smooth) velocity field.

viscous-diffusive subrange: $k \gg 2\pi/\eta_\theta$. The temperature fluctuations are strongly damped and the temperature range is laminar after ν_θ, whose effect is the last one to be felt by the temperature field, is in action.

Having said this, are there relevant cases of Pr much larger or much smaller than 1 in nature, to justify the theoretical effort? Yes! Hill and Clifford (1978) give two important examples:

- Temperature in water: $\mathrm{Pr} \simeq 8$.

- Salt in Water: $\mathrm{Pr} \simeq 700$.

Hill (1978) developed several analytical models to represent the several features of the scalar (in our case represented by the temperature) spectrum. Figure ?? shows the fitting of Hill's 4 models to the data of temperature measured in the surface layer by Champagne et al. (1977): Hill calls the bump in the figure a viscous-convective subrange *even though* $\mathrm{Pr} = 0.72$ *for air*! Clearly, there is an inconsistency here.
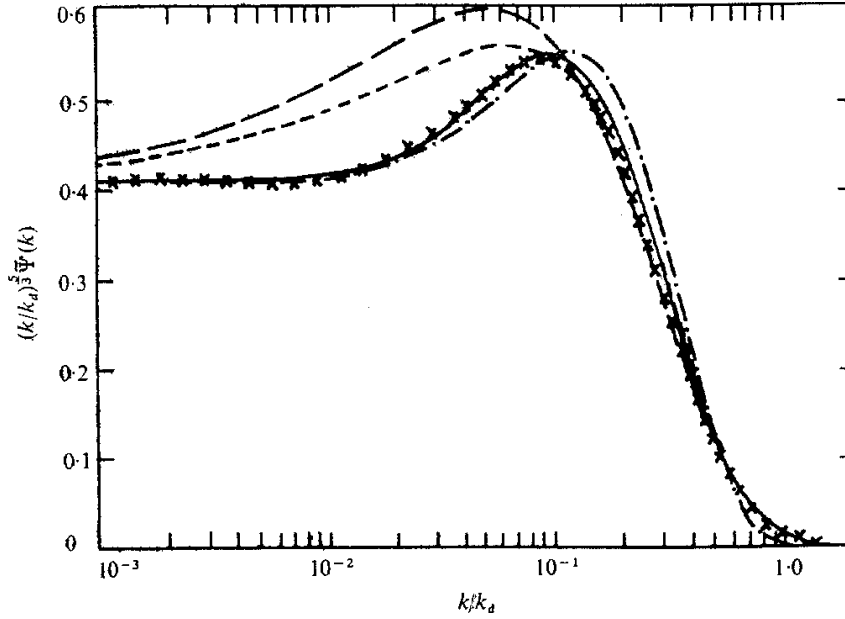
Yet, the proposal by Hill that a viscous-convective subrange exists in the temperature spectra in the air still holds, in spite of the inner contradiction. Here is Hartogensis (2006), p. 6–7 (symbols have been changed to follow this text's notation):

> The existence of the Hill bump can be understood as follows. For Pr $\approx$ 0.72 the inertial-dissipation range transition is of a viscous-convective nature, i.e. viscosity already starts to break up TKE when θ-diffusion still is characterised by convection (the inertial range). Since ν_u is much smaller than the turbulent u-diffusion coefficient the breaking up of turbulent eddies halts, but at the same time the θ-diffusion is still at its convective intensity thus leading to a build up of spectral energy at these scales (a bump). At smaller scales, the θ gradients are finally large enough for the molecular diffusivity to compensate the lack of turbulent mixing.

A

O fator 2 nos espectros de escalares

Uma boa notícia é que Monin and Yaglom (1975) usam na página 139 a mesma notação que eu, quando escrevem

$$\int_0^\infty E_{\vartheta\vartheta}(k)\,dk = \overline{\vartheta'^2}.$$

Na página 123 nós encontramos o espectro de energia cinética da turbulência (ECT), na forma

$$E(k,t) = 4\pi k^2 F(k,t)$$

Ao que tudo indica, por comparação com (11.6),

$$F(k,t) = \frac{\phi_{ii}(k,t)}{2}$$

Isto é confirmado na página 20, equação 11.58:

$$F(\boldsymbol{k}) = \frac{1}{2}F_{jj}(\boldsymbol{k}).$$

Começo a compilar uma tabela de equivalência de símbolos:

A primeira aparição da lei dos 5/3 é (parece ser) na equação (16.37):

$$E(k) = C_1\epsilon^{2/3}k^{-5/3}.$$

As diversas relações entre as constantes de Kolmogorov aparecem na equação (21.25), página 355. Em Monin and Yaglom (1975), tudo parece girar em torno da função de esturutura longitudinal para velocidade, que eles definem como (eq. (21.10))

$$D_{LL}(r) = \overline{(\Delta_r u_L)^2}.$$

Table A.1: M, Y & Eu

M& Y	Eu
$F_{ij}(\boldsymbol{k})$	$\Phi_{i,j}(\boldsymbol{k})$
$F(\boldsymbol{k})$	—
$E(k)$	$E_e(k)$
$E_{\vartheta\vartheta}(k)$	$E_{\theta,\theta}(k)$
$\overline{\epsilon}$	ϵ_e
$\overline{N}$	$\epsilon_{\theta,\theta}$

Vamos agora em direção à temperatura, que é o que nos interessa no momento. Monin and Yaglom (1975) definem a taxa de dissipação de semi-variância de temperatura na página 379, logo após a equação (21.80). O símbolo, $\overline{N}$, vai para a tabela A.1.

Agora um pouco de confusão: na página 385 nós vamos encontrar $E_{\vartheta\vartheta}(k) = E^{(\vartheta)}(k)$, e logo em seguida (equação (21.89))

$$E^{(\vartheta)}(k) = B^{(\vartheta)}\overline{N}\overline{\epsilon}^{-1/3}k^{-5/3}$$

A função de estrutura de temperatura é

$$D_{\vartheta\vartheta}(r) = C_\vartheta \overline{N}\overline{\epsilon}^{1/3}r^{2/3}$$

e

$$B^{(\vartheta)} = \frac{10C_\vartheta}{9\Gamma(1/3)}.$$

Compare com (11.28), que eu repito aqui,

$$D_{\theta,\theta}(r_1) = \underbrace{\frac{9}{10}\Gamma\left(\frac{1}{3}\right)(2\alpha_{\theta,\theta})}_{C_\vartheta = C_{\theta,\theta}}\epsilon_e^{-1/3}\epsilon_{\theta,\theta}r_1^{2/3} \Rightarrow$$

$$(2\alpha_{\theta,\theta}) = \frac{10C_{\theta,\theta}}{9\Gamma(1/3)},$$

o que e *valida* minha interpretação:

$$B^{(\vartheta)} = 2\alpha_{\theta,\theta}.$$

B

Divagações equacionais

Considere a equação da difusão,

$$\frac{\partial \phi}{\partial t} = k \frac{\partial^2 \phi}{\partial x^2}. \tag{B.1}$$

Vou procurar uma solução de similaridade sem recorrer diretamente à análise dimensional, ou seja: vou supor que é possível reduzir (B.1) a uma equação diferencial ordinária via a mudança de variável

$$\xi = a x^b t^c k^d \tag{B.2}$$

```
(C1) writefile('difu-simples.out')
     Starts dribbling to difu-simples.out (2001/10/17, 11:22:44).
(D1)                               FALSE
(C2) linel : 100 ;
(D2)                                 100
(C3) ksi : a*x^b*t^c*k^d ;
                                  d  c  b
(D3)                            a k  t  x
(C4) depends(fi,ksi);
                                  d  c  b
(D4)                          [fi(a k  t  x )]
```

Agora introduzo a equação diferencial (B.1):

```
(C5) diff(fi,t) - k*diff(fi,x,2);
                                            2
         dfi      d  c - 1  b       2 2   d fi     2 d  2 c  2 b - 2
(D5) a c ----------- k  t        x  - k (a  b  ------------- k    t      x
         d  c  b                           d  c  b 2
       da k  t  x                       d(a k  t  x )

                                         dfi      d  c  b - 2
                          + a (b - 1) b ----------- k  t  x      )
                                        d  c  b
                                      da k  t  x
```

Note que o último termo em $d\phi/d\xi$ será anulado se, e somente se, $b = 1$. É sempre possível impor esta condição elevando (B.3) a $1/b$, de forma que vamos tentar a transformação alternativa

$$\xi = a x t^c k^{2d} \tag{B.3}$$

Na sequência, eu reinicializo a seção com `kill(all)` e em seguida redefino `ksi`:

```
(C6) kill(all);
(D0)                                DONE
(C1) ksi : a*x*t^c*k^d ;
                                   d  c
(D1)                             a k  t  x
(C2) depends(fi,ksi);
```

```
                                          d  c
(D2)                                   [fi(a k  t  x)]
(C3) diff(fi,t) - k*diff(fi,x,2);
                                                2
               dfi      d  c - 1      2      d fi      2 d + 1  2 c
(D3)        a c --------- k  t        x  - a ------------- k        t
               d  c                         d  c  2
             da k  t  x                    d(a k  t  x)
```

Para o resultado ficar mais claro, removo a variável `ksi` e então uso o comando
`scsimp` para substituir no resultado acima $axt^c k^d$ por ξ:

```
(C4) kill(ksi);
(D4)                                       DONE
(C5) scsimp(d3,ksi=a*x*t^c*k^d);
                             dfi
                          c ---- ksi      2
                            dksi         2 d fi   2 d + 1  2 c
(D5)                      ----------- - a ----- k        t
                               t            2
                                         dksi
(C6) ratsimp(%);
                         2
                       2 d fi   2 d + 1  2 c + 1     dfi
                      a ----- k        t         - c ---- ksi
                          2                          dksi
                       dksi
(D6)                 - -------------------------------------
                                         t
```

Agora está claro também que para tornar a equação acima totalmente adimen-
sional, preciso de $c = -1/2$, $d = -1/2$; finalmente, a escolha de a é arbitrária, e em
nome da tradição usarei $a = 1/2$.

```
(C7) %,[c=-1/2,d=-1/2] ;
                          dfi
                          ---- ksi      2
                          dksi         2 d fi
                          -------- + a  -----
                             2             2
                                        dksi
(D7)                     - -------------------
                                    t
(C8) %, a=1/2 ;
                                         2
                                       d fi
                           dfi         -----
                           ---- ksi      2
                           dksi        dksi
                           -------- + -----
                              2         4
(D8)                      - ----------------
                                   t
(C9) %*(-t);
                                         2
                                       d fi
                           dfi         -----
                           ---- ksi      2
                           dksi        dksi
(D9)                       -------- + -----
                              2         4
(C10) ratsimp(%);
                                         2
                           dfi         d fi
                         2 ---- ksi + -----
                           dksi          2
                                       dksi
(D10)                    ------------------
                                  4
(C11) %*(4);
                                         2
                           dfi         d fi
(D11)                    2 ---- ksi + -----
```

```
                              dksi           2
                                          dksi
(C12) quit();
```

Portanto, a equação diferencial ordinária que precisa ser resolvida é

$$2\xi\frac{d\phi}{d\xi} + \frac{d^2\phi}{d\xi^2} = 0, \tag{B.4}$$

a partir da mudança de variável

$$\xi = \frac{x}{(2k\sqrt{t})} \;\blacksquare \tag{B.5}$$

Para não perder muito tempo, vou deixar por sua conta verificar que para as condições de contorno:

$$\phi(x,0) = 0, \tag{B.6}$$

$$\phi(0,t) = \phi_0, \tag{B.7}$$

$$\phi(\infty,t) = 0, \tag{B.8}$$

a solução é

$$\phi(x,t) = \phi_0\left[1 - \operatorname{erf}(\xi)\right] = \phi_0\operatorname{erfc}(\xi) \;\blacksquare \tag{B.9}$$

Exercício Suponha que você use a solução acima para resolver o problema de Sutton,

$$u_0\frac{\partial\phi}{\partial x} = K_0\frac{\partial^2\phi}{\partial z^2}. \tag{B.10}$$

Suponha $u_0 = 5\,\text{m s}^{-1}$, $u_* = 0.5\,\text{m s}^{-1}$, $K_0 = \kappa(10\text{m})u_*$, $T_0 = 28°C$ e $T_a = 24°C$. Plote o perfil do fluxo de calor sensível

$$H(z) = \rho c_p K_0\frac{\partial T}{\partial z} \tag{B.11}$$

para $x = 200$m. Este perfil obedece à condição de constância com z usualmente aceita na teoria de similaridade de Monin-Obukhov?

Solução
Se $k = K_0/u_0$, a solução para o perfil de temperatura é

$$T(x,z) = T_0 + [T_a - T_0]\operatorname{erfc}\left(\frac{zu_0}{2K_0(z)\sqrt{x}}\right), \tag{B.12}$$

Note que o enunciado está utilizando a formulação de condições neutras para a difusividade turbulenta a uma altura equivalente a 10m, *a qual a rigor depende de z*: então,

$$H(x,z) = \rho c_p(\kappa z u_*) \tag{B.13}$$

A sequência de comandos de MAXIMA abaixo calcula a "fórmula" para $H(x,z)$:

```
(C1) K0 : kappa*10*ustar ;

(D1)                          10 kappa ustar
(C2) k : K0/u0 ;

                              10 kappa ustar
```
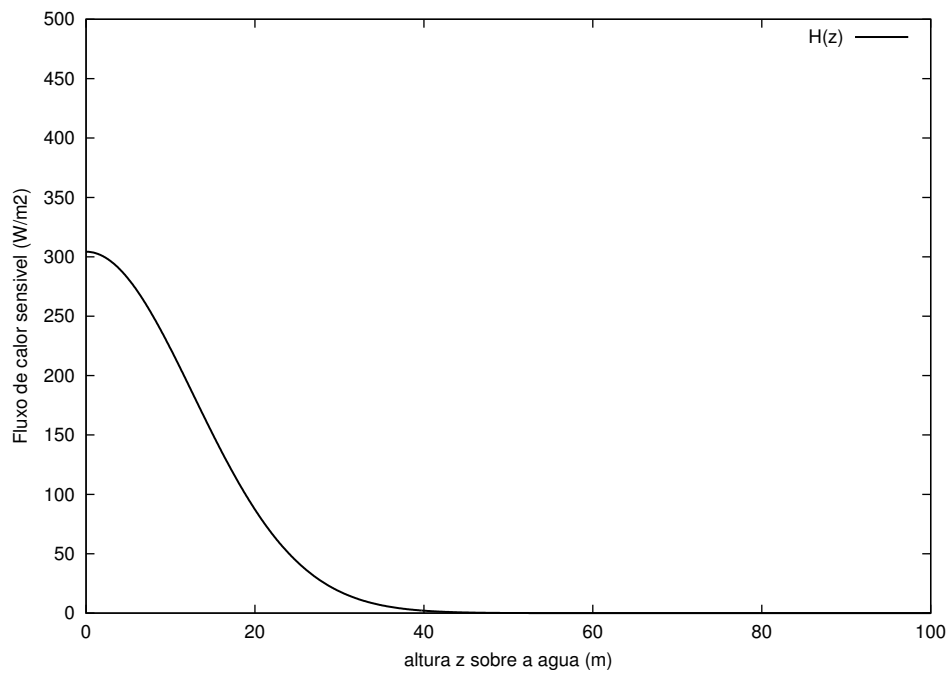
Figure B.1: Perfil do fluxo de calor sensível previsto pela solução de Sutton com $u_0 = $ const., $K_0 = $ const.

```
(D2)                                    --------------
                                             u0
(C3) ksi : z/(2*sqrt(k*x));

                                            z
(D3)                          ------------------------------
                                         kappa ustar x
                              2 SQRT(10) SQRT(------------)
                                                  u0
(C4) T : T0 + (Ta-T0)*(1 - erf(ksi));

                                           z
(D4)              (Ta - T0) (1 - ERF(-----------------------------)) + T0
                                            kappa ustar x
                              2 SQRT(10) SQRT(------------)
                                                   u0
(C5) diff(T,z);

                                             2
                                          u0 z
                                    - ----------------
                                       40 kappa ustar x
                      (Ta - T0) %E
(D5)             - ------------------------------------
                                        kappa ustar x
                    SQRT(10) SQRT(%PI) SQRT(------------)
                                                u0
(C6)
```

O resultado deste exercício é mostrado na figura B.1.

References

Adkins, C. J. (1983). *Equilibrium thermodynamics.* New York: Cambridge University Press.

Alduchov, O. A. and R. E. Eskridge (1996). Improved Magnus form approximation of saturation vapor pressure. *J Appl Meteorol 35*, 601–609.

Batchelor, G. K. (1967). *An introduction to fluid dynamics.* Cambridge: Cambridge University Press.

Bendat, J. S. and A. G. Piersol (1986). *Random Data* (2 ed.). New York: John Wiley & Sons. 566 pp.

Billingsley, P. (1986). *Probability and Measure* (2nd ed.). New York: John Wiley and Sons.

Bird, R. B., W. E. Stewart, and E. N. Lightfoot (1960). *Transport phenomena.* New York: John Wiley and Sons.

Brunt, D. (1932). Notes on radiation in the atmosphere, 1. *Q J Roy Meteorol Soc 58*, 389–420.

Brutsaert, W. (1975). On a derivable formula for long-wave radiation from clear skies. *Water Resour Res 11*, 742–744.

Brutsaert, W. (1982). *Evaporation into the atmosphere.* Dordrecht: D. Reidel. 309 pp.

Brutsaert, W. (1992, March). Stability correction functions for the mean wind speed and temperature in the unstable surface layer. *Geophys Res Lett 19*(5), 469–472.

Butenhoff, C. L. and M. A. K. Khalil (2002). Correction for water vapor in the measurement of atmospheric trace gases. *Chemosphere 47*(8), 823–836.

Chamecki, M., N. L. Dias, and L. S. Freire (2018). A reduced tke phase space for studying disturbed atmospheric surface layer flows: Application to vertical velocity variance over a forest canopy. In *23rd Symposium on Boundary Layers and Turbulence*, Number 1B.5, Oklahoma City. American Meteorological Society.

Champagne, F. H., C. A. Friehe, J. C. LaRue, and J. C. Wyngaard (1977). Flux measurements, flux estimation techniques, and fine-scale turbulence measurements in the unstable surface layer over land. *J Atmos Sci 34*, 515–530.

Cheng, Y. and W. Brutsaert (2005). Flux-profile relationships for wind speed and temperature in the stable atmospheric boundary layer. *Boundary-Layer Meteorol 114*, 519–538.

CHOI, K.-S. and J. L. LUMLEY (2001, Jun). The return to isotropy of homogeneous turbulence. *Journal of Fluid Mechanics 436*, 59–84.

COESA (1976). U.S. Standard Atmosphere, 1976. Technical report, U.S. Government Printing Office.

Cram?r, H. and M. R. Leadbeter (2004). *Stationary and related stochastic processes.* Mineola, New York: Dover.

Dake, J. M. (1972). Evaporative cooling of a body of water. *Water Resources Research 8*(4), 1087–1091.

Davidson, P. A. (2004). *Turbulence. An introduction for scientists and engineers.* Oxford: Oxford University Press. 657 pp.

Dias, N. L. (1986). Estimativas climatológicas de evaporação em lagos. Master's thesis, COPPE/UFRJ.

Dias, N. L. (1994). *The structure of temperature and humidity turbulent fluctuations in the stable surface layer.* Ph. D. thesis, Cornell University, Ithaca, NY.

Dias, N. L. (2017). *An introduction to mathematical methods for engineering (in Portuguese).* Curitiba: Author's edition. Available at https://nldias.github.io/pdf/matappa-1ed.pdf.

Dias, N. L. (2021). Uma revisão do efeito da composição química da atmosfera sobre a constante de gás do ar seco em múltiplas escalas de tempo. *Rev Bras Met 36*(1), 1–11.

Dias, N. L. and W. Brutsaert (1996). Similarity of scalars under stable conditions. *Boundary-Layer Meteorol 80*, 355–373.

Dias, N. L., H. F. Duarte, S. R. Maggiotto, and L. Grodzki (2007). An attenuated eddy covariance method for latent heat flux measurements. *Water Resour Res 43*, W04415.

Dias, N. L., J. Hong, M. Leclerc, Black, Z. Nesic, and P. Krishnan (2009). A simple method of estimating scalar fluxes over forests. *Boundary-Layer Meteorol 132*, 401–414.

Dilley, A. C. (1968). On the computer calculation of vapor pressure and specific humidity gradients from psychrometric data. *J Appl Meteorol 7*, 717–719.

Duarte, H. F., N. L. Dias, and S. R. Maggiotto (2006). Assessing daytime downward longwave radiation estimates for clear and cloudy skies in Southern Brazil. *Agric For Meteorol 139*, 171–181.

Finnigan, J. J. (2009). Response to comment by Dr. A.S. Kowalski on "The storage term in eddy flux calculations". *Agr Forest Meteorol 149*, 725 – 729.

Finnigan, J. J., R. Clement, Y. Malhi, R. Leuning, and H. A. Cleugh (2003). A re-evaluation of long-term flux measurement techniques part i: averaging and coordinate rotation. *Boundary-Layer Meteorol 107*, 1–48.

Fleagle, R. G. and J. A. Businger (1980). *An introduction to atmospheric physics.* Orlando: Academic Press.

Fox, R. W. and A. T. McDonald (1981). *Introdução à Mecânica dos Fluidos.* Rio de Janeiro: Guanabara Dois.

Garratt, J. (1994). *The Atmospheric Boundary Layer.* Cambridge University Press, U.K. 316 pp.

Hartogensis, O. (2006). *Exploring Scintillometry in the Stable Atmospheric Surface Layer.* Ph. D. thesis, Wageningen Universiteit.

Hauf, T., U. Finke, J. Neisser, G. Bull, and J.-G. Stangenberg (1996). A ground-based network for atmospheric pressure fluctuations. *J Atmos Oceanic Technol 13*, 1001–1023.

Henderson-Sellers, B. (1984). A new formula for latent heat of vaporization of water as a function of temperature. *Quarterly Journal of the Royal Meteorological Society 110*(466), 1186–1190.

Hicks, B. B. (1981). An examination of turbulence statistics in the surface boundary layer. *Boundary-Layer Meteorol 21*, 389–402.

Hill, R. J. (1978). Models of the scalar spectrum for turbulent advection. *J Fluid Mech 88*, 541–562.

Hill, R. J. (1989). Implications of Monin-Obukhov similarity theory for scalar quantities. *J Atmos Sci 46*, 2236–2244.

Hill, R. J. and S. F. Clifford (1978). Modified spectrum of atmospheric temperature fluctuations and its application to optical propagation. *J Opt. Soc Am. 68*(7), 892–899.

Hinze, J. O. (1975). *Turbulence.* New York: McGraw-Hill Publishing Company.

Holton, J. R. (1992). *An introduction to dynamic meteorology.* Sand Diego: Academic Press.

Houghton, J. T. (1986). *The physics of atmospheres* (2$^{\underline{nd}}$ ed.). Cambridge University Press.

Huang, J. (2018). A simple accurate formula for calculating saturation vapor pressure of water and ice. *J Appl Meteorol and Climatol 57*(6), 1265–1272.

Högström, U. (1988). Non-dimensional wind and temperature profiles in the atmospheric surface layer: a re-evaluation. *Boundary-Layer Meteorol 42*, 55–78.

Högström, U. (1990). Analysis of turbulence structure in the surface layer with a modified similarity formulation for near neutral conditions. *J Atmos Sci 47*, 1949–1972.

Iribarne, J. V. and W. L. Godson (1981). *Atmospheric Thermodynamics* (2$^{\underline{nd}}$ ed.). Dordrecht: D. Reidel.

Jacobs, J. D. (1978). Radiation climate of broughton island. In R. G. Barry and J. D. Jacobs (Eds.), *Energy Budget Studies in Relation to Fast-ice Breakup Processes in Davis Strait.*, Number Occas. Paper No 26, pp. 105–120. Boulder, CO: Inst. of Arctic and Alp. Res, University of Colorado.

Kader, B. A. and A. M. Yaglom (1990). Mean fields and fluctuation moments in unstably stratified turbulent boundary layers. *J Fluid Mech 212*, 637–662.

Kolmogorov, A. N. (1991). The local structure of turbulence in incompressible viscous fluid for very large Reynolds numbers. In J. C. R. Hunt, O. M. Phillips, and D. Williams (Eds.), *Turbulence and stochastic processes: Kolmogorov's ideas 50 years on*, Volume 434 of *Proceedings A*, pp. 9–13. The Royal Society.

Kumar, P. and M. Sharan (2010). An analytical model for dispersion of pollutants from a continuous source in the atmospheric boundary layer. *Proceedings of the Royal Society A 466*, 383–406.

Kundu, P. K. (1990). *Fluid Mechanics.* San Diego: Academic Press.

Kustas, W. P., J. H. Blanford, D. I. Stannard, C. S. T. Daughtry, W. D. Nichols, and M. A. Weltz (1994). Local energy flux estimates for unstable conditions using variance data in semiarid rangelands. *Water Resour Res 30*(5), 1351–1361.

Landau, L. D. and E. M. Lifshitz (1959). *Fluid Mechanics.* Oxford: Pergamon Press.

Lawrence, R. S. and J. W. Strohbehn (1970). A survey of clear-air propagation effects relevant to optical communications. *Proceedings of the IEEE 58*, 1523–1545.

Lee, X. and W. J. Massman (2011). A perspective on thirty years of the Webb, Pearman and Leuning density corrections. *Boundary-Layer Meteorol 139*, 37 – 59.

Lumley, J. L. and G. R. Newman (1977, Aug). The return to isotropy of homogeneous turbulence. *Journal of Fluid Mechanics 82*(01), 161.

Lumley, J. L. and H. A. Panofksy (1964). *The structure of atmospheric turbulence.* New York: Interscience. 239 pp.

Massman, W. J. and X. Lee (2002). Eddy covariance flux corrections and uncertainties in long-term studies of carbon and energy exchanges. *Agric For Meteorol 113*, 121–144.

Monin, A. S. and A. M. Yaglom (1971). *Statistical fluid mechanics: Mechanics of turbulence*, Volume 1. Cambridge, Massachusetts: MIT Press.

Monin, A. S. and A. M. Yaglom (1975). *Statistical fluid mechanics: Mechanics of turbulence*, Volume 2. Cambridge, Massachusetts: MIT Press.

Murray, F. W. (1966). On the computation of saturation vapor pressure. *J Appl Meteorol 6*, 203–204.

NIST (2020). Nist chemistry web book, srd69. Available at https://webbook.
    nist.gov/chemistry/mw-ser/. Retrieved in 2020-04-10T09:05:36.

Obukhov, A. M. (1946 1971). Turbulence in an atmosphere with non-uniform tem-
    perature. *Boundary-Layer Meteorol 2*, 7–29.

Pahlow, M., M. B. Parlange, and F. Porté-Agel (2001). On Monin-Obukhov simi-
    larity in the stable atmospheric boundary layer. *Boundary-Layer Meteorol 99*,
    225–248.

Pope, S. B. (2000). *Turbulent Flows*. Cambridge: Cambridge University Press.

Rannik, U. and T. Vesala (1999). Autoregressive filtering versus linear detrending
    in estimation of fluxes by the eddy covariance method. *Boundary-Layer Meteo-
    rol 91*(2), 259–280.

Reynolds, O. (1895). On the dynamical theory of incompressible viscous fluids and
    the determination of the criterion. *Philos. Trans. R. Soc. Lond. A 186*, 123–164.

Rotta, J. (1951a). Statistische theorie nichthomogener turbulenz, 1. *Z Phys 129*,
    547–572.

Rotta, J. (1951b). Statistische theorie nichthomogener turbulenz, 2. *Z Phys 131*,
    51–77.

Ruelle, D. (1994, July). Where can one hope to profitably apply the ideas of chaos?
    Physics Today 47(7), 24–30.

Schlyter, P. (2019). How to compute planetary positions. Internet: http://www.
    stjarnhimlen.se/comp/ppcomp.html. Retrieved in 2019-04-22T16:45:34.

Stull, R. (1988). *An Introduction to Boundary-Layer Meteorology*. Dordrecht: Kluwer.

Stull, R. B. (1995). *Meteorology today for scientists and engineers*. Minneapolis / St.
    Paul: West Publishing Company.

Taylor, G. I. (1921). Diffusion by continuous movements. *Proceedings of the London
    Mathematical Society 20*(2), 196–211.

Tennekes, H. and J. L. Lumley (1972). *A first course in turbulence*. Cambridge,
    Massachusetts: The MIT Press.

Tillman, J. E. (1972). The indirect determination of stability, heat and momentum
    fluxes in the atmospheric boundary layer from simple scalar variables during
    dry unstable conditions. *J Appl Meteorol 11*, 783–792.

United States Naval Observatory (2022). Earth's seasons – equinoxes, sol-
    stices, perihelion, and aphelion. https://aa.usno.navy.mil/calculated/
    seasons?year=2020&tz=0&tz_sign=-1&tz_label=false&dst=false&
    submit=Get+Data. Retrieved 2022-04-04T17:09:25.

van Flandern, T. C. and K. F. Pulkkinen (1979). Low-precision formulae for plane-
    tary positions. *Astrophys J Suppl S 41*, 391–411.

Wallace, J. M. and P. V. Hobbs (2006). *Atmospheric Science: an introductory survey* (2ⁿᵈ ed.). Amsterdam: Elsevier.

Webb, E. K., G. I. Pearman, and R. Leuning (1980). Correction of flux measurements for density effects due to heat and water vapor transfer. *Q J Roy Meteorol Soc 106*, 85–100.

Wesely, M. L. (1988). Use of variance techniques to measure dry air-surface exchange rates. *Boundary-Layer Meteorol 44*, 13–31.

Wikipedia (2019). Okta. https://en.wikipedia.org/wiki/Okta. Retrieved in 2019-05-22T10:40:15.

Wikipedia (2020). Atmosphere of earth. Available at https://en.wikipedia.org/wiki/Atmosphere_of_Earth. Retrieved in 2020-04-08T11:25:15.

Wilczak, J. M., S. P. Oncley, and S. A. Stage (2001). Sonic anemometer tilt correction algorithms. *Boundary-Layer Meteorol 99*, 127–150.

Wyngaard, J. C. (1981). Boundary-layer modeling. In F. T. M. Niewstadt and H. van Dop (Eds.), *Atmospheric turbulence and air pollution modelling*, Chapter 3, pp. 69–106. Dordrecht: D. Reidel Publishing Company.

Wyngaard, J. C. (2010). *Turbulence in the atmosphere.* Cambridge.

Wyngaard, J. C., O. R. Coté, and Y. Izumi (1971). Local free convection, similarity, and the budgets of shear stress and heat flux. *J Atmos Sci 28*, 1171–1182.